

## LEADING ARTICLE

# Design and standardization of PCR primers and protocols for detection of clonal immunoglobulin and T-cell receptor gene recombinations in suspect lymphoproliferations: Report of the BIOMED-2 Concerted Action BMH4-CT98-3936

JJM van Dongen<sup>1</sup>, AW Langerak<sup>1</sup>, M Brüggemann<sup>2</sup>, PAS Evans<sup>3</sup>, M Hummel<sup>4</sup>, FL Lavender<sup>5</sup>, E Delabesse<sup>6</sup>, F Davi<sup>7</sup>, E Schuurin<sup>8,9</sup>, R García-Sanz<sup>10</sup>, JHM van Krieken<sup>11</sup>, J Droese<sup>2</sup>, D González<sup>10</sup>, C Bastard<sup>12</sup>, HE White<sup>5</sup>, M Spaargaren<sup>13</sup>, M González<sup>10</sup>, A Parreira<sup>14</sup>, JL Smith<sup>5</sup>, GJ Morgan<sup>3</sup>, M Kneba<sup>2</sup> and EA Macintyre<sup>6</sup>

<sup>1</sup>Department of Immunology, Erasmus MC, University Medical Center Rotterdam, Rotterdam, The Netherlands; <sup>2</sup>II Medizinische Klinik des Universitätsklinikums Schleswig-Holstein, Campus Kiel, Kiel, Germany; <sup>3</sup>Academic Unit of Haematology and Oncology, University of Leeds, Leeds, UK; <sup>4</sup>Institute of Pathology, Free University Berlin, Berlin, Germany; <sup>5</sup>Wessex Immunology Service, Molecular Pathology Unit, Southampton University Hospitals NHS Trust, Southampton, UK; <sup>6</sup>Laboratoire d'Hématologie and INSERM EMI 210, Hôpital Necker-Enfants Malades, Paris, France; <sup>7</sup>Department of Hematology, Hôpital Pitié-Salpêtrière, Paris, France; <sup>8</sup>Department of Pathology, Leiden University Medical Center, Leiden, The Netherlands; <sup>9</sup>Department of Pathology and Laboratory Medicine, University Medical Center Groningen, Groningen, The Netherlands; <sup>10</sup>Servicio de Hematología, Hospital Universitario de Salamanca, Salamanca, Spain; <sup>11</sup>Department of Pathology, University Medical Center Nijmegen, Nijmegen, The Netherlands; <sup>12</sup>Laboratoire de Genetique Oncologique, Centre Henri Becquerel, Rouen, France; <sup>13</sup>Department of Pathology, Academic Medical Center, Amsterdam, The Netherlands; and <sup>14</sup>Department of Hematology, Instituto Português de Oncologia, Lisboa, Portugal

In a European BIOMED-2 collaborative study, multiplex PCR assays have successfully been developed and standardized for the detection of clonally rearranged immunoglobulin (Ig) and T-cell receptor (TCR) genes and the chromosome aberrations t(11;14) and t(14;18). This has resulted in 107 different primers in only 18 multiplex PCR tubes: three VH–JH, two DH–JH, two Ig kappa (IGK), one Ig lambda (IGL), three TCR beta (TCRB), two TCR gamma (TCRG), one TCR delta (TCRD), three BCL1-Ig heavy chain (IGH), and one BCL2-IGH. The PCR products of Ig/TCR genes can be analyzed for clonality assessment by heteroduplex analysis or GeneScanning. The detection rate of clonal rearrangements using the BIOMED-2 primer sets is unprecedentedly high. This is mainly based on the complementarity of the various BIOMED-2 tubes. In particular, combined application of IGH (VH–JH and DH–JH) and IGK tubes can detect virtually all clonal B-cell proliferations, even in B-cell malignancies with high levels of somatic mutations. The contribution of IGL gene rearrangements seems limited. Combined usage of the TCRB and TCRG tubes detects virtually all clonal T-cell populations, whereas the TCRD tube has added value in case of TCR $\gamma\delta^+$  T-cell proliferations. The BIOMED-2 multiplex tubes can now be used for diagnostic clonality studies as well as for the identification of PCR targets suitable for the detection of minimal residual disease.

Leukemia (2003) 17, 2257–2317. doi:10.1038/sj.leu.2403202

**Keywords:** PCR; clonality; immunoglobulin genes; T-cell receptor genes; lymphoproliferative disorders; IGH; IGK; IGL; TCRB; TCRG; TCRD; t(14;18); t(11;14); BCL1; BCL2; GeneScanning; heteroduplex; multiplex PCR; BIOMED-2

## Preface

In most patients with suspect lymphoproliferative disorders, histomorphology or cytomorphology supplemented with immunohistology or flow cytometric immunophenotyping can discriminate between malignant and reactive lymphoproliferations. However, in 5–10% of cases, making the diagnosis is more complicated. The diagnosis of lymphoid malignancies can be supported by clonality assessment based on the fact that, in

principle, all cells of a malignancy have a common clonal origin.

The majority of lymphoid malignancies belong to the B-cell lineage (90–95%) with only a minority being T-cell (5–7%) or NK-cell lineage (<2%). Acute lymphoblastic leukemias (ALLs) are of T-cell origin in 15–20% of cases, but in the group of mature lymphoid leukemias and in non-Hodgkin lymphomas (NHLs) T-cell malignancies are relatively rare, except for specific subgroups such as cutaneous lymphomas (Table 1). The vast majority of lymphoid malignancies (>98%) contains identically (clonally) rearranged immunoglobulin (Ig) and/or T-cell receptor (TCR) genes, and in 25–30% of cases well-defined chromosome aberrations are found, all of which can serve as markers for clonality.<sup>1,2</sup>

## Ig and TCR gene rearrangements

The Ig and TCR gene loci contain many different variable (V), diversity (D), and joining (J) gene segments, which are subject to rearrangement processes during early lymphoid differentiation.<sup>3,4</sup> The V–D–J rearrangements are mediated via a recombinase enzyme complex in which the RAG1 and RAG2 proteins play a key role by recognizing and cutting the DNA at the recombination signal sequences (RSS), which are located downstream of the V gene segments, at both sides of the D gene segments, and upstream of the J gene segments (Figure 1). Inappropriate (mutated or crippled) RSS reduce or even completely prevent rearrangement.

The rearrangement process generally starts with a D to J rearrangement followed by a V to D–J rearrangement in case of Ig heavy chain (IGH), TCR beta (TCRB), and TCR delta (TCRD) genes (Figure 1) or concerns direct V to J rearrangements in case of Ig kappa (IGK), Ig lambda (IGL), TCR alpha (TCRA), and TCR gamma (TCRG) genes. The sequences between rearranging gene segments are generally deleted in the form of a circular excision product, also called TCR excision circle (TREC) or B-cell receptor excision circle (Figure 1).

The Ig and TCR gene rearrangements during early lymphoid differentiation generally follow a hierarchical order. During B-cell differentiation, first the IGH genes rearrange, then IGK, potentially resulting in IgH $\kappa$  expression or followed by IGK

Correspondence: Professor JJM van Dongen, Department of Immunology, Erasmus MC, University Medical Center Rotterdam, Dr Molewaterplein 50, 3015 GE Rotterdam, The Netherlands; Fax: +31 10 40 89456; E-mail: j.j.m.vandongen@erasmusmc.nl  
Received 10 July 2003; accepted 10 October 2003

**Table 1** B, T, and NK lineage of lymphoid malignancies<sup>a</sup>

Lineage	ALL		Chronic lymphocytic leukemias (%)	NHL			Multiple myeloma (%)
	Childhood (%)	Adult (%)		Nodal (%)	Extranodal (%)	Skin (%)	
B	82–86	75–80	95–97	95–97	90–95	30–40	100
T	14–18	20–25	3–5	3–5	5–10	60–70	0
NK	<1	<1	1–2	<2	<2	<2	0

<sup>a</sup>See van Dongen *et al*,<sup>1</sup> Jaffe *et al*,<sup>2</sup> and van Dongen *et al*.<sup>5</sup>

deletion and *IGL* rearrangement, potentially followed by IgH/λ expression.<sup>5</sup> This implies that virtually all Igλ<sup>+</sup> B cells have monoallelic or biallelic *IGK* gene deletions. During T-cell differentiation, first the *TCRD* genes rearrange, then *TCRG*, potentially resulting in TCRγδ expression or followed by further *TCRB* rearrangement and *TCRD* deletion with subsequent *TCRA* rearrangement, potentially followed by TCRαβ expression. The Ig and TCR gene rearrangement patterns in lymphoid malignancies generally fit with the above-described hierarchical order, although unusual rearrangement patterns can be found as well, particularly in ALL.<sup>6</sup>

### Ig and TCR repertoire

The many different combinations of V, D, and J gene segments represent the so-called combinatorial repertoire (Table 2), which is estimated to be  $\sim 2 \times 10^6$  for Ig molecules,  $\sim 3 \times 10^6$  for TCRαβ molecules, and  $\sim 5 \times 10^3$  for TCRγδ molecules. At the junction sites of the V, D, and J gene segments, deletion and random insertion of nucleotides occurs during the rearrangement process, resulting in highly diverse junctional regions, which significantly contribute to the total repertoire of Ig and TCR molecules, estimated to be  $> 10^{12}$ .<sup>5</sup>

Mature B-lymphocytes further extend their Ig repertoire upon antigen recognition in germinal centers via *somatic hypermutation*, a process leading to affinity maturation of the Ig molecules. The somatic hypermutation process focuses on the V(D)J exon of *IGH* and Ig light-chain genes and concerns single-nucleotide

mutations and occasional insertions or deletions of nucleotides. Somatic mutated Ig genes are therefore found in mature B-cell malignancies of germinal center or postgerminal center origin.<sup>7</sup>

### Monotypic Ig and TCR molecules as indirect evidence of clonality

Functionally rearranged Ig and TCR genes result in surface membrane expression of Ig, TCRαβ, or TCRγδ molecules. Based on the concept that only a single type of Ig or TCR molecule is expressed by a lymphocyte or lymphoid clone, the clonally rearranged genes of mature lymphoid malignancies might be detectable at the protein level. The detection of single Ig light-chain expression (Igκ or Igλ) has for a long time been used to discriminate between reactive (polyclonal) B-lymphocytes (normal Igκ/Igλ ratio: 0.7–2.8) vs aberrant (clonal) B-lymphocytes with Igκ/Igλ ratios of  $> 4.0$  or  $< 0.5$ .<sup>8–10</sup> In the vast majority ( $> 90\%$ ) of mature B-cell malignancies, single Ig light-chain expression can support the clonal origin of the malignancy. In tissue sections, however, reliable detection of Ig light-chain expression is often difficult to assess due to soluble Ig molecules overlaying the cellular Ig expression.

The development of many different antibodies against variable domains of the various TCR chains also allows the detection of monotypic Vβ, Vγ and Vδ domains, when compared with appropriate reference values.<sup>11–16</sup> In the interpretation of monotypic Vβ results using 20–25 antibodies against different Vβ families (Table 2), one should realize that

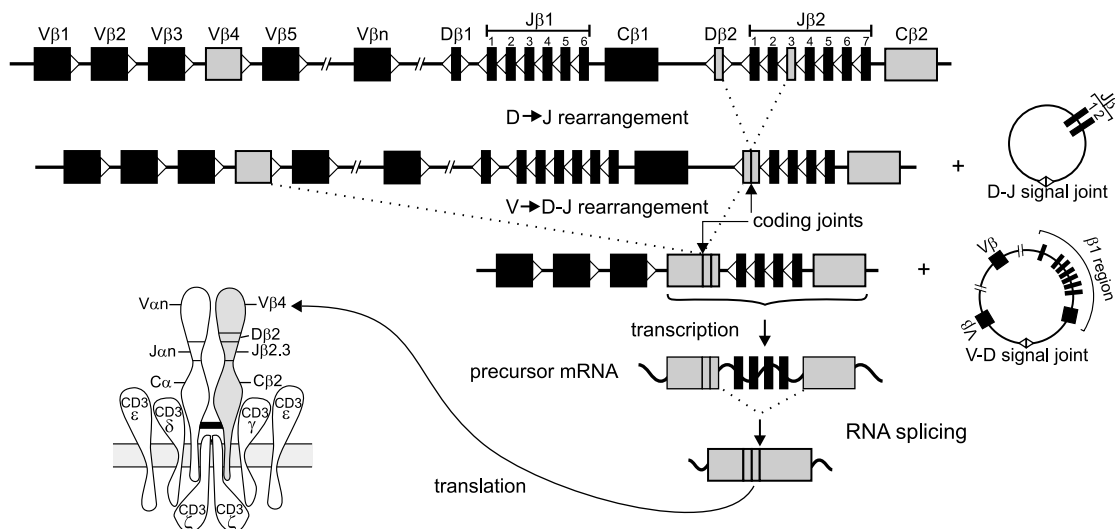


**Figure 1** Schematic diagram of sequential rearrangement steps, transcription, and translation of the *TCRB* gene. In this example, first a Dβ2 to Jβ2.3 rearrangement occurs, followed by Vβ4 to Dβ2–Jβ2.3 rearrangement, resulting in the formation of a Vβ4–Dβ2–Jβ2.3 coding joint. The rearranged *TCRB* gene is transcribed into precursor mRNA, spliced into mature mRNA, and finally translated into a TCRβ protein chain. The two extrachromosomal TRECs that are formed during this recombination process are indicated as well; they contain the D–J signal joint and V–D signal joint, respectively.

**Table 2** Estimated number of nonpolymorphic human V, D, and J gene segments that can potentially be involved in Ig or TCR gene rearrangements<sup>a</sup>

Gene segment	IGH	IGK	IGL	TCRA	TCRB	TCRG	TCRD
<i>V segments</i>							
Functional (family)	44 (7)	43 (7)	38 (10)	46 (32)	47 (23)	6 (4)	8
Rearrangeable (family)	66 (7) <sup>b</sup>	76 (7)	56 (11)	54 (32)	67 (30)	9 (4)	8
<i>D segments</i>							
Rearrangeable (family)	27 (7)	—	—	—	2	—	3
<i>J segments</i>							
Functional	6 <sup>c</sup>	5 <sup>d</sup>	4	53	13	5	4
Rearrangeable	6 <sup>c</sup>	5 <sup>d</sup>	5 <sup>e</sup>	61	13	5	4

<sup>a</sup>Only nonpolymorphic gene segments with a suitable RSS are included in this table.<sup>62,63</sup>

<sup>b</sup>This estimation does not include the recently discovered (generally truncated) VH pseudogenes, which are clustered in three clans.

<sup>c</sup>The six JH gene segments are highly homologous over a stretch of ~20 nucleotides, which is sufficient for the design of a consensus primer.

<sup>d</sup>The J $\kappa$  segments have a high homology, which allows the design of two to three J $\kappa$  consensus primers.

<sup>e</sup>Five of the seven J $\lambda$  gene segments have a suitable RSS.

clinically benign clonal TCR $\alpha\beta^+$  T-cell expansions (frequently CD8<sup>+</sup>) are regularly found in peripheral blood (PB) of older individuals.<sup>13,17</sup> These clonal T-cell expansions in PB are, however, relatively small in size: <40% of PB T-lymphocytes and <0.5  $\times 10^6$ /ml PB.<sup>13</sup> It is not yet clear to what extent such clinically benign T-cell clones can also be found in lymphoid tissues.

The results of monotypic V $\gamma$  and V $\delta$  domain expression should be interpreted with caution, because in healthy individuals a large fraction of normal polyclonal TCR $\gamma\delta^+$  T-lymphocytes has been selected for V $\gamma$ 9–J $\gamma$ 1.2 and V $\delta$ 2–J $\delta$ 1 usage.<sup>18,19</sup> Consequently, high frequencies of V $\gamma$ 9<sup>+</sup>/V $\delta$ 2<sup>+</sup> T-lymphocytes in PB should be regarded as a normal finding, unless the absolute counts are over 1–2  $\times 10^6$ /ml PB. It should be noted that most TCR $\gamma\delta^+$  T-cell malignancies express V $\delta$ 1 or another non-V $\delta$ 2 gene segment in combination with a single V $\gamma$  domain (generally not V $\gamma$ 9).<sup>15,20</sup>

The detection of Ig $\kappa$ - or Ig $\lambda$ -restricted expression or monotypic V $\beta$ , V $\gamma$  or V $\delta$  expression is relatively easy in flow cytometric studies of PB and bone marrow (BM) samples of patients with mature B- or T-cell leukemias. However, it appears to be more difficult in tissue samples with suspect lymphoproliferative disorders that are intermixed with normal (reactive) lymphocytes.

In contrast to the antibody-based techniques, molecular techniques are broadly applicable for the detection of clonally rearranged Ig/TCR genes and certain chromosome aberrations. This previously concerned Southern blot analysis, which has gradually been replaced by PCR techniques.

### Molecular clonality diagnostics in hemato-oncology

Difficulties in making a final diagnosis of lymphoid malignancy occur in a proportion of cases (5–10%) despite extensive immunophenotyping. Therefore, additional (molecular clonality) diagnostics are needed to generate or to confirm the final diagnosis, such as in case of:

- any suspect B-cell proliferation when morphology and immunophenotyping are not conclusive;
- all suspect T-cell proliferations (caution: T-cell-rich B-NHL);
- lymphoproliferations in immunodeficient patients, including post-transplant patients;

- evaluation of the clonal relationship between two lymphoid malignancies in one patient or discrimination between a relapse and a second malignancy;
- further classification of a malignancy, for example, via Ig/TCR gene rearrangement patterns or particular chromosome aberrations;
- occasionally, staging of lymphomas.

### Southern blot analysis and PCR techniques for clonality studies

**Southern blot analysis:** For a long time, Southern blot analysis has been the gold standard technique for molecular clonality studies. Southern blotting is based on the detection of non-germline ('rearranged') DNA fragments, obtained after digestion with restriction enzymes. Well-chosen restriction enzymes (resulting in fragments of 2–15 kb) and well-positioned DNA probes (particularly downstream J segment probes) allow the detection of virtually all Ig and TCR gene rearrangements as well as chromosome aberrations involving J gene segments.<sup>21–28</sup> It should be noted that Southern blot analysis focuses on the rearrangement diversity of Ig/TCR gene segments and therefore takes advantage of the combinatorial repertoire.

Optimal Southern blot results for clonality assessment can particularly be obtained with the IGH, IGK, and TCRB genes, because these genes have an extensive combinatorial repertoire as well as a relatively simple gene structure that can be evaluated with only one or two DNA probes.<sup>22,24,28</sup> The IGL and TCRA genes are more complex and require multiple probe sets.<sup>25,26,29</sup> Finally, the TCRG and TCRD genes have a limited combinatorial repertoire, which is less optimal for discrimination between monoclonality and polyclonality via Southern blot analysis.<sup>20,21</sup>

Despite the high reliability of Southern blot analysis, it is increasingly replaced by PCR techniques, because of several inherent disadvantages: Southern blot analysis is time-consuming, technically demanding, requires 10–20  $\mu$ g of high-quality DNA, and has a limited sensitivity of 5–10%.<sup>21</sup>

**PCR analysis:** The detection of rearranged Ig/TCR genes and chromosome aberrations by PCR techniques requires precise knowledge of the rearranged gene segments in order to design

appropriate primers at opposite sides of the junctional regions and breakpoint fusion regions, respectively.

In routine PCR-based clonality studies, the distance between the primers should be less than 1 kb, preferably less than 500 bp, and in formalin-fixed tissues preferably less than 300 bp (see also Section 10). This is particularly important for discrimination between PCR products from monoclonal vs polyclonal Ig/TCR gene rearrangements, which is based on the diversity of the junctional regions (diversity in size and composition). To date, *IGH* and *TCRG* gene rearrangements have most commonly been used for PCR-based clonality studies, because of the limited number of primers needed to detect VH-JH and V $\gamma$ -J $\gamma$  rearrangements.

The main advantages of PCR techniques are their speed, the low amounts of DNA required, the possibility to use DNA of lower quality, and the relatively good sensitivity of 1–5%, for some types of rearrangements even <1%. Consequently, PCR techniques allow the use of small biopsies (eg fine-needle aspiration biopsies), or the use of formaldehyde-fixed paraffin-embedded samples, which generally results in DNA of lower quality, that is, partly degraded into smaller fragments. Therefore archival material may also be used, if needed.

### Limitations and pitfalls of molecular clonality studies

Molecular clonality studies can be highly informative, but several limitations and pitfalls might hamper the interpretation of the results:

1. *Limited sensitivity, related to normal polyclonal background:* The detection limit varies between 1 and 10% (or even 15%), dependent on the applied technique (Southern blot analysis or PCR techniques) and on the relative size of the 'background' of normal (polyclonal) B- and T-lymphocytes. A limited sensitivity might hamper the detection of small clonal cell populations with less than 5–10% clonal lymphoid cells.

2. *Clonality is not equivalent to malignancy:* The detection of clonality does not always imply the presence of a malignancy. Some clinically benign proliferations have a clonal origin, such as many cases of CD8<sup>+</sup> (or sometimes CD4<sup>+</sup>) T-lymphocytosis, benign monoclonal gammopathies, initial phases of EBV<sup>+</sup> lymphoproliferations (frequently being oligoclonal) in immunodeficient patients, and benign cutaneous T-cell proliferations, such as lymphomatoid papulosis, etc. This implies that results of molecular clonality studies should always be interpreted in the context of the clinical, morphological, and immunophenotypic diagnosis, that is, in close collaboration with hematologists, cytomorphologists, pathologists, and immunologists.

3. *Ig and TCR gene rearrangements are not markers for lineage:* In contrast to the initial assumption, it has now been clear for more than a decade that Ig and TCR gene rearrangements are not necessarily restricted to B- and T-cell lineages, respectively. Crosslineage TCR gene rearrangements occur relatively frequently in immature B-cell malignancies, particularly in precursor B-ALL (>90% of cases),<sup>30</sup> but also acute myeloid leukemias (AMLs) and mature B-cell malignancies might contain TCR gene rearrangements.<sup>31–33</sup> Crosslineage Ig gene rearrangements, mainly involving the *IGH* locus, also occur in T-cell malignancies and AML, albeit at a lower frequency.<sup>33,34</sup>

Virtually all (>98%) TCR $\alpha\beta$ <sup>+</sup> T-cell malignancies have *TCRG* gene rearrangements (generally biallelic) and many TCR $\gamma\delta$ <sup>+</sup> T-cell malignancies have *TCRB* gene rearrangements, implying that the detection of *TCRB* or *TCRG* rearrangements is not

indicative of T cells of the  $\alpha\beta$  or  $\gamma\delta$  T-cell lineage, respectively, either.<sup>15,27,28</sup>

In addition to these crosslineage rearrangements, it has been established that several lymphoid malignancies have unusual Ig/TCR gene rearrangement patterns. This information is available in detail for precursor B-ALL and T-ALL, but not yet for most other lymphoid malignancies.<sup>6</sup>

4. *Pseudoclonality and oligoclonality:* The erroneous detection of a seemingly clonal or seemingly oligoclonal lymphoid cell population (pseudoclonality) is rare by Southern blot analysis, unless genes with a limited combinatorial repertoire, such as *TCRG* or *TCRD*, are used. This might result in faint rearranged bands, for example, representing V $\gamma$ 9-J $\gamma$ 1.2 or V $\delta$ 2-J $\delta$ 1 rearrangements derived from antigen-selected TCR $\gamma\delta$ <sup>+</sup> T-lymphocytes. This is, however, a well-known pitfall of Southern blot analysis and will not result in rearranged bands of high density.

Pseudoclonality in PCR-based clonality studies is more difficult to recognize. The high sensitivity of PCR can cause the amplification of the few Ig or TCR gene rearrangements derived from a limited number of B or T-cells in the tissue sample analyzed. In particular, the few reactive (polyclonal) T cells in a small-needle biopsy or in a B-NHL sample with high tumor load might result in (oligo)clonal PCR products. Frequently, the amount of such PCR products is limited. This is particularly seen when *TCRG* genes are used as PCR targets. Duplicate or triplicate PCR analyses followed by mixing of the obtained PCR products should help to clarify whether the seemingly clonal PCR products are in fact derived from different lymphocytes.

Finally, reactive lymph nodes can show reduced diversity of the Ig/TCR repertoire, caused by predominance of several antigen-selected subclones (oligoclonality). In particular, lymph nodes or blood samples of patients with an active EBV or CMV infection can show a restricted TCR repertoire or TCR gene oligoclonality. Also clinical pictures of immunosuppression are frequently associated with restricted TCR repertoires, for example, in transplant patients or patients with hairy cell leukemia.<sup>35</sup> Recovery from transplantation and hematological remission are followed by restoration of the polyclonal TCR repertoire.<sup>36,37</sup>

5. *False-positive results:* False-positive results are rare by Southern blot analysis and can generally be prevented by checking for underdigestion and by excluding polymorphic restriction sites.<sup>21</sup>

False-positive PCR results have shown to be a serious problem, if no adequate analysis of the obtained PCR products is performed to discriminate between monoclonal, oligoclonal, or polyclonal PCR products. Such discrimination can be achieved via single-strand conformation polymorphism analysis,<sup>38</sup> denaturing gradient gel electrophoresis,<sup>39</sup> heteroduplex analysis,<sup>40,41</sup> or GeneScanning.<sup>42,43</sup> These techniques exploit the junctional region diversity for discrimination between monoclonal cells with identical junctional regions and polyclonal cells with highly diverse junctional regions.

6. *False-negative results:* False-negative results are rare in Southern blot analysis if appropriate J gene segment probes are used. Nevertheless, some uncommon rearrangements (generally nonfunctional rearrangements) might be missed, such as V-D rearrangements or deletions of the J regions.

PCR analysis of Ig and TCR genes might be hampered by false-negative results because of improper annealing of the applied PCR primers to the rearranged gene segments. This improper primer annealing can be caused by two different phenomena. Firstly, precise detection of all different V, D, and J

gene segments would require many different primers (Table 2), which is not feasible in practice. Consequently, family primers are designed, which specifically recognize most or all members of a particular V, D, or J family. Alternatively, consensus primers are used, which are assumed to recognize virtually all V and J gene segments of the locus under study. Family primers and particularly consensus primers are generally optimal for a part of the relevant gene segments, but show a lower homology (70–80%) to other gene segments. This may eventually lead to false-negative results, particularly in Ig/TCR genes with many different gene segments. In *TCRG* and *TCRD* genes this problem is minimal, because of the limited number of different gene segments.

The second phenomenon is the occurrence of somatic hypermutations in rearranged Ig genes of germinal center and postgerminal center B-cell malignancies, particularly B-cell malignancies with class-switched *IGH* genes.

Sufficient knowledge and experience can prevent the first four pitfalls, because they mainly concern interpretation problems. The last two pitfalls concern technical problems, which can be solved by choosing reliable techniques for PCR product analysis and by the design of better primer sets.

## Can Southern blot analysis be replaced by PCR technology?

Optimization of Southern blot analysis of Ig/TCR genes during the past 10 years has resulted in the selection of reliable combinations of restriction enzymes (fragments between 2 and 15 kb, avoiding polymorphic restriction sites) and probes (mainly downstream of J gene segments). Although Southern blot analysis is a solid 'gold standard' technique, many laboratories have gradually replaced Southern blot analysis by

PCR technology, because PCR is fast, requires minimal amounts of medium-quality DNA, and has overall good sensitivity.

Despite the obvious advantages, replacement of Southern blot analysis by PCR techniques for reliable Ig/TCR studies is hampered by two main technical problems:

- false-negative results due to improper primer annealing; and
- difficulties in discrimination between monoclonal and polyclonal Ig/TCR gene rearrangements.

Several individual diagnostic laboratories tried to solve the problems of the PCR-based clonality studies, but no reliably standardized PCR protocols were obtained. In contrast, many different primer sets are being used, which all differ in their sensitivity and applicability. We therefore initiated the BIOMED-2 Concerted Action BMH4-CT98-3936, entitled 'PCR-based clonality studies for early diagnosis of lymphoproliferative disorders' with the aim to develop standardized PCR protocols and PCR primer sets for clonality diagnostics.

## Introduction

In order to introduce reliable and easy PCR technology for routine clonality diagnostics in suspect lymphoproliferations, the BIOMED-2 Concerted Action BMH4-CT98-3936 had two main objectives, addressed in two separate Work Packages:

*Work Package 1:* Development and standardization of PCR protocols and PCR primer sets for the detection of Ig and TCR gene rearrangements and well-defined chromosome aberrations as targets for clonality assessment. This included the development of guidelines for interpretation of the results obtained.

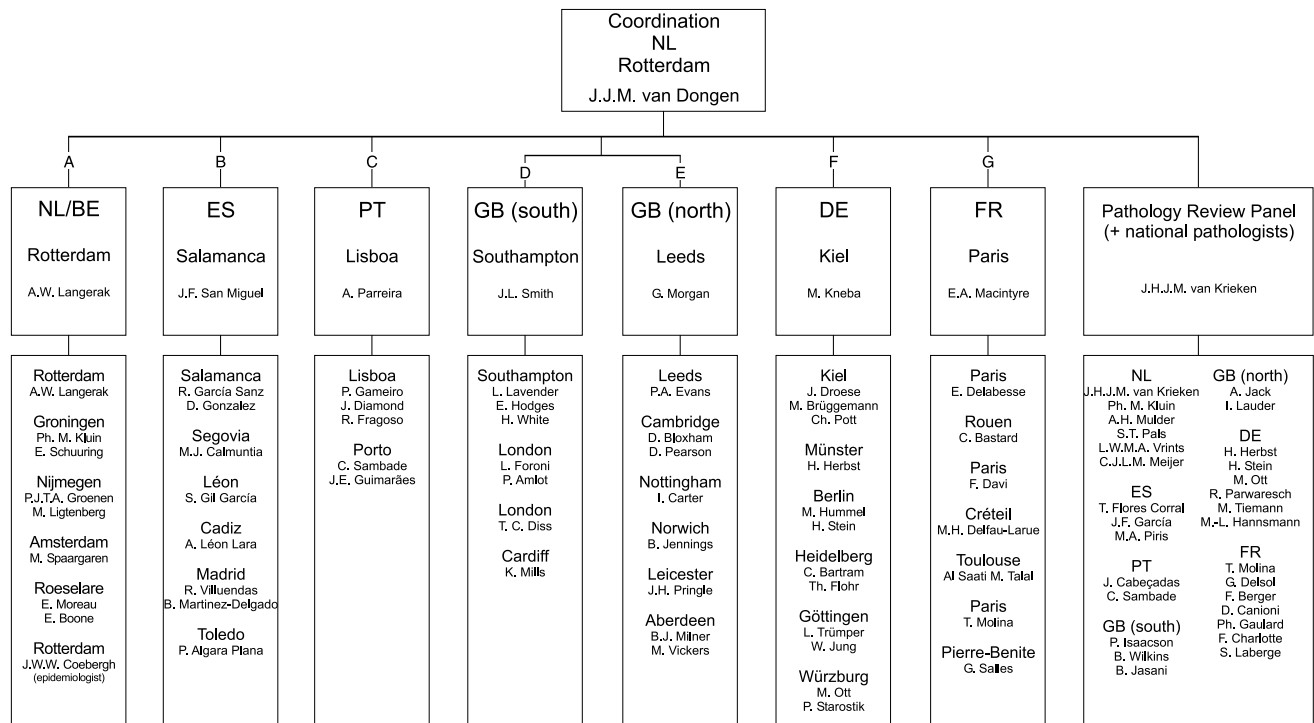


**Figure 2** Schematic diagram of management structure of the BIOMED-2 Concerted Action BMH4-CT98-3936. The collaboration between the 47 European institutes was structured via seven National Networks and a Pathology Review Panel.

**Work Package 2:** Evaluation of the applicability of the standardized PCR protocols and PCR primer sets for clonality studies in the various categories of WHO-defined lymphoid malignancies.

A total of 47 institutes from seven European countries (Netherlands, Belgium, Spain, Portugal, UK, Germany, and France) participated in the BIOMED-2 Concerted Action with one to four participants per institute (~90 active participants in total). This included laboratory specialists in the field of molecular biology, immunology, hematology, and pathology. To facilitate the organization and management of this complex and large-scale European collaboration, the Concerted Action activities were organized via seven National Networks (each coordinated by a National Network Leader) and an international Pathology Review Panel (Figure 2). The National Networks played a central role in the collection of tissue samples and corresponding DNA samples for use in Work Packages 1 and 2. The national pathologists were responsible for reviewing all nationally collected samples. All difficult cases and a 10% randomly selected set of additional cases were reviewed by the international Pathology Review Panel (coordinator: JJM van Krieken).

Work Package 1 and most of Work Package 2 were performed in the period June 1998–November 2002, evaluated and coordinated via a total of 12 international meetings (Table 3). This report describes the organization, experimentation, and results of Work Package 1.

## Materials and methods

### Organization and experimentation of Work Package 1

Work Package 1 focused on the development of standardized PCR protocols and PCR primer sets for the detection of clonally rearranged Ig/TCR gene rearrangements and well-defined chromosome aberrations. This included the selection of the PCR targets, the development of PCR primer sets to be used in multiplex tubes, and the selection of techniques for the analysis of PCR products.

### Selection of PCR targets: aiming for complementarity

It was decided to aim for the availability of at least one PCR-detectable clonality target in each lymphoid malignancy. In mature B-cell malignancies this aim might be hampered by the occurrence of somatic hypermutations in Ig genes, which are particularly found in germinal center and postgerminal center-derived B-cell malignancies. Therefore, it was decided to include PCR targets that have some degree of complementarity.

Several rationales were used for target selection:

- *IGH* genes: not only complete VH–JH rearrangements but also incomplete DH–JH rearrangements were included as PCR targets, because DH–JH rearrangements are probably not affected by somatic hypermutation;
- *IGK* and *IGL* genes: both Ig light-chain genes were included as PCR targets, because this increases the chance of finding a PCR-detectable Ig gene rearrangement in each mature B-cell malignancy;
- *IGK* genes: not only V $\kappa$ –J $\kappa$  rearrangements were included, but also rearrangements of the kappa deleting element (Kde), because they occur on one or both alleles in (virtually) all Ig $\lambda^+$  B-cell malignancies and in one-third of Ig $\kappa^+$  B-cell malignancies, and because Kde rearrangements are probably not affected by somatic hypermutation;
- *TCRB* genes: both complete V $\beta$ –J $\beta$  and incomplete D $\beta$ –J $\beta$  rearrangements, because complete and incomplete *TCRB* gene rearrangements occur in all mature TCR $\alpha\beta^+$  T-cell malignancies and also in many TCR $\gamma\delta^+$  T-cell malignancies;
- *TCRG* genes: this classical PCR clonality target is useful in all T-cell malignancies of the TCR $\gamma\delta$  and the TCR $\alpha\beta$  lineage.
- *TCRD* genes: this is a potentially useful target in immature T-cell malignancies as well as in TCR $\gamma\delta^+$  T-cell malignancies;
- *TCRA* genes: this gene was not included as PCR target, because of its high degree of complexity with 54 V and 61 J gene segments. Furthermore, all T-cell malignancies with *TCRA* gene rearrangements contain *TCRB* gene rearrangements and generally also have *TCRG* gene rearrangements;

**Table 3** Meetings of the BIOMED-2 Concerted Action BMH4-CT98-3936

Date	Town	Type of meeting <sup>a</sup>	Topics <sup>a</sup>
June 1998	Rotterdam, Netherlands	Network leaders (national)	Organization/planning/finances
Oct 1998	Rotterdam, Netherlands	General	Presentation of participants/task divisions primer design+testing
Jan 1999	Rotterdam, Netherlands	Primer design	Computerized primer design for WP1
Nov 1999	Rotterdam, Netherlands	Primer design	Initial primer evaluation/Southern blot evaluation
Jan 2000	Berlin, Germany	General	Primer evaluation/pathology review
April 2000	Dordrecht, Netherlands	Network leaders (national/target)	Primer evaluation
June 2000	Birmingham, UK	Network leaders (national/target)	Primer evaluation/plannings and organization of WP2
Nov 2000	Salamanca, Spain	General	General primer testing evaluation/pathology review
April 2001	Paris, France	Network leaders (national/target)	Final primer approval/start testing WP2
Sep 2001	Rotterdam, Netherlands	Network leaders (national/target/disease)	Initial WP2 evaluation/pathology review
Nov 2001	Rotterdam, Netherlands	General	Final WP2 evaluation/pathology review
May 2002	Siena, Italy	EAHP <sup>b</sup> satellite symposium	International presentation of WP1 and WP2 results for international audience

<sup>a</sup>The Network Leaders meetings included: National Network leaders meeting for management and organization of the Work Packages; Target Network leaders meetings for organization and evaluation of Work Package 1 (WP1); Disease Category Network leaders meeting for organization and evaluation of Work Package 2 (WP2).

<sup>b</sup>EAHP, European Association for Hematopathology.

- *functional gene segments*: most suspect lymphoproliferations concern mature lymphocytes, which consequently have functional Ig or TCR gene rearrangements. Therefore, PCR primer design aimed at inclusion of (virtually) all functional Ig/TCR gene segments; and
- *well-defined chromosome aberrations*: t(11;14) with *BCL1-IGH* and t(14;18) with *BCL2-IGH* were included as additional targets, because these two aberrations are PCR detectable at relatively high frequencies in lymphomas, that is, in 30–40% of mantle cell lymphoma (MCL) and in 60–70% of follicular lymphomas (FCL), respectively.

### Primer design for multiplex PCR

Precise detection of all V, D, and J gene segments in rearranged Ig and TCR genes would require many different primers (Table 2). For some gene complexes this might be possible (eg *TCRG* and *TCRD*), but for other loci in practice this is impossible because of the high number of different gene segments. To solve this problem, family primers can be designed, which recognize most or all gene segments of a particular family (Table 2). Alternatively, consensus primers can be made, which recognize conserved sequences that occur in many or all involved gene segments.

The design of family primers and consensus primers balances between a limited number of primers and maximal homology with all relevant gene segments. In this Concerted Action, we aimed at maximal homology with all relevant gene segments (particularly functional gene segments) in order to prevent suboptimal primer annealing, which might cause false-negative results. Furthermore, we aimed at the design of specific family primers without crossannealing to other families.

In order to limit the number of PCR tubes per locus, multiplexing of PCR primers became essential. Consequently, special guidelines were developed to ensure maximal possibilities for designing primers useful in multiplex PCR tubes. For this purpose, Dr W Rychlik (Molecular Biology Insights, Cascade, CO, USA) provided his specially adapted OLIGO 6.2 software program and supported the development of the guidelines for optimal primer design.

The general guidelines for primer design were as follows:

- the position of the primers should be chosen in such a way that the size of the PCR products would preferably be <300bp (preferably 100–300bp) in order to be able to use paraffin-embedded material;
- a minimal distance to the junctional region of preferably >10–15bp should be taken into account (in order to avoid false-negativity due to the impossibility of the 3'-end of the primer to anneal to the rearranged target because of nucleotide deletion from the germline sequence); and
- primers preferably should not be too long (eg <25 nucleotides).

The following parameters were used for primer design with the OLIGO 6.2 program:

- search for primers should be performed with *moderate* stringency;
- priming efficiency (PE) value should preferably be ~400 (and >630, if the primer is to be used as a consensus primer for other gene segments as well);
- the most stable 3' dimer of upper/upper, lower/lower, or upper/lower primers should not exceed –4 Kcal (moderate

search strategy), the most stable dimer overall being less important; and

- in view of multiplex PCR, the following guidelines were taken into account: a common primer would have to be designed in the most consensus region (ie high PE in consensus search), whereas individual primers (family or member) would have to be designed in the least consensus region (ie low PE value of that primer for gene segments that should not be covered) to avoid crossannealing to other gene segments and thereby multiple (unwanted) PCR products.

### PCR primers and commercial availability

To ensure the usage of identical primers in all participating laboratories during the here reported study, the primers were produced in bulk quantities by Applied Biosystems (Foster City, CA, USA) or by Sigma-Genosys Ltd (Pampisford, UK), that is, one large batch of each primer per testing phase. The obtained primers were aliquoted centrally in Rotterdam and distributed in standard packages to all participating centers (AW Langerak c.s.).

Since the completion of the BIOMED-2 study, all primers and ready-to-go multiplex tubes are available on a commercial basis exclusively from InVivoScribe Technologies (Carlsbad, CA, USA; www.invivoscribe.com). See Discussion for rationale.

### PCR protocol

A standardized BIOMED-2 PCR protocol was developed based on pre-existing experience from earlier European collaborative studies. After initial testing and approval, the protocol was accepted as summarized in Table 4.

The reaction conditions were developed for a final volume of 50 µl. At a later stage 25 µl was also tested and approved, always using 100 ng of DNA. During all testing phases the same batch of dNTP was used, kindly produced and reserved for the BIOMED-2 Concerted Action by Amersham Pharmacia Biotech (Roosendaal, Netherlands).

**Table 4** Standardized BIOMED-2 PCR protocol

#### Reaction conditions

Buffer: ABI Buffer II or ABI Gold Buffer

50 µl final volume

100 ng DNA

10 pmol of each primer (unlabeled or 6-FAM labeled) irrespective of total numbers of primers in each multiplex PCR tube

dNTP: 200 µM final concentration

MgCl<sub>2</sub>: 1.5 mM final concentration (to be optimized per target)

Taq enzyme<sup>a</sup>: 1 U in most tubes; 2 U in tubes with many primers

#### Cycling conditions

Preactivation 7 min at 95°C

Annealing temperature: 60°C

Cycling times:

	'Classical' PCR equipment	'Newer' PCR equipment
Denaturation	45 s	30 s
Annealing	≥45 s	≥30 s
Extension	1.30 min	≥30 s
Final extension	≥10 min	≥10 min
Number of cycles: 35		
Hold 15°C (or room temperature)		

<sup>a</sup>AmpliTaq Gold (Applied Biosystems, Foster City, CA, USA) was used in combination with 1 × ABI Buffer II or 1 × ABI Gold Buffer (Applied Biosystems), depending on the target.

MgCl<sub>2</sub> was used at 1.5 mM final concentration, but needed optimization for some multiplex PCR tubes (see later). In most tubes 1 U of AmpliTaq Gold (Applied Biosystems) was used, but in tubes with many primers (>15), 2 U of AmpliTaq Gold were used.

The cycling conditions started with preactivation of the AmpliTaq Gold for 7 min at 95°C. The cycling times of the subsequent 35 amplification cycles were dependent on the PCR equipment (classical equipment vs newer and faster equipment). See Table 4 for details.

### Techniques for the analysis of PCR products obtained from Ig/TCR gene rearrangements

The PCR products obtained from Ig and TCR gene rearrangements have to be analyzed for discrimination between monoclonal lymphoid cells with identical junctional regions and polyclonal lymphoid cells with highly diverse junctional regions.

Based on the combined experience of the participating laboratories, two techniques were selected: heteroduplex analysis and GeneScanning. Heteroduplex analysis uses double-stranded PCR products and takes advantage of the length and composition of the junctional regions, whereas in GeneScanning single-stranded PCR products are separated in a high-resolution gel or polymer according to their length only (Figure 3).

**Heteroduplex analysis of PCR products:** PCR products obtained with *unlabeled* primers are denatured at high temperature (~95°C for 5 min), followed by rapid random renaturation at low temperature (preferably at 4°C for 1 h). This enforced duplex formation results in many different heteroduplexes with different migration speed in case of polyclonal lymphoproliferations, but results in homoduplexes with identical rapid migration in case of monoclonal lymphoproliferations. Electrophoresis of the homoduplexes in a 6% polyacrylamide gel results in a single band within a predictable size range, whereas the heteroduplexes form a smear at a higher position (Figure 3).

The heteroduplex technique is rapid, simple, and cheap (Table 5), and has a detection limit of ~5%.<sup>40,41</sup> The detection limit is influenced by the frequency of polyclonal lymphocytes, because the formation of many heteroduplexes will also consume a part of the monoclonal PCR products.<sup>41</sup> Since heteroduplex analysis separates PCR products on the basis of junctional diversity in addition to PCR product size, it is particularly useful in the analysis of loci with restricted junctional diversity.

**GeneScanning of PCR products:** The PCR primers for GeneScanning need to be labeled with a fluorochrome to allow detection of the PCR products with automated sequencing equipment (Figure 3).

The fluorochrome-labeled single-strand (denatured) PCR products are size separated in a denaturing polyacrylamide

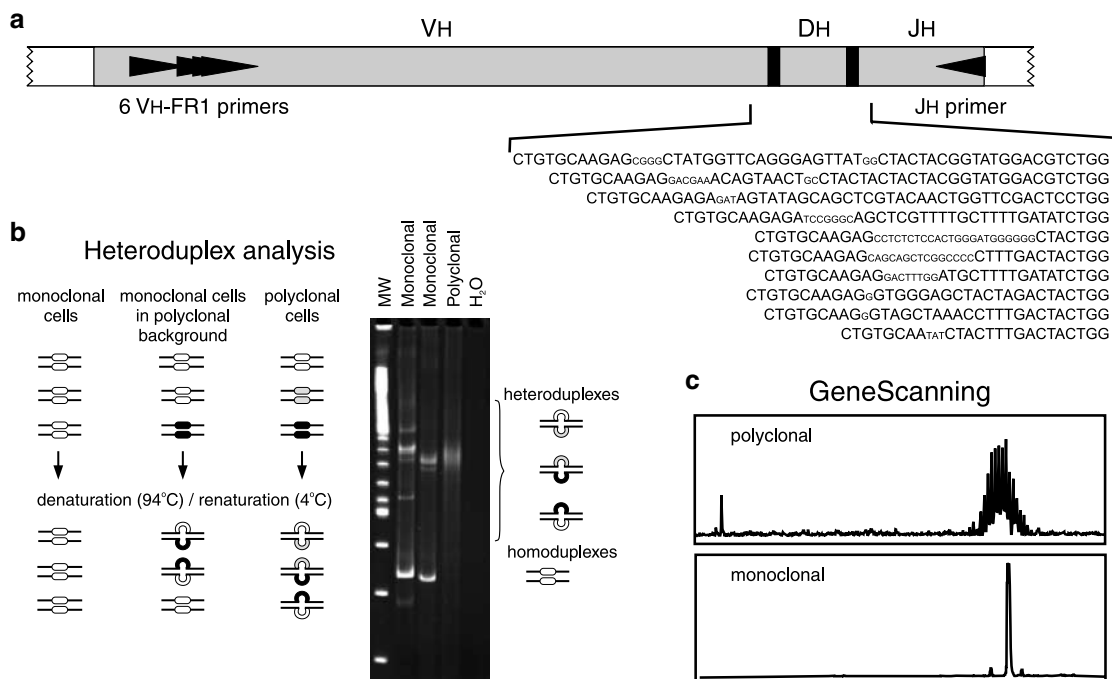


**Figure 3** Schematic diagram of heteroduplex analysis and GeneScanning of PCR products, obtained from rearranged Ig and TCR genes. (a) Rearranged Ig and TCR genes (*IGH* in the example) show heterogeneous junctional regions with respect to size and nucleotide composition. Germline nucleotides of V, D, and J gene segments are given in large capitals and randomly inserted nucleotides in small capitals. The junctional region heterogeneity is employed in heteroduplex analysis (size and composition) and GeneScanning (size only) to discriminate between products derived from monoclonal and polyclonal lymphoid cell populations. (b) In heteroduplex analysis, PCR products are heat denatured (5 min, 94°C) and subsequently rapidly cooled (1 h, 4°C) to induce duplex (homo- or heteroduplex) formation. In cell samples consisting of clonal lymphoid cells, the PCR products of rearranged *IGH* genes give rise to homoduplexes after denaturation and renaturation, whereas in samples that contain polyclonal lymphoid cell populations the single-strand PCR fragments will mainly form heteroduplexes, which result in a background smear of slowly migrating fragments upon electrophoresis. (c) In GeneScanning fluorochrome-labeled PCR products of rearranged *IGH* genes are denatured prior to high-resolution fragment analysis of the resulting single-stranded fragments. Monoclonal cell samples will give rise to PCR products of identical size (single peak), whereas in polyclonal samples many different *IGH* PCR products will be formed, which show a characteristic Gaussian size distribution.



**Table 5** Standardized protocol for heteroduplex analysis of PCR products

*PCR product preparation*

Tube with 10–20  $\mu$ l of PCR product  
Denaturation of PCR product: 5 min at 95°C  
Reannealing of PCR product: 60 min at 4°C

*Electrophoresis conditions (noncommercial polyacrylamide gels)*

Gel: 6% nondenaturing polyacrylamide (acrylamide: bisacrylamide ratio of 29:1)  
Buffer: ratio of 0.5  $\times$  TBE  
Loading buffer: 5  $\mu$ l ice-cold nondenaturing bromophenol blue loading buffer  
Electrophoresis: typically 2–3 h at 110 V or overnight at 40–50 V<sup>a</sup>

*Electrophoresis conditions (commercial polyacrylamide gels)*

Gel: nondenaturing polyacrylamide (eg BioRad PreCast Gel System or Amersham Pharmacia Biotech Gene Gel Excel Kit)  
Buffer: 1  $\times$  TBE  
Loading buffer: ice-cold nondenaturing bromophenol blue loading buffer  
Electrophoresis: 1.5 h at 100 V

*Visualization*

Staining: 5–10 min in 0.5  $\mu$ g/ml EtBr in H<sub>2</sub>O  
Destaining/washing: 2  $\times$  5–10 min in H<sub>2</sub>O  
Visualization: UV illumination  
Alternative: silver staining using Amersham Pharmacia Biotech DNA Silver stain kit

<sup>a</sup>Voltage and electrophoresis time depend on PCR amplicon sizes, thickness of polyacrylamide gel, and type of PCR equipment, and should be adapted accordingly.

sequencing gel or capillary sequencing polymer and detected via automated scanning with a laser (see Table 6 for technical details). This results in a Gaussian distribution of multiple peaks, representing many different PCR products in case of polyclonal lymphoproliferations, but gives a single peak consisting of one type of PCR product in case of a fully monoclonal lymphoproliferation (Figure 3).

GeneScanning is rapid and relatively simple, but needs expensive equipment. GeneScanning is generally more sensitive than heteroduplex analysis and can reach sensitivities of 0.5–1% of clonal lymphoid cells. In addition, the precise determination of the size of the PCR product can potentially be used for global monitoring of the clonal proliferation during follow-up of the patient.

*Development and testing of new primers and multiplex tubes in two phases*

**Phase 1: Development and initial testing of primers:** All PCR primers for the detection of Ig and TCR rearrangements as well as for *BCL1* and *BCL2* rearrangements were newly designed. This concerned a total of 108 primers for the nine selected PCR targets: *IGH* VH–JH, *IGH* DH–JH, *IGK*, *IGL*, *TCRB*, *TCRG*, *TCRD*, *BCL1-IGH*, and *BCL2-IGH*.

Initial testing was performed in nine small Target Networks (one network per target) of three to five experienced laboratories. The new primers were tested in parallel to in-house PCR primer sets, using in-house positive controls (cell lines and patient material) with well-defined rearrangements. The 108 initial primers were tested in single PCR analyses, implying that approximately 425 PCR primer combinations had to be evaluated.

Whenever needed, the primers were redesigned (11% of the primers) and tested again. Finally, the primers were combined into 18–21 multiplex tubes, which appeared to give reproducible results within the small networks. Finally, 107 primers in 18 multiplex tubes were approved.

*Phase 2: General testing on 90 Southern-blot defined DNA samples:*

After approval of the new PCR primers and multiplex tubes, a total of 30 PCR laboratories were involved in the general testing of the multiplex tubes: five to 20 laboratories were performing the general testing of each PCR target. All laboratories used the same DNA samples, extracted from 90 freshly collected or frozen malignant or reactive samples, derived from the seven national networks.

All 90 samples were evaluated for their cytomorphology or histomorphology and for their immunophenotype by the local or national hematologists or pathologists. Difficult cases were also evaluated by the Pathology Review Panel (Figure 2). The 90 selected cases could be clustered as follows:

- eight prefollicular B-cell malignancies: one precursor-B-ALL and seven MCL;
- 16 cases of B-cell chronic lymphocytic leukemia (B-CLL);
- 25 (post)follicular B-cell malignancies, including 11 cases of FCL and 11 cases with diffuse large B-cell lymphoma (DLBCL);
- 18 T-cell malignancies, including several T-ALL and peripheral T-NHL;
- 15 reactive lesions, particularly reactive lymph nodes and tonsils; and
- eight cases of miscellaneous origin, for example, three cases of T-cell-rich B-NHL.

The DNA samples of the General Testing phase were carefully analyzed for their clonality status by Southern blotting of the *IGH*, *IGK*, *IGL*, *TCRB*, *TCRG*, and *TCRD* genes, using the *IGH*J6, *IGK*J5, *IGK*DE, *IGK*C, *IGL*C1D, *IGL*J2, *TCRB*J1, *TCRB*J2, *TCRB*C, *TCRG*J13, *TCRG*J21, and *TCRD*J1 probes in *Eco*RI, *Hind*III, *Bgl*II, *Bam*HI, and *Pst*I digests.<sup>22–28</sup> The probe/enzyme combinations and the preferred successive hybridizations are summarized in Table 7. The Southern blot analyses were performed by eight laboratories and coordinated in Rotterdam by AW Langerak c.s. The results are summarized in Table 8.

In practice, the 90 DNA samples represented a typical broad spectrum of pathology samples with sufficient diversity for the General Testing of the PCR primers and multiplex tubes in the 30 PCR laboratories.

*Control genes and paraffin-embedded tissues*

In several European countries, fresh tissue material is not easily available for molecular diagnostics such as PCR-based clonality studies. Therefore, one of the aims of the BIOMED-2 Concerted Action was to develop a strategy for PCR-based clonality studies in paraffin-embedded tissues.

To control for the quality and amplifiability of DNA from paraffin-embedded material, a special multiplex control gene PCR was developed, resulting in a ladder of five fragments (100, 200, 300, 400, and 600 bp).

From 45 of the aforementioned 90 cases sufficient paraffin-embedded tissue was available for DNA extraction. These DNA samples were tested in parallel to the freshly obtained DNA samples, using the Control Gene multiplex tube as well as the Ig/

**Table 6** Standardized protocol for GeneScanning of PCR products**A. Gel-based sequencers***PCR product preparation*

1. PCR product dilution: initially 1:10 in formamide or H<sub>2</sub>O (can be altered if fluorescent signal is outside optimal range; see electrophoresis conditions)
2. Sample volume: 2  $\mu$ l diluted PCR product
3. Loading buffer volume: 0.5  $\mu$ l blue dextran loading buffer+0.5  $\mu$ l TAMRA internal standard+2  $\mu$ l deionized formamide
4. Denaturation of PCR product: 2 min at 95°C or higher temperature
5. Cooling of PCR product at 4°C

*Electrophoresis conditions*

6. Gel: 5% denaturing polyacrylamide
7. Buffer: 1  $\times$  TBE
8. Electrophoresis: 2–3.5 h<sup>a</sup> (see Table 25)
9. Optimal fluorescent signal intensity:  
600–4000 fluorescent units (373 platforms)  
400–7000 fluorescent units (377 platforms)

**B. Capillary sequencers (to be optimized per sequencer)***PCR product preparation*

1. 1  $\mu$ l PCR product (volume of PCR product or sampling times can be altered if fluorescent signal is outside optimal range; see electrophoresis conditions)
2. Sample volume: 1  $\mu$ l PCR product+9.5  $\mu$ l (Hi-Di) formamide+0.5  $\mu$ l ROX-400 heteroduplex analysis internal standard
3. Denaturation of PCR product: 2 min at 95°C or higher temperature
4. Cooling of PCR product at 4°C for an hour

*Electrophoresis conditions*

5. Polymer: e.g. 3100 POP4 polymer
6. Buffer: e.g. 1  $\times$  3100 buffer with EDTA
7. Electrophoresis: 45 min<sup>b</sup>
8. Optimal fluorescent signal intensity:  
Up to 10000 fluorescent units

<sup>a</sup>Electrophoresis time depends on amplicon sizes and on employed platform.

<sup>b</sup>For 36 cm capillary; time taken depends on the capillary used.

TCR/*BCL1*/*BCL2* multiplex tubes for clonality diagnostics (see Section 10).

*Presentation of the results per PCR target*

The coordination of the Initial Testing and General Testing of the PCR primers for each PCR target was coordinated by the following Target Network Leaders: *IGH* (V–J), M Hummel (Berlin, Germany) and R Garcia Sanz (Salamanca, Spain); *IGH* (D–J), AW Langerak (Rotterdam, Netherlands); *IGK*, AW Langerak; *IGL*, F Davi (Paris, France); *TCRB*, M Brüggemann (Kiel, Germany); *TCRG*, EA Macintyre (Paris, France); *TCRD*, FL Lavender (Southampton, UK); *BCL1-IGH*, E Schuurin (Groningen, Netherlands); *BCL2-IGH*, PAS Evans (Leeds, UK); and control genes, HE White (Southampton, UK).

The results of these 10 Target Networks are described in 10 sections, followed by a General Discussion.

**SECTION 1. Complete *IGH* gene rearrangements: VH–JH**

M Hummel<sup>1</sup>, R García-Sanz<sup>2</sup>, D González<sup>2</sup>, A Balanzategui<sup>2</sup>, PAS Evans<sup>3</sup>, F Davi<sup>4</sup>, E Delabesse<sup>5</sup>, E Schuurin<sup>6,7</sup>, M Spaargaren<sup>8</sup>, GI Carter<sup>9</sup>, M Brüggemann<sup>10</sup>, P Algara<sup>11</sup>, A Jack<sup>12</sup>, L Trümper<sup>13</sup> and TJ Molina<sup>14</sup>

<sup>1</sup>Institute of Pathology, Free University Berlin, Germany; <sup>2</sup>Servicio de Hematología, Hospital Universitario de Salamanca, Spain; <sup>3</sup>Academic Unit of Haematology and Oncology, University of Leeds, Leeds, UK; <sup>4</sup>Department of Hematology, Hôpital Pitié-Salpêtrière, Paris, France; <sup>5</sup>Laboratoire d'Hématologie and INSERM EMI 210, Hôpital Necker-Enfants Malades, Paris, France; <sup>6</sup>Department of Pathology, Leiden University Medical Center, The Netherlands; <sup>7</sup>Department of Pathology and Laboratory Medicine, University Medical Center Groningen, The Netherlands; <sup>8</sup>Department of Pathology, Academic Medical Center, Amsterdam, The Netherlands; <sup>9</sup>Department of

**Table 7** Southern blot hybridization scheme for consecutive Ig/TCR probe hybridizations per digest<sup>a</sup>

Restriction enzyme	1st hybridization	2 <sup>nd</sup> hybridization	3rd hybridization	4th hybridization	5th hybridization	Additional hybridization round (optional)
<i>EcoRI</i>	TCRBJ2	TCRBJ1	TCRGJ13	TCRDJ1		(TCRBC)
<i>HindIII</i>	TCRBJ2	TCRBJ1	TCRDJ1	IGLC1D		
<i>BglII</i>	IGHJ6	IGKJ5	IGKDE	IGLC1D	IGLJ2	(IGKC)
<i>BamHI/HindIII</i>	IGHJ6	IGKJ5	IGKDE			
<i>PstI</i>	TCRGJ21					

<sup>a</sup>See Beishuizen *et al*,<sup>22,24</sup> Breit *et al*,<sup>23</sup> Tümkaya *et al*,<sup>25,26</sup> Moreau *et al*,<sup>27</sup> and Langerak *et al*<sup>28</sup> for detailed information about preferred restriction enzyme digest and position of probe per locus.

**Table 8** Summary of Southern blot results of the 90 WP1 cases

Sample	Category <sup>a</sup>	Diagnosis <sup>b</sup>	Tumor load (%) <sup>c</sup>	IGH <sup>d</sup>	IGK <sup>d</sup>	IGL <sup>d</sup>	TCRB <sup>d</sup>	TCRG <sup>d</sup>	TCRD <sup>d</sup>
<i>B-cell malignancies – pregerminal center</i>									
1-DE-9	A	Common ALL	> 50	R/R	R/R	R/R	R/G	ND	D/D
2-NL-15	A	MCL		R/R	R/G		R/R		
3-NL-16	A	MCL		R/R	R/R		R/G		
4-ES-4	A	MCL	> 50	R/R	R/R	R/G			
5-PT-10	A	MCL	> 50	R/R	R/G				
6-GBS-1	A	MCL	> 50	R/R	R/R	R/G			
7-GBS-17	A	MCL	> 50	R/R	R/R	R/G	R/R		
8-FR-4	A	MCL	> 50	R/R	R/R				
<i>B-cell malignancies – B-CLL</i>									
9-NL-10	A	B-CLL		R/R	R/R	D/R			
10-NL-11	A	B-CLL	> 50	R/R	R/G				R/G
11-NL-19	A	B-CLL	> 50	R/R	R/R		R/G		
12-ES-1	A	B-CLL	> 50	R/R	R/G				
13-ES-2	A	B-CLL	> 50	R/R	R/G				
14-ES-3	A	B-CLL	> 50	R/R	R/G				
15-GBS-2	A	B-CLL	> 50	R/R	R/R	R/G			
16-GBS-3	A	B-CLL		R/R	R/R	R/G			R/G
17-GBS-14	A	B-CLL	> 50	R/R	R/R				
18-GBN-10	A	B-CLL	> 50	R/G	R/R	R			
19-GBN-11	A	B-CLL	> 50	R/R	R/G				
20-DE-6	A	B-CLL	> 50	R/R	R/R	R/G			
21-DE-7	A	B-CLL	> 50	R/R	R/R				
22-FR-1	A	B-CLL	> 50	R/R	R/G				
23-FR-2	A	B-CLL	> 50	D/R	R/G				
24-FR-3	A	B-CLL	> 50	R/R	R/G				
<i>B-cell malignancies – (post)germinal center</i>									
25-NL-4	A	FCL		RwRw/G					
26-NL-5	A	FCL	> 50	R/R	R/G				
27-NL-13	A	FCL		Rw/Rw/G	R/G	Rw/G			
28-ES-7	A	FCL	> 50	R/R	R/R				
29-PT-7	A	FCL	> 50	R/R	R/G				
30-PT-8	A	FCL	15–50	Rw/Rw	Rw/Rw		R/G		
31-GBS-6	A	FCL		R/G	R/R	R/G		R/G	
32-GBS-7	A	FCL	< 15	Rw/Rw/Rww/ Rww/G	Rw/Rw/G	Rw/Rw			
33-GBN-3	A	FCL	> 50	R/R	R/G				
34-FR-5	A	FCL	> 50	R/R	R/R	Rw/G			
35-FR-8	A	FCL	> 50	R/R/Rw	R/Rw	R/G			
36-NL-6	A	DLBCL	> 50	R/R	R/R				
37-ES-5	A	DLBCL	> 50	D/R	R/G				
38-ES-6	A	DLBCL		R/R	R/G				
39-PT-11	A	DLBCL	> 50	R/R	R/G				
40-PT-13	A	DLBCL	> 50	R/G	R/G				
41-PT-14	A	DLBCL	> 50	R/R	R/R				
42-GBS-4	A	DLBCL	> 50	R/R	R/G				
43-GBS-16	A	DLBCL	> 50	R/G	R/R				
44-GBN-2	A	DLBCL	15–50	Rw/G	Rw/Rw/G		Rw/Rw		
45-GBN-4	A	DLBCL	> 50	R/R	R/R				
46-FR-6	A	DLBCL	> 50	R/R	R/R		R/R		
47-FR-7	A	DLBCL	> 50	R/R	R/R		R/R		
48-ES-8	A	MM	15–50	Rw/G	Rw/G				
49-NL-12	A	PC leukemia	> 50	R/R	R/R				
<i>T-cell malignancies</i>									
50-ES-9	B	T-LBL	> 50	R/G			R/R	R/R	D/R or Rr
51-DE-1	B	T-ALL/T-LBL	> 50				R/R	Rr	
52-DE-10	B	T-ALL	> 50				R/R	R/G	R/R
53-FR-12	B	T-ALL	> 50					R/G	R/R
54-GBS-15	B	T-PLL	> 50				R/R	R/G	
55-NL-17	B	MF	> 50	R/G			R/R	R/R	
56-ES-10	B	SS	< 15				Rww/ Rww		
57-NL-2	B	AILT-NHL					Rww/G	Rww/G	
58-PT-3	B	PTCL	> 50				Rw/Rw	Rw/G	
59-PT-5	B	PTCL	15–50				Rw/Rw	Rw/Rw	
60-GBN-1	B	PTCL	> 50				R/G		D/G
61-GBN-5	B	PTCL	> 50				R/R	R/G	D/G

**Table 8** Continued

Sample	Category <sup>a</sup>	Diagnosis <sup>b</sup>	Tumor load (%) <sup>c</sup>	IGH <sup>d</sup>	IGK <sup>d</sup>	IGL <sup>d</sup>	TCRB <sup>d</sup>	TCRG <sup>d</sup>	TCRD <sup>d</sup>
62-FR-9	B	PTCL	15–50				Rww/G	Rww/G	
63-FR-10	B	PTCL	> 50				R/R	R/R	D/D
64-NL-18	B	PTCL	15–50				Rw/G	Rw/G	
65-PT-4	B	EATL	< 15				Rw/G	Rw/G	
66-NL-3	B	ALCL	> 50				R/R	R/G	
67-NL-1	B	T-LGL	< 15				Rww/ Rww	Rww/ Rww	
<i>Reactive lesions</i>									
68-ES-14	C	Normal PB	NA						
69-PT-2	C	Normal PB	NA						
70-FR-14	C	Normal PB	NA						
71-NL-7	C	Reactive tonsil	NA						
72-NL-8	C	Reactive tonsil	NA						
73-NL-14	C	Reactive tonsil	NA						
74-ES-11	C	Reactive tonsil	NA						
75-ES-13	C	Reactive tonsil	NA						
76-GBS-11	C	Reactive tonsil	NA						
77-GBS-12	C	Reactive tonsil	NA						
78-GBS-13	C	Reactive tonsil	NA						
79-PT-1	C	Reactive LN	NA						
80-GBN-7	C	Reactive LN	NA						
81-GBN-9	C	Reactive LN	NA						
82-DE-5	C	Reactive LN	NA						
<i>Miscellaneous</i>									
83-PT-9	D	MZL (splenic)	> 50				Rw/G	Rw/G	
84-PT-12	D	DLBCL	> 50	Rw/Rw/G					
85-PT-6	D	T-cell-rich B-NHL	15–50	Oligo	Oligo		Rw/Rw		
86-DE-2	D	T-cell-rich B-NHL	< 5						
87-GBS-9	D	T-cell-rich B-NHL	< 5						
88-GBS-10	D	T-LBL ?	> 50	R/G	R/R				R/G
89-GBN-8	D	Hypocellular-regenerating BM	> 50	R/R	R/R		R/G		
90-ES-12	D	Hodgkin's disease and few B cells	NA						

<sup>a</sup>Four categories of WP1 cases were identified: A, clonal B-cell malignancies (pregerminal center, B-CLL, germinal center/postgerminal center); B, clonal T-cell malignancies; C, reactive lesions without clonal Ig/TCR gene rearrangements; D, miscellaneous, that is, cases that were difficult to classify in any of the other categories and/or showing unexpected Ig/TCR gene results.

<sup>b</sup>*Diagnosis*: ALL, acute lymphoblastic leukemia; MCL, mantle cell lymphoma; B-CLL, B-cell chronic lymphocytic leukemia; FCL, follicular center cell lymphoma; DLBCL, diffuse large B-cell lymphoma; MM, multiple myeloma; PC leukemia, plasma cell leukemia; T-LBL, T-cell lymphoblastic lymphoma; T-ALL, T-cell acute lymphoblastic leukemia; T-PLL, T-cell prolymphocytic leukemia; MF, mycosis fungoides; SS, Sézary syndrome; AIT-NHL, angioimmunoblastic T-cell lymphoma; PTCL, peripheral T-cell lymphoma; EATL, enteropathy type T-cell lymphoma; ALCL, anaplastic large-cell lymphoma; T-LGL, T-cell large granular lymphocyte leukemia; MZL, marginal zone lymphoma.

<sup>c</sup>*Tumor load*: In most cases at least 50% tumor cells were present; in some cases 15 to 50%, and in six cases < 15%. Finally, in nine cases the tumor load could not be estimated.

<sup>d</sup>Rearrangement patterns of *IGH*, *IGK*, *IGL*, *TCRB*, *TCRG* and *TCRD* genes: R, rearranged allele; D, deleted allele; G, germline allele; ND, not determined; Rw, weak rearranged band; Rww, very weak rearranged band; Rr, two comigrating rearranged bands.

NA = not applicable.

*Molecular Diagnostics and Histopathology, Nottingham City Hospital, UK;* <sup>10</sup>*II Medizinische Klinik des Universitätsklinikums Schleswig-Holstein, Campus Kiel, Germany;* <sup>11</sup>*Unidad de Genética, Hospital Virgen de la Salud, Toledo, Spain;* <sup>12</sup>*Department of Molecular Haematology, Leeds General Hospital, Leeds, UK;* <sup>13</sup>*Department of Internal Medicine, Georg August Universität, Göttingen, Germany;* and <sup>14</sup>*Department of Pathology, Hotel-Dieu de Paris, France*

## Background

The functional rearrangement of the *IGH* gene, first DH to JH and subsequently V to DH–JH, is followed by antibody expression, the hallmark of mature B cells. The *IGH* gene is located on chromosome 14q32.3 in an area covering approxi-

mately 1250 kb. In all, 46–52 functional VH segments (depending on the individual haplotype) have been identified, which can be grouped according to their homology in six or seven VH subgroups. In addition, approximately 30 nonfunctional VH segments have been described. Furthermore, 27 functional DH segments and six functional JH segments have been consistently found (Table 2 and Figure 4a).<sup>44</sup> The most frequently used VH gene segments in normal and malignant B cells belong to the VH3 family (30–50%), VH4 family (20–30%), and VH1 family (10–20%), together covering 75–95% of VH usage (Table 9).<sup>45–47</sup> However, in precursor B-ALL also VH6 gene segments are used relatively frequent.<sup>48</sup>

The VH segments contain three framework (FR) and two complementarity-determining regions (CDRs) (Figure 4b). The FRs are characterized by their similarity among the various VH segments, whereas the CDRs are highly different even within the

same VH family. Furthermore, the CDRs represent the preferred target sequences for somatic hypermutations in the course of the germinal center reaction, which increase the variability within those regions. Although the FRs are usually less affected by somatic mutations, nucleotide substitutions may also occur within these regions, especially in B cells under a heavy mutational process.

The highly variable V–D–JH regions can be amplified by PCR to detect clonal B-cell populations indicative of the presence of a malignant B-cell disorder. Clonal B cells can be discriminated from polyclonal B cells (ie normal or reactive lymphoid tissues) based on the identical size and composition of the clonal PCR products as compared to the many different polyclonal PCR products with a size range of approximately 60 bp, arranged in a Gaussian distribution. PCR-based strategies for the detection of clonal B-cell populations in histological sections and cell suspensions have already been established in the early 1990s. However, the initial PCR protocols used single VH consensus primers, which were able to bind to one of the three FR regions, mainly FR3. Such consensus primers were not suitable to amplify all VH segments with the same efficiency leading to nondetectability of a significant number of clonal rearrangements. In addition, somatic mutations introduced in the course of the germinal center reaction are not restricted to the CDRs, but can also occur in FRs, thereby preventing primer annealing and consequently leading to the absence of clonal PCR products despite the presence of a neoplastic B-cell population. This is especially true for FCLs, diffuse large B-cell lymphomas, and multiple myelomas, which usually contain high numbers of somatic mutations.

To further increase the detection rate of the *IGH* PCR, several attempts have been made to design family-specific primers to overcome the limitations of consensus primers. However, these family-specific primers are largely based on the sequences of the previous consensus primers. Although these PCR strategies have helped to improve the detection rate, there is still a need of primer systems, which are less sensitive to somatic hypermutations, thus allowing the amplification of (virtually) all possible V–D–JH rearrangements.

### Primer design

According to the BIOMED-2 guidelines, three sets of VH primers were designed with the help of the OLIGO 6.2 program corresponding to the three VH FR regions (FR1, FR2, and FR3) (Figure 4b). Each set of primers consisted of six or seven oligonucleotides capable of annealing to their corresponding VH segments (VH1–VH7) with no mismatches for most VH segments and one or at most two mismatches for some rare VH segments. The design was such that mismatches would be located at the very 5′-end of the primer. These VH primer sets were used in conjunction with a single JH consensus primer, designed to anneal to the most homologous 3′-end of the six JH segments, approximately 35 bp downstream of the JH RSS. This ensures that all JH segments are detectable with the same binding efficiency and that the primer binding will not easily be affected by extensive nucleotide deletion in the course of the rearrangement process. In addition, there was no crossannealing between the VH primers and the JH primer as evaluated by the OLIGO 6.2 program.

The JH primer was also designed to be used for the amplification of other PCR targets, such as incomplete DH–JH rearrangements as well as t(11;14) (*BCL1-IGH*) and t(14;18) (*BCL2-IGH*). This allows the detection of different PCR products by GeneScanning employing the same labeled JH primer.

### Results of initial testing phase

The initial testing of the newly designed VH–JH PCR was carried out by separate application of each VH primer together with the JH primer in an individual PCR. For this purpose, DNA extracted from B-cell lines and well-defined clonal patient samples were used. Furthermore, clonal rearrangements were tested for sensitivity by serial dilution in DNA extracted from reactive tonsils. Clonal control samples were not available for each possible *IGH* rearrangement, but all major VH segments and several rarely rearranged VH segments have been included in the initial testing phase.

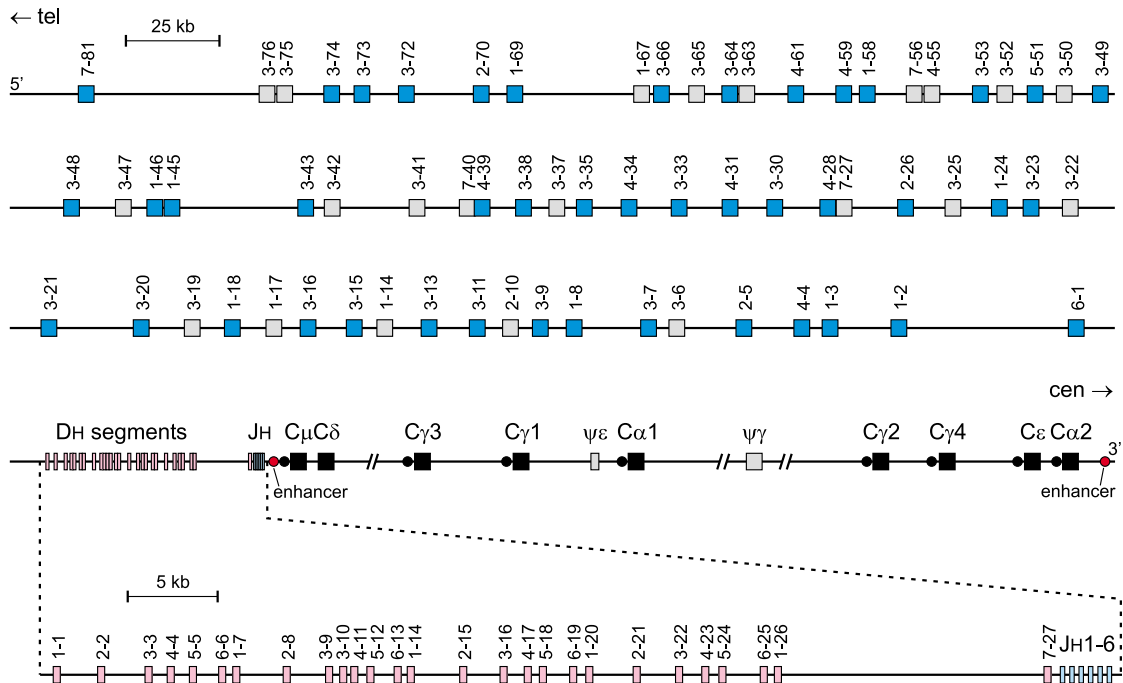
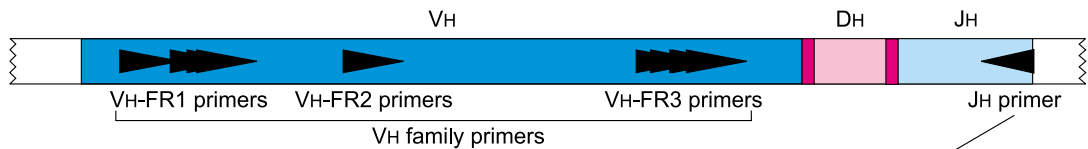
All primer pairs worked with high efficiency and sensitivity. The expected clonal VH rearrangements were detectable and the sensitivity was at least 1% ( $10^{-2}$ ). There was no background within the expected size range and the amplification of tonsillar DNA gave the expected Gaussian distribution curve (Figure 4c–e).

Based on these results, we started the next phase of the initial primer testing by combining the VH primers into three sets, each specific for one of the three FR regions, which were used together with the common JH primer (Figure 4b). The results were the same as those obtained with single primer pairs, but with a slightly lower sensitivity. In addition, no nonspecific products were amplified within the expected size range, with the exception of a 340 bp PCR product, which appeared in the FR1 multiplex PCR. This PCR product was generated irrespective of the source of the DNA (lymphoid and nonlymphoid) used for PCR, whereas no PCR product was obtained when no DNA template was applied. Furthermore, this amplicon was only detectable in heteroduplex analysis, not in GeneScanning. This indicates that the fluorescent-labeled JH primer was not involved in the generation of this PCR product. Sequence analysis of this PCR product disclosed a VH4 fragment amplified by the FR1 VH4 primer in conjunction with the FR1 VH2 primer, which apparently acted as a downstream primer by binding to the intronic VH4 sequence. This problem was solved by designing a new FR1 VH2 primer that was located 25 bp upstream to the previous primer binding site.

### Results of general testing phase

The approved *IGH* PCR was applied to the 90 Southern blot-defined DNA samples, which were derived from well-characterized cases. Six of the 11 laboratories involved in the general testing phase performed GeneScanning of the PCR products and five performed heteroduplex analysis. In addition, several polyclonal as well as monoclonal samples (cell line DNA) were included as controls; 45 of these cases displayed dominant PCR products after GeneScanning and 40 cases after heteroduplex analysis, indicating the presence of a monoclonal B-cell population. The clonal rearrangements were detectable with all three FR primer sets in 33 of the 45 clonal cases (GeneScanning), and in the remaining 12 with one or two of the three FR primer sets. It was concluded that most negative results were caused by somatic hypermutations in the primer binding site, preventing primer annealing and thus amplification.

The comparison of the VH–JH PCR results with the Southern blot results revealed a high degree of concordance: 85% (46 out of 55) and 76% (42 out of 55) of the samples with rearranged JH genes by Southern blot analysis showed a dominant amplification product by GeneScanning and heteroduplex analysis, respectively. In contrast, all but two samples harboring germline

**a** *IGH* gene complex (#14q32.3)**b****IGH tube A**

5' 3'

VH1-FR1 (1-2) (-252) GGCCTCAGTGAAGGTCTCCTGCAAG  
 VH2-FR1 (2-5) (-284) GTCTGGTCTACGCTGGTGAACCC  
 VH3-FR1 (3-7) (-256) CTGGGGGGTCCCTGAGACTCTCCTG  
 VH4-FR1 (4-4) (-256) CTTGGGAGACCCTGTCCCTCACCTG  
 VH5-FR1 (5-51) (-255) CGGGGAGTCTCTGAAGATCTCCTGT  
 VH6-FR1 (6-1) (-263) TCGCAGACCCTCTCACTCACCTGTG

**IGH tube B**

VH1-FR2 (1-2) (-192) CTGGGTGCGACAGGCCCTGGACAA  
 VH2-FR2 (2-5) (-190) TGGATCCGTGACCCCCAGGGAAGG  
 VH3-FR2 (3-7) (-189) GGTCCGCCAGGCTCCAGGGAA  
 VH4-FR2 (4-4) (-188) TGGATCCGCCAGCCCCAGGGAAGG  
 VH5-FR2 (5-51) (-190) GGGTGCGCCAGATGCCCGGGAAGG  
 VH6-FR2 (6-1) (-194) TGGATCAGGCAGTCCCCATCGAGAG  
 VH7-FR2 (7) (-192) TTGGGTGCGACAGGCCCTGGACAA

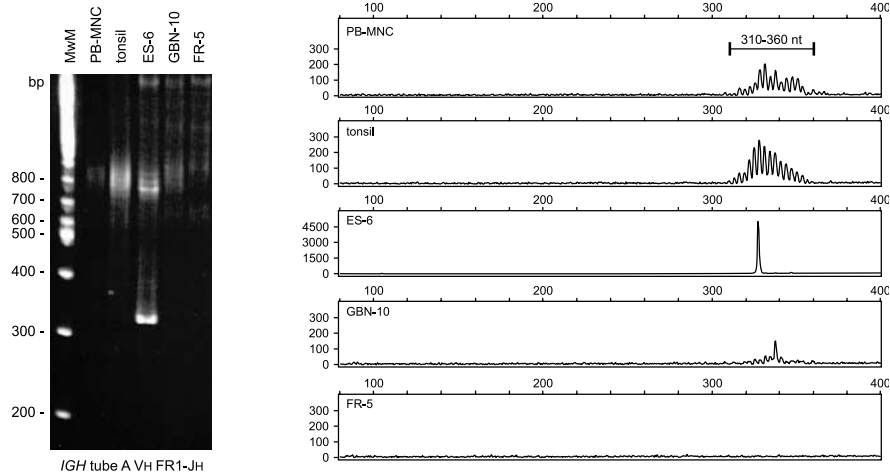
**IGH tube C**

VH1-FR3 (1-2) (-55) TGGAGCTGAGCAGCCTGAGATCTGA  
 VH2-FR3 (2-5) (-54) CAATGACCAACATGGACCCTGTGGA  
 VH3-FR3 (3-7) (-57) TCTGCAAATGAACAGCCTGAGAGCC  
 VH4-FR3 (4-4) (-48) GAGCTCTGTGACCGCCGCGGACACG  
 VH5-FR3 (5-51) (-69) CAGCACCGCCTACCTGCAGTGGAGC  
 VH6-FR3 (6-1) (-63) GTTCTCCCTGCAGCTGAACCTGTG  
 VH7-FR3 (7) (-69) CAGCACGGCATATCTGCAGATCAG

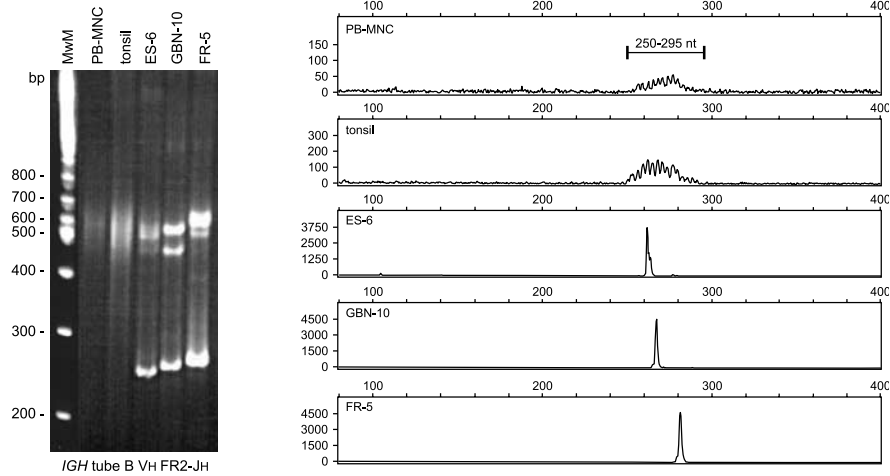
3' 5' IGH tubes A, B, and C  
 CCAGTGGCAGAGGAGTCCATTC (+57) JH consensus

**Figure 4** PCR analysis of *IGH* (VH–JH) rearrangements. (a) Schematic diagram of *IGH* gene complex on chromosome band 14q32.3 (adapted from ImMunoGeneTics database).<sup>62,63</sup> Only rearrangeable nonpolymorphic VH gene segments are included in blue (functional VH) or in gray (rearrangeable pseudogenes). Recently discovered (generally truncated) VH pseudogenes are not indicated. (b) Schematic diagram of *IGH* VH–JH rearrangement with three sets of VH primers and one JH consensus primer, combined in three multiplex tubes. The relative position of the VH and JH primers is given according to their most 5' nucleotide upstream (–) or downstream (+) of the involved RSS. The VH gene segment used as a representative VH family member for primer design is indicated in parentheses. (c, d, and e) Heteroduplex analysis and GeneScanning of the same polyclonal and monoclonal cell populations, showing the typical heteroduplex smears and homoduplex bands (left panels) and the typical polyclonal Gaussian curves and monoclonal peaks (right panels). The approximate distribution of the polyclonal Gaussian curves is indicated in nt.

**c. *IGH* tube A Vh FR1-Jh**



**d. *IGH* tube B Vh FR2-Jh**



**e. *IGH* tube C Vh FR3-Jh**

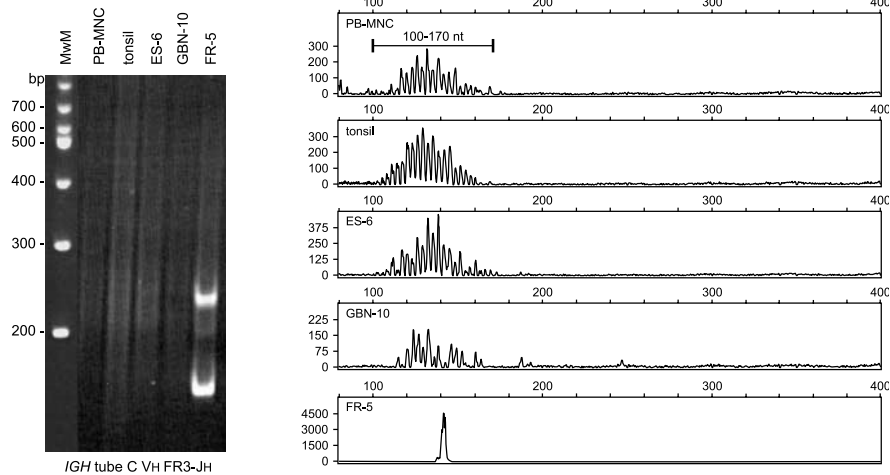


**Figure 4** Continued.

JH genes by Southern blot displayed a polyclonal pattern by GeneScanning and heteroduplex analysis.

There are a few exceptional cases with rearranged JH genes by Southern blot analysis, but without clonality by VH-JH PCR

and vice versa. The detailed evaluation of these cases demonstrate that all but three samples showing *IGH* clonality in Southern blot concerned FCLs or diffuse large B-cell lymphomas that are known to harbor many somatic mutations

**Table 9** VH family usage in normal and malignant B cells

VH family	Normal B cells <sup>a</sup>		Malignant B cells						Clonal controls
	BM (%)	PB (%)	Precursor-B-ALL <sup>a</sup>		MCL (%) <sup>b</sup>	B-CLL (%) <sup>c</sup>	B-NHL (%) <sup>d</sup>	MM (%) <sup>e</sup>	
			Adult (%)	Childhood (%)					
VH1/VH7	14	12	20	14	20	28	17	18	EHEB
VH2	5	7	5	11	2	11	4	6	Patient
VH3	52	40	36	43	46	30	47	47	DAUDI
VH4	24	30	19	17	29	10	20	19	Granta-519
VH5	4	8	3	4	3	13	8	8	L428
VH6	1	5	17	11	0	2	2	1	Patient

<sup>a</sup>Mortuza *et al.*<sup>48</sup><sup>b</sup>Camacho *et al.*<sup>45</sup><sup>c</sup>Pritsch *et al.*<sup>46</sup><sup>d</sup>Hummel and co-workers (unpublished results from many hundreds of B-NHL cases).<sup>e</sup>Rettig *et al.*<sup>47</sup>

in most cases. In two cases without monoclonally rearranged JH genes by Southern blotting, the PCR clonality was embedded in a strong polyclonal background, indicating the presence of many reactive B cells in these samples. Therefore, the Southern blot technique was probably not sensitive enough to detect the weak clonal rearrangement.

## Conclusion

In conclusion, the three multiplex PCRs for the detection of clonal VH–JH rearrangements designed in the context of the BIOMED-2 Concerted Action provide a new and reliable assay to identify clonal B-cell proliferations. The combined use of standardized primers in the three different FRs helps to decrease significantly the rate of false-negative results due to somatic hypermutation in primer binding sites of the involved VH gene segments.

## SECTION 2. Incomplete IGH gene rearrangements: DH–JH

AW Langerak<sup>1</sup>, E Moreau<sup>2</sup>, T Szczepanski<sup>1</sup>, MECM Oud<sup>1</sup>, FM Raaphorst<sup>3</sup>, PJTA Groenen<sup>4</sup>, D González<sup>5</sup>, C Sambade<sup>6</sup>, KI Mills<sup>7</sup>, GI Carter<sup>8</sup>, M Brüggemann<sup>9</sup>, K Beldjord<sup>10</sup>, EA Macintyre<sup>10</sup>, L Bassegio<sup>11</sup>, JF Garcia<sup>12</sup> and JJM van Dongen<sup>1</sup>

<sup>1</sup>Department of Immunology, Erasmus MC, University Medical Center Rotterdam, The Netherlands; <sup>2</sup>Laboratory of Clinical Biology, H Hartziekenhuis, Roeselare, Belgium; <sup>3</sup>Department of Pathology, Free University Medical Center, Amsterdam, The Netherlands; <sup>4</sup>Department of Pathology, University Medical Center Nijmegen, The Netherlands; <sup>5</sup>Servicio de Hematología, Hospital Universitario de Salamanca, Spain; <sup>6</sup>Department of Pathology, Medical Faculty of Porto and IPATIMUP (Institute of Molecular Pathology and Immunology of the University of Porto), Porto, Portugal; <sup>7</sup>Department of Haematology, University of Wales College of Medicine, Cardiff, UK; <sup>8</sup>Department of Molecular Diagnostics and Histopathology, Nottingham City Hospital, UK; <sup>9</sup>II Medizinische Klinik des Universitätsklinikums Schleswig-Holstein, Campus Kiel, Germany; <sup>10</sup>Laboratoire d'Hématologie and INSERM EMI 210, Hôpital Necker-Enfants Malades, Paris, France; <sup>11</sup>Department of Hematology, Centre

Hospitalier Lyon-Sud, Pierre-Benite, France; and <sup>12</sup>Department of Pathology, Centro Nacional de Investigaciones Oncológicas, Madrid, Spain

## Background

The formation of complete V–D–J rearrangements in the *IGH* locus on chromosome 14q32.3 is a sequential process that occurs in two steps: VH coupling is generally preceded by an initial rearrangement between DH and JH gene segments in early precursor-B cells (reviewed by Ghia *et al.*<sup>49</sup>). In addition to the many distinct VH gene segments and the six functional JH gene segments (see Section 1), the human *IGH* locus also contains 27 DH gene segments.<sup>50</sup> Based on sequence homology, the 27 DH segments can be grouped into seven families: DH1 (formerly known as DM), DH2 (DLR), DH3 (DXP), DH4 (DA), DH5 (DK), DH6 (DN), and DH7 (DQ52); all families comprise at least four members, except for the seventh that consists of the single DH7–27 segment just upstream of the JH region (Figure 4a).<sup>50,51</sup>

Recombination between any of the DH and JH segments will result in the formation of incomplete DH–JH joints, which can easily be detected in BM-derived CD10<sup>+</sup>/CD19<sup>+</sup> precursor B cells,<sup>52,53</sup> and hence also in a subset (20–25%) of precursor B-cell ALLs, which show an immature genotype.<sup>54</sup> Sequencing revealed a predominance of DH2 (DH2–2), DH3 (DH3–9), and DH7–27 gene segments in precursor B-ALL, comprising 36, 33, and 19% of all identified segments, respectively.<sup>54</sup>

However, also in mature B-cell malignancies incomplete DH–JH rearrangements have been reported.<sup>53,55</sup> Moreover, even in a subset of IgH-negative multiple myelomas, which can be considered as the most mature type of B-lineage malignancy, DH–JH joints were observed.<sup>56</sup> These DH–JH rearrangements were derived from the noncoding second allele and involved segments from DH1 to DH4 families.<sup>56</sup> Based on the description of DH–JH joints in precursor B-ALL and multiple myelomas, it is assumed that incomplete DH–JH rearrangements are also present in other types of B-cell leukemias and lymphomas. In immature T-cell malignancies, DH–JH couplings have been identified as crosslineage rearrangements,<sup>34</sup> interestingly, these almost exclusively occurred in the more immature non-TCRαβ<sup>+</sup> T-ALL subset and mainly involved the more downstream DH6–19 and DH7–27 segments. The latter segment is frequently (up to 40%) used in fetal B cells but rarely in adult B cells.<sup>57,58</sup>



Human adult precursor and mature B cells mainly seem to use DH2 and DH3 family segments, as evidenced from sequences of complete VH–DH–JH rearrangements.<sup>58</sup>

Although the exact frequencies of incomplete DH–JH couplings in different types of mature B-cell malignancies are largely unknown, it is clear that they will at least be lower than those of VH–JH joinings. Nevertheless, DH–JH rearrangements might still represent an important complementary target for PCR-based clonality assessment. This presumed contribution of DH–JH rearrangements as PCR target is based on the assumption that incomplete rearrangements in the *IGH* locus will not contain somatic hypermutations, because transcription starting from the promoters in the V gene segments does not occur, which is regarded as an essential prerequisite for somatic hypermutation to take place.<sup>59,60</sup> Especially in those types of B-lineage proliferations in which somatic hypermutations are frequent, PCR analysis of a possible DH–JH recombination product might therefore be relevant, and sometimes even the only possibility to detect the B-cell clone.

### Primer design

Based on the high degree of homology within each DH family, seven family-specific DH primers were designed (Figure 5a) in combination with the consensus JH primer that is also used for the detection of VH–JH rearrangements (see Section 1) and t(11;14) (*BCL1-IGH*) and t(14;18) (*BCL2-IGH*) (Sections 8 and 9). Primers were designed such that crossannealing to other DH family segments would be minimal or preferably absent, resulting in distinct positions for the various family primers relative to the RSS elements (Figure 5a). The expected PCR product sizes of DH–JH joints range from 100–130 bp (for DH7–JH joinings) to 390–420 bp (for DH3–JH rearrangements) (see Table 10 for expected size ranges). Of note, due to the position of the DH7–27 segment close to the segments in the JH region, PCR products of 211 bp (and also 419, 1031, 1404, 1804, and 2420 bp in case of primer annealing to downstream JH gene segments) will be amplified from nonrearranged alleles and will be detected as a ladder of germline bands in virtually every sample.

### Results of initial testing phase

For initial testing of the individual DH primers, high tumor load precursor B-ALL or T-ALL samples with well-defined clonal DH–JH rearrangements were used. Under standard PCR conditions using 1.5 mM MgCl<sub>2</sub> and ABI Gold Buffer, all seven primer combinations appeared to detect the clonal DH–JH targets with product lengths within the expected size ranges. Crossannealing of the DH primers to rearranged gene segments from other DH families was only very weak or not observed at all. Furthermore, also in healthy control tonsillar or MNC DNA PCR products of the correct size ranges were observed. Nonspecific annealing of the primers was not observed for virtually all primers sets, using nontemplate-specific control DNA; only in case of the DH2/JH primer set, a (sometimes faint) 340–350 bp product was observed in HeLa DNA. Further sequencing revealed that this nonspecific product was due to false priming of the DH2 primer to a DNA sequence upstream of the JH4 segment. However, as the size of this nonspecific product was so different from the sizes of any of the true DH–JH PCR products, it was decided not to design a new DH2 primer. In fact, the nonspecific 350 bp band can be employed as an internal marker for successful DNA amplification and hence the quality of the template DNA, being

hardly or only faintly visible when enough clonal or polyclonal DH–JH template is available (eg in tonsillar DNA or DNA from particular leukemic samples), but being especially strong in samples containing low numbers of lymphoid cells with DH–JH rearrangements.

Serial dilutions of DNA from the clonal reference samples into tonsillar DNA generally resulted in sensitivities of 5% or lower (0.5–1% in case of the DH6–JH rearrangement) using heteroduplex analysis; sensitivities in GeneScanning were generally 1–2 dilution steps better, that is, 1% or lower. The clonal DH7–JH target could only be detected with a sensitivity of ~10%, which is most probably caused by primer consumption in PCR amplicons involving the nonrearranged germline DH7 and JH gene segments.

Although the initial multiplex strategy, as suggested from the OLIGO 6.2-assisted primer design, was to divide the various DH primers over two tubes, it was decided after testing various multiplex approaches to combine all primers into one multiplex tube (tube D of *IGH* clonality assay), except for the DH7 primer, which was included in a separate tube (tube E of *IGH* clonality assay). The reason to exclude the DH7 primer was the complicated germline pattern, due to easy amplification of alleles with nonrearranged DH7 segments. Using this two-tube multiplex approach, all clonal reference samples were still detectable. Under multiplex conditions, the detection limits for these various clonal targets were logically less optimal as compared to the single assays, ranging from ~5% (DH3, DH4, and DH6) to ~10% (DH2, and DH5). For the DH1 clonal reference sample that was available, a sensitivity of ~20% was observed; at a later stage, the DH1–JH rearrangement of cell line KCA was found to be detectable down to 10% in the multiplex assay. As tube E only contains the DH7 primer, the 10% sensitivity for this tube was the same as mentioned before. The same multiplex analysis performed with 500 ng instead of 100 ng DNA of the serial dilutions, resulted in slightly better sensitivities. The use of serial dilutions in MNC DNA instead of tonsillar DNA did not clearly affect detection limits of the assays for DH–JH recombinations.

### Results of general testing phase

Following initial testing in the three laboratories involved in primer design (Rotterdam, Roeselare, Amsterdam-VUMC), the developed *IGH* DH–JH multiplex PCR assay was further evaluated using the 90 Southern blot-defined samples (Figure 5b and c). Every sample was analyzed in parallel in four laboratories by heteroduplex analysis and in five laboratories by GeneScanning; in another two laboratories all samples were analyzed by both techniques. All together a total of six heteroduplex analysis and seven GeneScanning results were obtained per sample per tube. Despite concordant results (>80% of laboratories with identical results) in the vast majority of samples, nine showed interlaboratory discordances in tube D. Further analysis revealed that these could be explained by either the presence of a small clone with weak clonal products or to large size products (~390 and larger). In a few cases, the products were so large that only after sequencing it became clear that they concerned true but extended DH–JH rearrangements, either from upstream DH (eg DH6–25–DH1–26–JH in NL-12) or from downstream JH gene segments (eg DH6–25–JH4–JH5 in PT-14). In all three cases (NL-17, mycosis fungoides; FR-1, B-CLL; FR-5, FCL) in which clonal products were found using tube E, the results were completely concordant between laboratories.

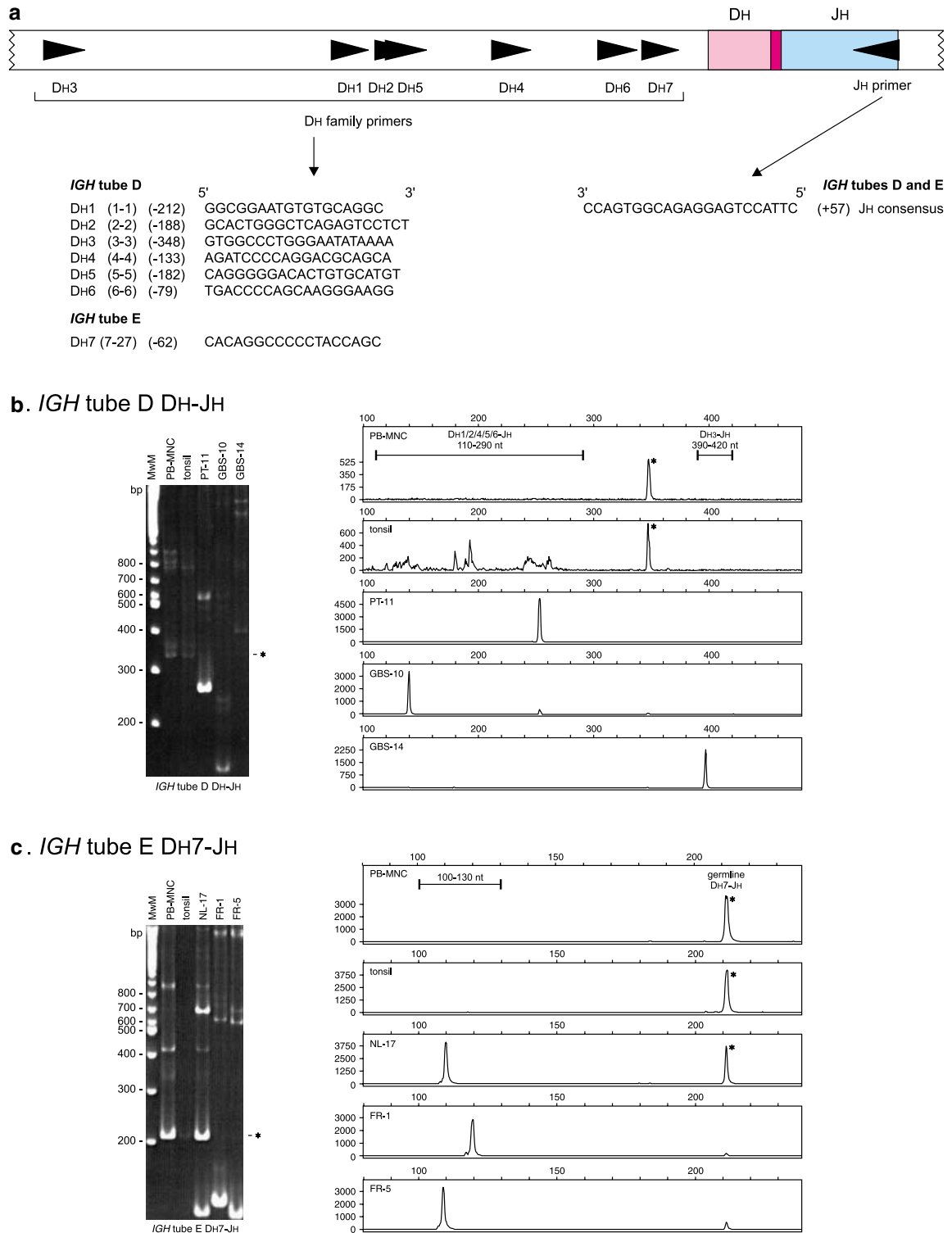


**Figure 5** PCR analysis of *IGH* (DH-JH) rearrangements. (a) Schematic diagram of *IGH* (DH-JH) rearrangement with seven DH family primers and one JH consensus primer, divided over two tubes (*IGH* tubes D and E). The DH7 (7-27) primer was separated from the other six DH primers, because the DH7 and JH consensus primer will give a germline PCR product of 211 nt. The relative position of the DH and JH primers is given according to their most 5' nucleotide upstream (–) or downstream (+) of the involved RSS. The DH gene segment used as a representative DH family member for primer design is indicated in parentheses. (b and c) Heteroduplex analysis (left panels) and GeneScanning (right panels) of the same polyclonal and monoclonal cell populations. The approximate distribution of the polyclonal and monoclonal peaks is indicated. The potential background band/peak in tube D is indicated with an asterisk and is located outside the expected range of DH-JH rearrangements. The germline DH-JH band of tube E is also indicated with an asterisk.

**Table 10** Size ranges of DH–JH BIOMED-2 PCR products

Primer set	Estimated size range <sup>a</sup>	Positive clonal control
DH1/JH	260–290 nt	KCA (271 nt)
DH2/JH	230–260 nt	Patient
DH3/JH	390–420 nt	ROS-15 (383 nt)
DH4/JH	175–205 nt	Patient
DH5/JH	225–255 nt	Patient
DH6/JH	110–150 nt	ROS-5 (148 nt)
DH7/JH	100–130 nt	Patient

<sup>a</sup>Estimation of size ranges is based on average deletion and insertion in DH–JH gene rearrangements.

When evaluating results from heteroduplex analysis and GeneScanning, it appeared that these were comparable, although in general the number of laboratories showing identical results was slightly higher upon heteroduplex analysis as compared to GeneScanning.

Direct comparison of DH–JH multiplex PCR results with Southern blot data are virtually impossible, as hybridization with a single probe (IGHJ6) in the JH region does not allow discrimination between VH–JH and DH–JH rearrangements. In three samples, it was clear that the detection of clonal products of the combined VH–JH and DH–JH assays did not fit with the configuration of the *IGH* locus in Southern blot analysis. Remarkably, no clonal DH–JH PCR products were observed in the prefollicular B-cell malignancies. In contrast, 11/16 B-CLL samples and 12/25 (post)follicular B-cell malignancy samples did contain clonally rearranged DH–JH PCR products. In three of the 18 T-cell malignancy cases (Table 8) clonal DH–JH rearrangements were seen; these concerned T-LBL (ES-9) and mycosis fungoides (NL-17) cases with Southern blot-detected *IGH* rearrangements, and a case of T-NHL/EATL (PT-4) without Southern blot-detected *IGH* rearrangements, probably because of the low tumor load of <15% (Table 8). All 15 reactive cases (Table 8) only showed polyclonal DH–JH PCR products, in accordance with Southern blot results. In category D with difficult diagnoses, three samples (PT-12, GBS-10, and GBN-8) showed clonal *IGH* DH–JH PCR products, which was in line with Southern blot data as well as *IGK* PCR data in two of three cases; in another two samples (PT-6 and GBS-9), both T-cell-rich B-NHL cases, clonal DH–JH products were found in addition to clonal *IGK* and/or *IGL* products, but without evidence for clonality from Southern blot analysis, which might best be explained by the small size of the B-cell clone in these samples (Table 8).

In order to determine the additional value of DH–JH PCR analysis, the results were compared to those of VH–JH PCR analysis. In five (NL-4, PT-14, GBN-2, FR-7, and NL-12) B-cell malignancies clonal DH–JH PCR products were found, whereas only polyclonal VH–JH PCR products were observed.

## Conclusion

In conclusion, based on the initial and general testing phases, DH–JH PCR analysis appears to be of added value for clonality assessment. Although heteroduplex analysis results might be interpreted slightly more easily, there is no clear preference for either heteroduplex analysis or GeneScanning, as they are both suitable for analyzing amplified PCR products. A potential difficulty in DH–JH PCR analysis is the relatively large size range of expected PCR products, due to scattered primer positions and to extended amplifications from upstream DH or downstream JH gene segments, implying that long runs are recommended for

GeneScanning. Finally, the remarkable position of the DH7–27 gene segment in the *IGH* locus causes a ladder of germline amplification products in tube E, with clonal products being easily recognizable as much smaller bands/peaks.

## SECTION 3. *IGK* gene rearrangements: Vκ–Jκ, Vκ–Kde/intronRSS–Kde

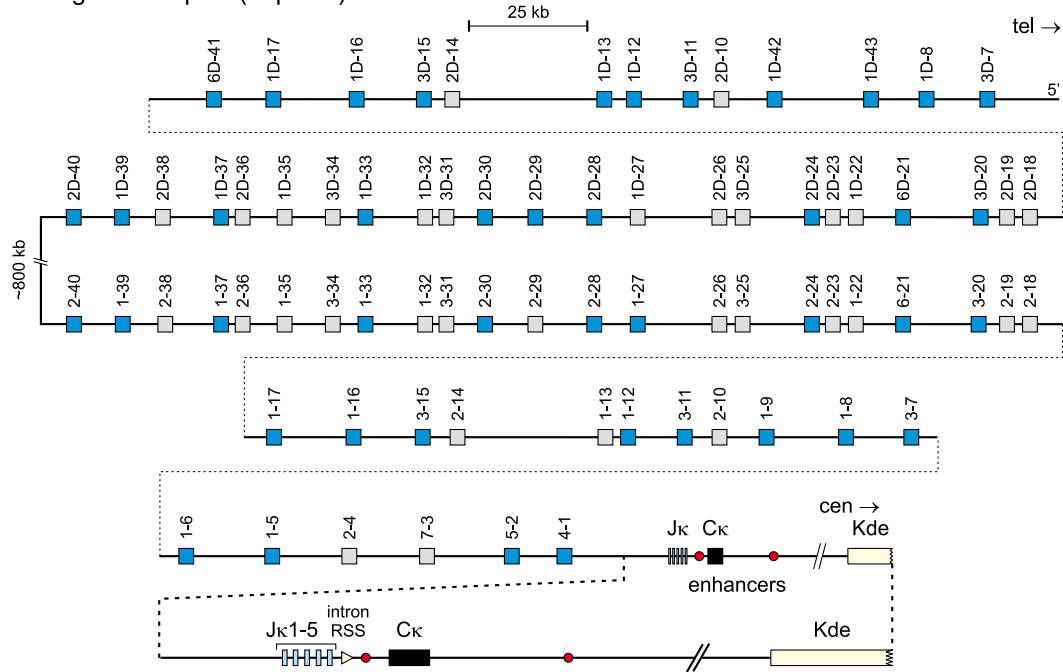
AW Langerak<sup>1</sup>, L Santos<sup>2</sup>, P Gameiro<sup>2</sup>, M Hummel<sup>3</sup>, F Davi<sup>4</sup>, EJ van Gastel-Mol<sup>1</sup>, ILM Wolvers-Tettero<sup>1</sup>, E Moreau<sup>5</sup>, R García-Sanz<sup>6</sup>, TC Diss<sup>7</sup>, PAS Evans<sup>8</sup>, T Flohr<sup>9</sup>, C Bastard<sup>10</sup>, M-H Delfau-Larue<sup>11</sup>, JM Cabeçadas<sup>12</sup>, A Parreira<sup>2</sup> and JJM van Dongen<sup>1</sup>

<sup>1</sup>Department of Immunology, Erasmus MC, University Medical Center Rotterdam, The Netherlands; <sup>2</sup>Department of Hemato-Oncology, Instituto Português de Oncologia, Lisboa, Portugal; <sup>3</sup>Institute of Pathology, Free University Berlin, Germany; <sup>4</sup>Department of Hematology, Hôpital Pitié-Salpêtrière, Paris, France; <sup>5</sup>Laboratory of Clinical Biology, H Hartziekenhuis, Roeselare, Belgium; <sup>6</sup>Servicio de Hematología, Hospital Universitario de Salamanca, Spain; <sup>7</sup>Department of Histopathology, Royal Free and UCL Medical School, London, UK; <sup>8</sup>Academic Unit of Haematology and Oncology, University of Leeds, Leeds, UK; <sup>9</sup>Institute of Human Genetics, University of Heidelberg, Germany; <sup>10</sup>Laboratoire de Genetique Oncologique, Centre Henri Becquerel, Rouen, France; <sup>11</sup>Service d'Immunologie Biologique, Hôpital Henri Mondor, Créteil, France; and <sup>12</sup>Department of Pathology, Instituto Português de Oncologia, Lisboa, Portugal

## Background

The human *IGK* light-chain locus (on chromosome 2p11.2) contains many distinct Vκ gene segments, grouped into seven Vκ gene families as well as five Jκ gene segments upstream of the Cκ region. Originally, the Vκ gene segments were designated according to the nomenclature as described by Zachau *et al.*<sup>61</sup> An alternative nomenclature groups the Vκ gene segments in seven families and is used in the ImMunoGeneTics database.<sup>62,63</sup> Here we follow the latter nomenclature. The Vκ1, Vκ2, and Vκ3 families are multimember families including both functional and pseudo gene segments, whereas the other families only contain a single (Vκ4, Vκ5, Vκ7) or a few segments (Vκ6).<sup>64</sup> Remarkably, all Vκ gene segments are dispersed over two large duplicated clusters, one immediately upstream and in the same orientation as the Jκ segments, and the other more distal and in an inverted orientation (Figure 6a).<sup>65</sup> The latter implies that the so-called inversion rearrangements are required to form Vκ–Jκ joints involving Vκ genes of the distal cluster. In addition to the Vκ and Jκ segments, there are other elements in the *IGK* locus that can be involved in recombination. The Kde, approximately 24 kb downstream of the Jκ–Cκ region, can rearrange to Vκ gene segments (Vκ–Kde), but also to an isolated RSS in the Jκ–Cκ intron (intronRSS–Kde) (Figure 6a).<sup>24,66</sup> Both types of rearrangements lead to functional inactivation of the *IGK* allele, through the deletion of either the Cκ exon (intronRSS–Kde rearrangement) or the entire Jκ–Cκ area (Vκ–Kde rearrangement).

As human *IGK* recombination starts in precursor B-cells in the BM, *IGK* rearrangements can also be detected in precursor B-ALL (40–60% of cases, depending on age) (Table 11).<sup>24,67</sup> Although Vκ–Jκ joinings are present, the *IGK* rearrangements in

a. *IGK* gene complex (#2p11.2)

## b

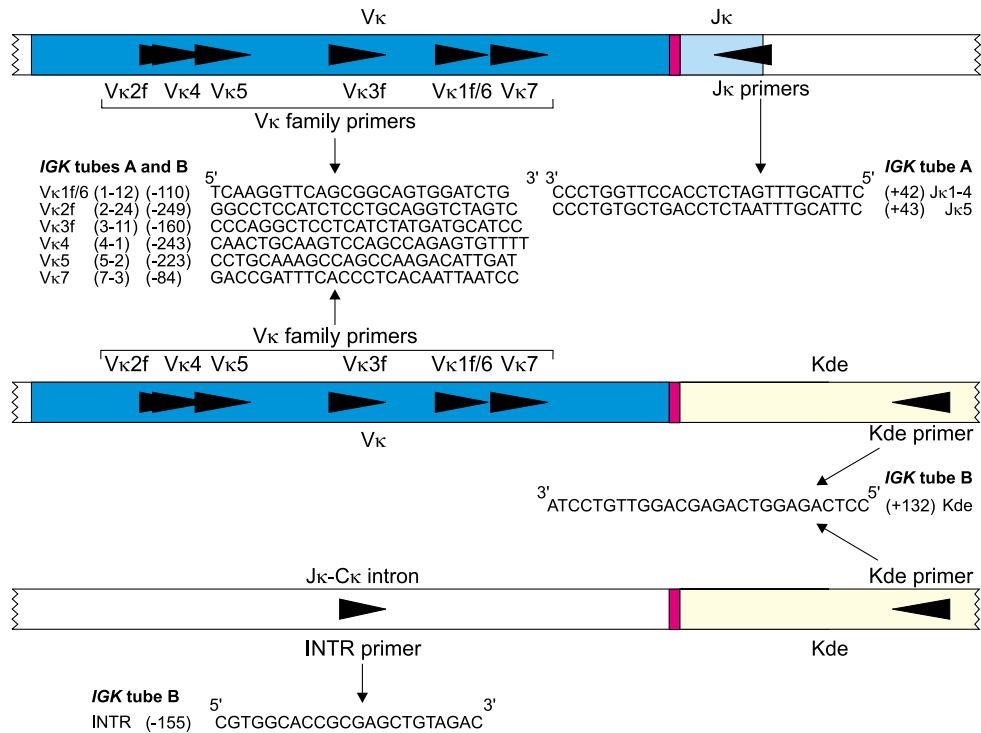
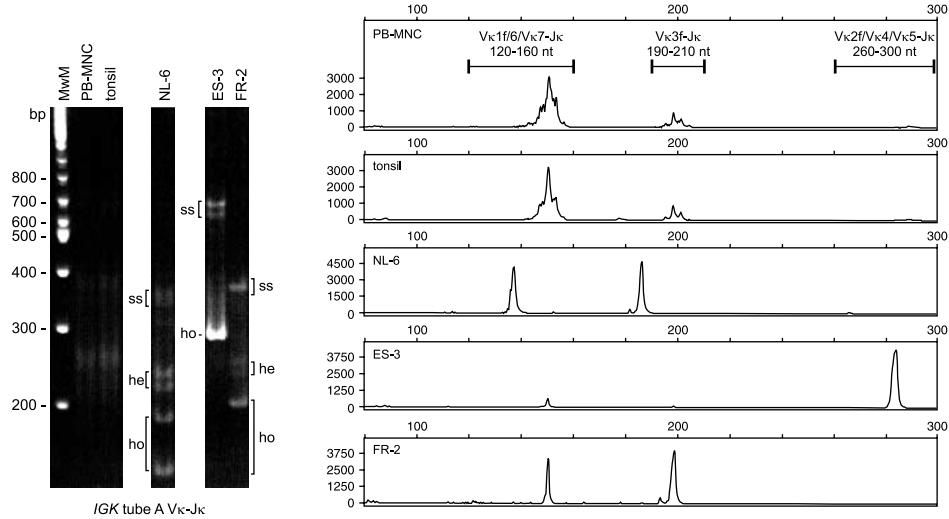


**Figure 6** PCR analysis of *IGK* gene rearrangements. (a) Schematic diagram of the *IGK* gene complex on chromosome band 2p11.2 (adapted from ImMunoGeneTics database).<sup>62,63</sup> Only rearrangeable nonpolymorphic *Vκ* gene segments are indicated in blue (functional *Vκ*) or in gray (nonfunctional *Vκ*). The cluster of inverted *Vκ* gene segments (coded with the letter D) is located ~800 kb upstream of the noninverted *Vκ* gene segments. (b) Schematic diagrams of *Vκ*-*Jκ* rearrangement and the two types of Kde rearrangements (*Vκ*-Kde and intronRSS-Kde). The relative position of the *Vκ*, *Jκ*, Kde, and intronRSS (INTR) primers is given according to their most 5' nucleotide upstream (-) or downstream (+) of the involved RSS. The *Vκ* gene segment used as a representative member of the *Vκ*1, *Vκ*2, and *Vκ*3 families are indicated in parentheses. *Vκ*4, *Vκ*5, and *Vκ*7 are single-member *Vκ* families. The primers are divided over two tubes: tube A with *Vκ* and *Jκ* primers and tube B with *Vκ*, intronRSS, and Kde primers. (c and d) Heteroduplex analysis and GeneScanning of the same polyclonal and monoclonal cell populations, showing the typical heteroduplex smears and homoduplex bands (left panels) and the typical Gaussian curves and monoclonal peaks (right panels). The approximate distribution of the polyclonal Gaussian curves is indicated in nt.

c. *IGK* tube A  $V_{\kappa}$ -J $\kappa$



d. *IGK* tube B  $V_{\kappa}$ /intron-Kde

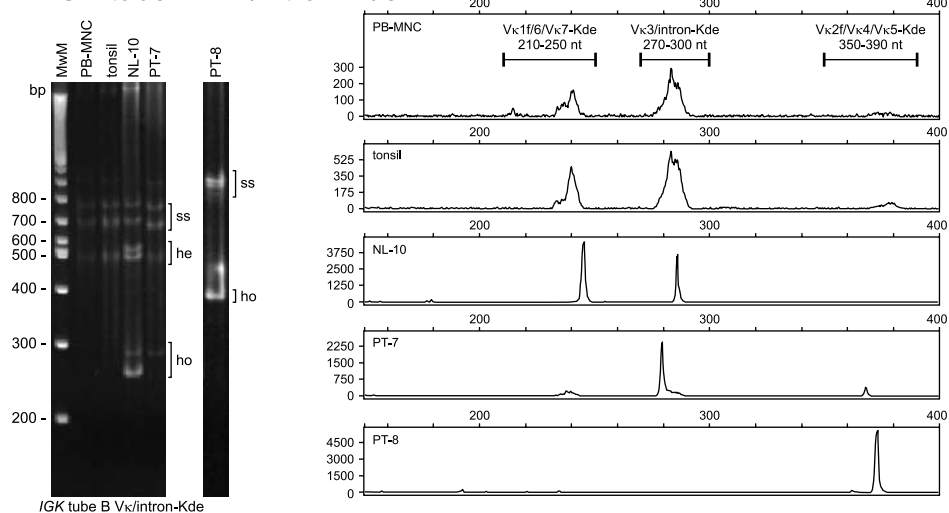


**Figure 6** Continued.

precursor B-ALL mainly concern recombinations involving Kde (35–50% of cases). In childhood precursor B-ALL,  $V_{\kappa}$ -Kde recombination predominates over intron-Kde, whereas in adult ALL the deletions exclusively concern  $V_{\kappa}$ -Kde couplings (Table 11).<sup>24,67,68</sup> In chronic B-cell leukemias, *IGK* rearrangements are even more frequent, being detectable in all  $Ig\kappa^+$  and  $Ig\lambda^+$  cases (Table 11). By definition, functional  $V_{\kappa}$ -J $\kappa$  rearrangements are found on at least one allele in  $Ig\kappa^+$  B-cell leukemias; the noncoding second allele is either in germline configuration (~50% of cases), contains an out-of-frame  $V_{\kappa}$ -J $\kappa$  rearrangement (~20% of cases), or is inactivated via a Kde rearrangement (~30% of cases).<sup>69</sup> Kde rearrangements occur in (virtually) all  $Ig\lambda^+$  B-cell leukemias (~85% of alleles), with a slight predominance of intronRSS-Kde recombinations over  $V_{\kappa}$ -Kde rearrangements (Table 11). This implies that (virtually) all  $Ig\lambda^+$  leukemias contain a Kde rearrangement, while potentially functional  $V_{\kappa}$ -J $\kappa$  couplings are relatively rare.<sup>24,69</sup> Several studies have shown that  $V_{\kappa}$  gene segment usage is almost identical between various normal and malignant B-cell populations and largely reflects the number of available gene segments

within each family (Table 12). Both in  $V_{\kappa}$ -J $\kappa$  as well as in  $V_{\kappa}$ -Kde rearrangements,  $V_{\kappa}$  gene segments from the first four families ( $V_{\kappa}1$ - $V_{\kappa}4$ ) predominate (Table 12).  $V_{\kappa}2$  gene usage appeared to be higher in precursor B-ALL than in more mature B-cell lymphoproliferations or normal B cells. Remarkably, the distal inverted  $V_{\kappa}$  cluster was rarely used in  $V_{\kappa}$ -J $\kappa$  rearrangements, whereas  $V_{\kappa}$  pseudogene segments were never involved, also not in  $Ig\lambda^+$  cases.<sup>70</sup> Little is known about J $\kappa$  gene segment usage, but sparse data show that J $\kappa$ 1, J $\kappa$ 2, and J $\kappa$ 4 are the most frequently used J $\kappa$  gene segments.<sup>69</sup>

$V_{\kappa}$ -J $\kappa$  rearrangements can be important complementary PCR targets for those types of B-cell proliferations in which somatic hypermutations may hamper amplification of the VH-JH target, but recombinations involving Kde are probably even more valuable. Deletion of intervening sequences in the J $\kappa$ -C $\kappa$  intron results in the removal of the *IGK* enhancer, which is thought to be essential for the somatic hypermutation process to occur. Rearrangements involving Kde are therefore assumed to be free of somatic hypermutations, and hence should be amplified rather easily.

**Table 11** Frequencies of *IGK* rearrangements (*Vκ-Jκ* and *Kde*) in different types of B-cell malignancies

B-cell malignancy	Rearranged <i>IGK</i> genes	<i>Vκ-Jκ</i> rearrangement	<i>Kde</i> rearrangement	Allelic distribution <i>Kde</i>	
	(%)	(%)	(%)	<i>Vκ-Kde</i> (%)	Intron- <i>Kde</i> (%)
Adult precursor-B-ALL <sup>a</sup>	46	15	35	100	0
Childhood prec-B-ALL <sup>b</sup>	62	30	50	69	31
Igκ <sup>+</sup> B-CLL <sup>b,c</sup>	100	100	32	53	47
Igλ <sup>+</sup> B-CLL <sup>b,c</sup>	100	83	100	45	55

<sup>a</sup>Szczepanski *et al.*<sup>67</sup><sup>b</sup>Beishuizen *et al.*<sup>24</sup><sup>c</sup>van der Burg *et al.*<sup>69</sup>

### Primer design

Using OLIGO 6.2 software, six family-specific *Vκ* primers were designed to recognize the various *Vκ* gene segments of the seven *Vκ* families; the *Vκ6* family gene segments were covered by the *Vκ1* family primer (Figure 6b). In case of the relatively large *Vκ1*, *Vκ2*, and *Vκ3* families only the functional *Vκ* gene segments were taken into consideration, as the less homologous pseudogene segments complicated optimal primer design too much. The family-specific *Vκ* primers were designed to be used in combination with either a set of two *Jκ* primers (*Jκ1*–4, covering the first four *Jκ* segments and *Jκ5* covering the fifth) or a *Kde* primer (Figure 6b). For the analysis of *Kde* rearrangements an additional forward primer recognizing a sequence upstream of the intronRSS was made. In order to show minimal crossannealing to other *Vκ* family segments and still be useful in multiplex reactions, the various primers could not be designed at similar positions relative to RSS elements (Figure 6b). The expected PCR product sizes of *Vκ-Jκ* joints range from 120–140 bp (for *Vκ7-Jκ* joints) to 280–300 bp (*Vκ2-Jκ* rearrangements) (see also Table 13 for size ranges). For the *Kde* rearrangements, product size ranges are from 210–230 bp (*Vκ7-Kde*) to 360–390 bp (*Vκ2-Kde*), whereas the intronRSS-*Kde* products are 270–300 bp (see also Table 13).

### Results of initial testing phase

For initial testing of the individual primers, several cell lines and patient samples with precisely defined clonal *Vκ-Jκ* or *Vκ-Kde*/intronRSS-*Kde* rearrangements were used (Table 13). The patient samples with *Vκ-Jκ* joints mostly concerned chronic B-cell leukemias, which were additionally selected on the basis of a high tumor load for easy and sensitive detection of the involved rearrangement. Unfortunately, clonal reference samples were not available for all *Vκ-Jκ* targets; especially the more rare types of rearrangements involving *Vκ5*, *Vκ7*, and/or *Jκ5* were not represented in the series of reference samples. For these targets and also for the targets for which clonal reference samples were available, healthy control tonsillar or MNC DNA samples were employed, in which PCR products of the correct expected sizes were indeed observed. The only exception was the *Vκ7/Jκ5* primer combination; most probably *Vκ7-Jκ5* joinings are so rare in normal B cells that these PCR products were hardly or not detectable in tonsils. Rearranged products within the expected size ranges could be detected in all clonal reference samples, under standard PCR conditions using 1.5 mM MgCl<sub>2</sub> and either ABI Gold Buffer or ABI Buffer II. However, in a few cases weak amplification of particular *Vκ-Jκ* rearrangements was observed with other *Vκ* family/*Jκ* primer sets, due to slight crossannealing of the *Vκ3* primer to a few *Vκ1* gene segments. Furthermore, in a

few of the clonal reference samples clear additional clonal PCR products were seen with other *Vκ/Jκ* or even *Vκ/Kde* and intronRSS/*Kde* primer sets; in most samples this could be explained by the complete configuration of the two *IGK* alleles. This occurrence of multiple clonal PCR products illustrates the complexity of *IGK* rearrangement patterns in a given cell sample, mainly caused by the potential occurrence of two clonal rearrangements on one allele (*Vκ-Jκ* and intronRSS-*Kde*). This complexity does not hamper but support the discrimination between polyclonality and monoclonality.

No nonspecific annealing of the primers was observed for any of the *Vκ-Jκ* and *Vκ-Kde*/intronRSS-*Kde* primer sets, when using HeLa DNA as a nontemplate-specific control. Serial dilutions of DNA from the clonal reference samples into tonsillar DNA generally resulted in sensitivities of 5–10% for *Vκ-Jκ* rearrangements and 1–10% for *Vκ-Kde* rearrangements, using heteroduplex analysis. In general, the sensitivities in GeneScanning were approximately one dilution step better. The only slightly problematic target was the intronRSS-*Kde* target that could only be detected down to the 10% serial dilution in the employed patient sample. This is probably caused by the fact that intronRSS-*Kde* rearrangements are abundant in DNA from both Igκ<sup>+</sup> and Igλ<sup>+</sup> tonsillar B cells, which were used in the dilution experiments.

The multiplex strategy that was chosen after testing several approaches consisted of two different multiplex PCR reaction tubes. In the *Vκ-Jκ* tube (tube A), all *Vκ* primers were combined with both *Jκ* primers, whereas tube B contained all *Vκ* primers plus the intronRSS primer in combination with the *Kde* reverse primer (Figure 6b). All before-mentioned clonal reference samples were detectable using this two-tube multiplex approach. Of note is the observation that in nonclonal tonsil samples a predominant, seemingly clonal band of ~150 bp was detected using the *Vκ-Jκ* multiplex tube A analysis. The presence of this product, which is seen especially in GeneScanning, can be explained by the limited heterogeneity of *Vκ-Jκ* junctional regions leading to a high frequency of products of an average size of ~150 bp. Furthermore, in some samples a sometimes weak 404 bp nonspecific band was observed in tube B. Although sensitivities were on average slightly better in other multiplex approaches in which the *Vκ* primers were further subdivided over multiple tubes, the feasibility of having only two tubes to analyze all relevant *IGK* rearrangements, finally, was the most important argument for choosing the two-tube multiplex strategy as given in Figure 6b. Detection limits for the various clonal targets in the two-tube multiplex approach were ~10% for most of the clonal *Vκ-Jκ* rearrangements (*Vκ1-Jκ4*, *Vκ2-Jκ4*, and *Vκ3-Jκ4*) derived from informative samples with a high tumor load; several of the *Vκ-Kde* targets were detectable with a still reasonable sensitivity of ~10%, but a few other samples containing *Vκ2-Kde*, *Vκ5-Kde*, and also intronRSS-

**Table 12** Allelic frequencies of V $\kappa$  family gene usage in V $\kappa$ -J $\kappa$  and V $\kappa$ -Kde rearrangements in different malignant and normal B-cell populations

V $\kappa$ family	V $\kappa$ -J $\kappa$ rearrangements					V $\kappa$ -Kde rearrangements	
	Precursor-B-ALL <sup>a</sup> (n = 6) (%)	B-CLL <sup>a</sup> (n = 23) (%)	B-NHL <sup>a</sup> (n = 23) (%)	MM <sup>a</sup> (n = 3) (%)	Normal B cells (%) <sup>d</sup>	Precursor-B-ALL <sup>e</sup> (n = 66) (%)	Chronic B-cell leukemia <sup>e</sup> (n = 38) (%)
V $\kappa$ 1	50	57	57	67	50–56	35	50
V $\kappa$ 2	33	13	13	0	6–10	29	13
V $\kappa$ 3	0	13	17	0	25–30	26	21
V $\kappa$ 4	17	17	13	33	4–19	3	10
V $\kappa$ 5	ND	ND	ND	ND	ND	0	0
V $\kappa$ 6	ND	ND	ND	ND	ND	0	3
V $\kappa$ 7	ND	ND	ND	ND	ND	7	3

ND, not determined.

<sup>a</sup>Data derived from Cannell *et al.*<sup>70</sup><sup>b</sup>Data derived from Wagner *et al.*<sup>205</sup><sup>c</sup>Data derived from Wagner *et al.*<sup>206</sup><sup>d</sup>Data derived from Solomon *et al.*<sup>207</sup> and Cuisinier *et al.*<sup>208</sup><sup>e</sup>Data derived from Beishuizen *et al.*<sup>194</sup>**Table 13** BIOMED-2 PCR product size ranges and control samples of different V $\kappa$ -J $\kappa$ , V $\kappa$ -Kde/intronRSS-Kde rearrangements

Primer set	Estimated size range <sup>a</sup>	Control reference sample(s)
V $\kappa$ 1f/6/J $\kappa$	140–160 nt	Patient (J $\kappa$ 1–4)/tonsil (J $\kappa$ 5)
V $\kappa$ 2f/J $\kappa$	280–300 nt	KCA (J $\kappa$ 1–4; 290 nt)/ROS-15 (J $\kappa$ 5; 288 nt)
V $\kappa$ 3f/J $\kappa$	190–210 nt	Patient (J $\kappa$ 1–4)/tonsil (J $\kappa$ 5)
V $\kappa$ 4/J $\kappa$	275–295 nt	Patient (J $\kappa$ 1–4)/tonsil (J $\kappa$ 5)
V $\kappa$ 5/J $\kappa$	260–280 nt	Tonsil (J $\kappa$ 1–4)/tonsil (J $\kappa$ 5)
V $\kappa$ 7/J $\kappa$	120–140 nt	Tonsil (J $\kappa$ 1–4)/none
V $\kappa$ 1f/6/Kde	225–245 nt	ROS-15 (241 nt)/380 <sup>b</sup>
V $\kappa$ 2f/Kde	360–390 nt	380 (372 nt)
V $\kappa$ 3f/Kde	270–300 nt	NALM-1
V $\kappa$ 4/Kde	355–385 nt	ROS-5 (371 nt)
V $\kappa$ 5/Kde	350–380 nt	Patient
V $\kappa$ 7/Kde	210–230 nt	Patient
IntronRSS/Kde	270–300 nt	NALM-1

<sup>a</sup>Estimation of size ranges is based on average deletion and insertion in V $\kappa$ -J $\kappa$  and V $\kappa$ -Kde/intronRSS-Kde gene rearrangements.<sup>b</sup>Cell line 380 shows a larger V $\kappa$ 1-Kde PCR product, due to an atypical rearrangement configuration.

Kde targets showed detection limits above 10%. Even the use of 500 ng serially diluted DNA instead of 100 ng hardly resulted in better sensitivities, whereas serial dilutions in MNC DNA did not affect the detection limits either. Nevertheless, detection limits of serial dilutions of reference DNA in water were all in the order of 0.5–1%, which shows that the chosen multiplex *IGK* PCR assay as such is good. It is important to note that potential clonal cell populations in lymph nodes or PB in practice will have to be detected within a background of polyclonal cells, which can hamper sensitive clonality detection, especially in samples with a relatively high background of polyclonal B cells.

### Results of general testing phase

Following initial testing in the four laboratories involved in primer design (Rotterdam, Lisbon, Berlin, and Paris-Salpetriere), the developed *IGK* multiplex PCR assay was further evaluated using 90 Southern blot-defined samples (Figure 6c and d). Every sample was analyzed in parallel via heteroduplex analysis (five

laboratories) and GeneScanning (two laboratories); in another four laboratories all samples were analyzed by both techniques. Taken together, eight heteroduplex analysis and five GeneScanning results were available per sample per tube. In the vast majority of samples >80% of laboratories produced identical results, that is, either clonal bands/peaks or polyclonal smears/curves in one or both tubes. However, in nine (~10%) samples discordances were found between laboratories, which remained after repetitive analysis of these samples. More detailed analysis revealed that in at least six cases the approximately 150 and 200 bp sizes of the clonal products in tube A could not easily be discriminated from polyclonal products of roughly the same size. This is an inherent difficulty in especially V $\kappa$ -J $\kappa$  analysis, which is caused by the relatively limited junctional heterogeneity of these rearrangements. In two samples, the results from tube B were however so clear in all laboratories with both techniques that in fact no discrepancy prevailed. In one sample (ES-8), a large product of around 500 bp appeared to be the reason for discrepant interlaboratory results; further sequencing revealed that amplification starting from the downstream J $\kappa$  segment caused the production of an extended V $\kappa$ 1-J $\kappa$ 3-J $\kappa$ 4 PCR product.

When evaluating results from heteroduplex analysis and GeneScanning, it appeared that these were rather comparable, although in general the number of laboratories showing identical results was slightly higher upon heteroduplex analysis as compared to GeneScanning (Figure 6c and d). Remarkably, in one sample (GBS-4) heteroduplex analysis revealed a clear product in both tubes, whereas GeneScanning only showed polyclonality. Cloning of the heteroduplex analysis product showed a peculiar V $\kappa$ 3-V $\kappa$ 5 PCR product, which was not observed in any other sample; the V $\kappa$ -V $\kappa$  configuration of this product explained why it was not detected with labeled J $\kappa$  primers in GeneScanning.

Comparison of PCR results with Southern blot data revealed no Southern blotting vs PCR discrepancies in the pregerminal center B-cell malignancies and B-CLL samples; in line with the presence of rearranged *IGK* bands in Southern blot analysis, all samples contained clonal *IGK* PCR products. In contrast, in the 25 (post)follicular B-cell malignancy samples clonal *IGK* PCR products were missed in four DLBCL cases (ES-5, PT-13, PT-14, and FR-7) and one PC leukemia (NL-19) with both techniques and in another DLBCL case (GBS-4, see above) with GeneScanning analysis only. In all cases this was most probably caused by

somatic hypermutation. Interestingly, in one FCL case (NL-4), a clonal PCR product was found, whereas Southern blot analysis revealed a germline band in case of the *IGK* genes and weak clonal bands upon *IGH* analysis. In all 18 T-cell malignancy cases and all 15 reactive cases polyclonal *IGK* PCR products were found in accordance with Southern blot results, except for one peripheral T-NHL case (FR-10). Next to the clonal TCR and *IGK* products this sample also showed clonal *IGH* and *IGL* PCR products, but no clonal Ig rearrangements in Southern blot analysis, probably reflecting the presence of a small additional B-cell clone in this sample. Finally, in the category with difficult diagnoses (D), two samples (GBS-10 and GBN-8) showed clonal *IGK* PCR products, in line with Southern blot data; however, in another two samples (PT-6 and GBS-9), both T-cell-rich B-NHL cases, clonal *IGK* PCR products were found as well as clonal *IGH* and/or *IGL* products, but without the evidence for clonality from Southern blot analysis. Also this discrepancy can probably be explained by the small size of the B-cell clone in these two patient samples.

To determine the additional value of analyzing the *IGK* locus, we compared the results of *IGK* PCR analysis to those of *IGH* PCR analysis. In five (ES-2, NL-4, PT-8, GBN-2, and ES-8) of the nine samples in which no clonal VH-JH PCR products were found, clonal products were readily observed in *IGK* analysis. When taking into account both VH-JH and DH-JH analysis, *IGK* PCR analysis was still complementary to *IGH* PCR analysis in three of these cases in detecting clonal Ig PCR products.

## Conclusion

In conclusion, based on the initial and general testing phases as well as preliminary evidence from use of these multiplex assays in pathologically well-defined series of lymphoproliferations (Work Package 2 of the BIOMED-2 project), PCR analysis of the *IGK* locus has clear (additional) value for clonality detection. Nevertheless, care should be taken with interpretation of seemingly clonal bands especially in tube A, due to the inherent restricted *IGK* junctional heterogeneity. As this problem is especially apparent in GeneScanning, heteroduplex analysis is slightly preferred over GeneScanning, although it should be marked that in some cases GeneScanning may facilitate proper interpretation of results. Another potential pitfall is the relatively large size range of expected rearranged *IGK* products, due to scattered primer positions, and to extended amplifications from downstream J $\kappa$  gene segments. This implies that long runs are recommended for GeneScanning. Finally, the inherent complexity of multiple rearrangements in the *IGK* locus (V $\kappa$ -J $\kappa$  and Kde rearrangements on the same allele), together with a low level of crossannealing of V $\kappa$  primers, may occasionally result in patterns with multiple bands or peaks, resembling oligoclonality. However, with these considerations in mind, the two-tube *IGK* multiplex PCR system can be valuable in PCR-based clonality diagnostics.

## SECTION 4. *IGL* gene rearrangements

F Davi<sup>1</sup>, C Sambade<sup>2</sup>, R García-Sanz<sup>3</sup>, C Colin<sup>1</sup>, H Hercher<sup>1</sup>, D González<sup>3</sup>, E Moreau<sup>4</sup>, TC Diss<sup>5</sup>, PAS Evans<sup>6</sup>, T Flohr<sup>7</sup> and TJ Molina<sup>8</sup>

<sup>1</sup>Department of Hematology, Hôpital Pitié-Salpêtrière, Paris, France; <sup>2</sup>Department of Pathology, Medical Faculty of Porto and

IPATIMUP (Institute of Molecular Pathology and Immunology of the University of Porto), Porto, Portugal; <sup>3</sup>Servicio de Hematología, Hospital Universitario de Salamanca, Spain; <sup>4</sup>Laboratory of Clinical Biology, H Hartziekenhuis, Roeselare, Belgium; <sup>5</sup>Department of Histopathology, Royal Free and UCL Medical School, London, UK; <sup>6</sup>Academic Unit of Haematology and Oncology, University of Leeds, Leeds, UK; <sup>7</sup>Institute of Human Genetics, University of Heidelberg, Germany; and <sup>8</sup>Department of Pathology, Hotel-Dieu de Paris, France

## Background

*IGL* gene rearrangements are present in 5–10% of Ig $\kappa$ <sup>+</sup> B-cell malignancies and in all Ig $\lambda$ <sup>+</sup> B-cell malignancies.<sup>69</sup> Therefore, V $\lambda$ -J $\lambda$  rearrangements potentially represent an attractive extra PCR target for clonality studies to compensate for false-negative *IGH* VH-JH PCR results, mainly caused by somatic mutations. The *IGL* locus spans 1 Mb on chromosome 22q11.2.<sup>71–73</sup> There are 73–74 V $\lambda$  genes spread over 900 kb, among which 30–33 are functional (Figure 7a). Based upon sequence homology, the V $\lambda$  genes can be grouped into 11 families (10 containing functional V $\lambda$  gene segments) and three clans. Members of the same family tend to be clustered on the chromosome (Figure 7a). The J $\lambda$  and C $\lambda$  genes are organized in tandem with a J $\lambda$  segment preceding a C $\lambda$  gene. Typically, there are seven J-C $\lambda$  gene segments, of which J-C $\lambda$ 1, J-C $\lambda$ 2, J-C $\lambda$ 3, and J-C $\lambda$ 7 are functional and encode the four Ig $\lambda$  isotypes (Figure 7a).<sup>74,75</sup> There is however a polymorphic variation in the number of J-C $\lambda$  gene segments, since some individual may carry up to 11 of them one allele, due to an amplification of the C $\lambda$ 2-C $\lambda$ 3 region.<sup>76,77</sup>

Several studies have shown that the *IGL* gene repertoire of both normal and malignant B cells is biased.<sup>78–81</sup> Thus, over 90% of V $\lambda$  genes used by normal B cells belong to the V $\lambda$ 1, V $\lambda$ 2, and V $\lambda$ 3 families, which comprise 60% of the functional genes (Table 14). Moreover, three genes (2–14, 1–40, and 2–8) account for about half of the expressed repertoire. While normal B cells use J-C $\lambda$ 1, J-C $\lambda$ 2, and J-C $\lambda$ 3 gene segments in roughly equivalent proportions, neoplastic B cells tend to use predominantly J-C $\lambda$ 2 and J-C $\lambda$ 3 gene segments (Table 15).<sup>81</sup> In both normal and malignant B cells, the J-C $\lambda$ 7 is used very rarely (1%). This latter finding was, however, challenged by a single-cell study of normal cells which found that more than half of the rearrangements employed the J-C $\lambda$ 7 gene segments.<sup>82</sup> This unexpectedly high usage of C $\lambda$ 7 has never been confirmed and might have been caused by a technical pitfall.<sup>81</sup>

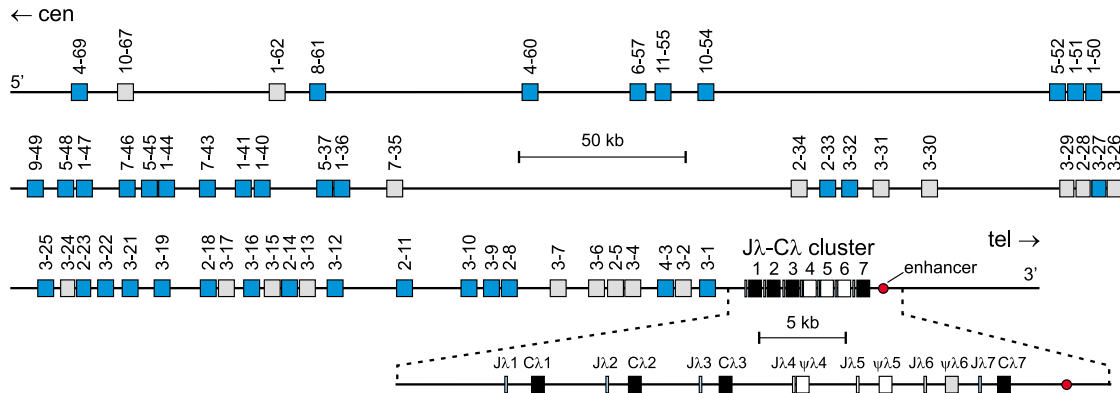
In contrast to the mouse, there is some junctional diversity due to exonuclease activity and N nucleotide addition in human *IGL* gene rearrangements.<sup>79,80,82,83</sup> It is however much less extensive than that of the *IGH* locus, and a number of rearrangements result from the directly coupling of germline V $\lambda$  and J $\lambda$  gene segments. Nevertheless, the *IGL* locus might represent an alternative complementary locus to *IGH* for B-cell clonality studies.

## Primer design

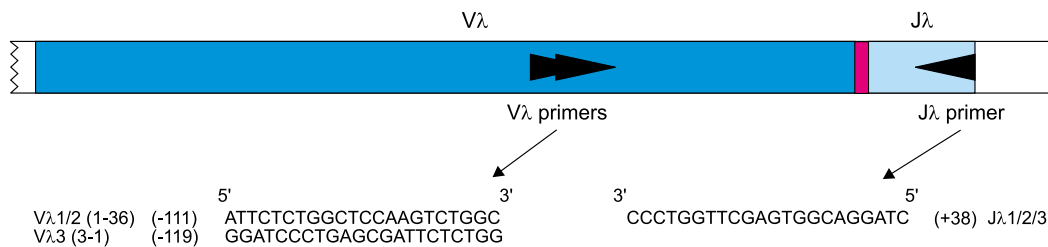
Considering the biased V $\lambda$  repertoire, we chose to amplify only rearrangements that used the V $\lambda$ 1, V $\lambda$ 2, and V $\lambda$ 3 gene segments. A single consensus primer recognizing both V $\lambda$ 1 and V $\lambda$ 2 gene segments, as well as a V $\lambda$ 3 primer, were designed in regions of high homology between members of the same family (Figure 7b).



### a. IGL gene complex (#22q11.2)



### b



### c. IGL tube Vλ-Jλ

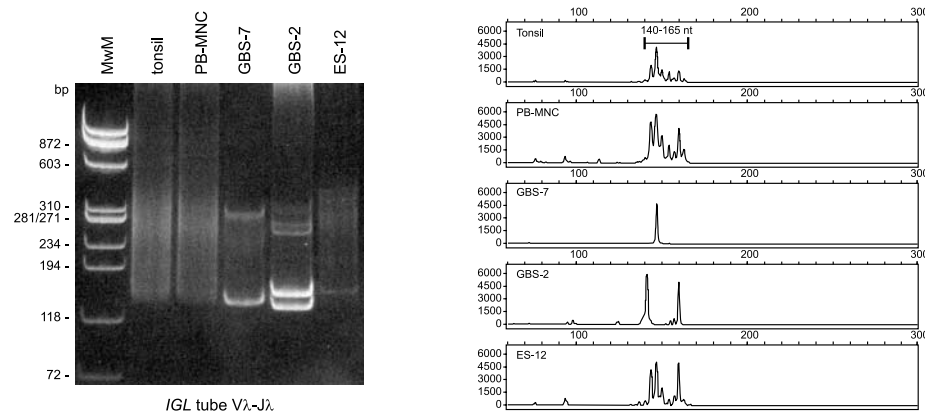


**Figure 7** PCR analysis of *IGL* gene rearrangements. (a) Schematic diagram of *IGL* gene complex on chromosome band 22q11.2 (adapted from ImMunoGenetics database).<sup>62,63</sup> Only rearrangeable nonpolymorphic *Vλ* gene segments are included in blue (functional *Vλ*) or in gray (nonfunctional *Vλ*). (b) Schematic diagram of *Vλ*-*Jλ* rearrangement with two *Vλ* family primers and one *Jλ* consensus primer. Only two *Vλ* primers were designed for *Vλ*1 plus *Vλ*2 and for *Vλ*3, because these three *Vλ* families cover approximately 70% of rearrangeable *Vλ* gene segments, and because approximately 90% of all *IGL* gene rearrangements involve *Vλ*1, *Vλ*2, or *Vλ*3 gene segments (Table 14).<sup>78</sup> Although five of the seven *Jλ* gene segments can rearrange, only a single *Jλ* consensus primer was designed for *Jλ*1, *Jλ*2, and *Jλ*3, because 98% of all *IGL* gene rearrangements involve one of these three gene segments (Table 15).<sup>81</sup> The relative position of the *Vλ* and *Jλ* primers is given according to their most 5' nucleotide upstream (−) or downstream (+) of the involved RSS. (c) Heteroduplex analysis and GeneScanning of the same polyclonal and monoclonal cell populations, showing the typical heteroduplex smears and homoduplex bands (left panel) and the polyclonal Gaussian curves and monoclonal peaks (right panel). The approximate position of the polyclonal Gaussian curves is indicated in nt. Two cases have major clonal rearrangements: GBS-7 (monoallelic), GBS-2 (biallelic). One case (ES-12) has a minor monoclonal rearrangement in a polyclonal background.

Initial experiments showed that they worked as well in multiplex as separately. However, crossannealing of the *Vλ*3 primer to some *Vλ*1 or even *Vλ*6 gene segments was observed when the *Vλ*3 primer was used separately. This was not seen in multiplex PCR, but could have important implications when the single assays are used for the identification of PCR targets in minimal residual disease (MRD) studies (AW Langerak, personal communication).

A single consensus primer was designed for the *Jλ*1, *Jλ*2, and *Jλ*3 gene segments and has one mismatch in its central portion compared to each of the germline sequences. In preliminary experiments, it was found to give rather better results than a combination of perfectly matched *Jλ*1 and *Jλ*2-*Jλ*3 primers. Since a single study reported the frequent usage of the *Jλ*7 gene in normal B cells,<sup>82</sup> we also designed a *Jλ*7-specific primer. When tested on various polyclonal B-cell samples, we could

**Table 14** V $\lambda$  gene usage, clonal controls, and size of PCR products

V $\lambda$ gene family	Number of functional V $\lambda$ segments <sup>a</sup>	V $\lambda$ gene usage in normal B cells (%) <sup>b</sup>	Clonal control for BIOMED-2 V $\lambda$ primers (product size)	Size range of BIOMED-2 V $\lambda$ -J $\lambda$ PCR products
V $\lambda$ 1	5 (17%)	30	} KCA (148 nt) EB-4B (160 nt) CLL1 (165 nt) NA <sup>c</sup>	140–155 nt
V $\lambda$ 2	5 (17%)	43		
V $\lambda$ 3	8 (27%)	19		150–165 nt
V $\lambda$ 4–V $\lambda$ 10	12 (40%)	8		NA

<sup>a</sup>Number (relative frequency) of nonpolymorphic functional V $\lambda$  gene segments per family.<sup>62,63</sup><sup>b</sup>Ignatovich *et al.*<sup>78</sup><sup>c</sup>NA, not applicable.**Table 15** Allelic J–C $\lambda$  gene usage in normal and malignant B cells

J–C $\lambda$ gene	Normal B cells (%) <sup>a</sup>	Malignant B cells <sup>b</sup>			
		Prec-B-ALL (n = 21) <sup>c</sup> (%)	B-CLL (n = 96) <sup>c</sup> (%)	B-NHL (n = 52) <sup>c</sup> (%)	MM (n = 35) <sup>c</sup> (%)
J–C $\lambda$ 1	27	0	11	14	3
J–C $\lambda$ 2	38	43	34	31	60
J–C $\lambda$ 3	34	38	55	53	37
J–C $\lambda$ 6	0.1	19	0	0	0
J–C $\lambda$ 7	0.6	0	0	2	0

<sup>a</sup>Ignatovich *et al.*<sup>78</sup><sup>b</sup>Tümekaya *et al.*<sup>81</sup><sup>c</sup>Number of investigated rearranged alleles.

hardly detect any signal in heteroduplex analysis, in contrast to amplifications performed on the same samples using the J $\lambda$ 1, J $\lambda$ 2–J $\lambda$ 3, or the J $\lambda$  consensus primers. Similarly, we could not detect any rearrangement with this primer when analyzing a collection of monoclonal B-cell tumors. Based on these results as well as the other reports in the literature,<sup>81</sup> we concluded that the nonconfirmed high frequency of J $\lambda$ 7 rearrangements in the one study had been caused by a technical pitfall, and consequently we decided not to include the J $\lambda$ 7 primer. The PCR assay for the detection of *IGL* gene rearrangements in clonality study therefore consists of a single tube containing three primers (Figure 7b). This single tube was expected to detect the vast majority of the rearrangements.

### Results of initial testing phase

Initial testing on a set of monoclonal and polyclonal samples showed they could be discriminated very well upon heteroduplex analysis of PCR products on 10% polyacrylamide gel electrophoresis (Figure 7c). Clonal *IGL* rearrangements were seen in the homoduplex region, with one or sometimes two weaker bands in the heteroduplex region, while polyclonal rearrangements appeared as a smear in the heteroduplex region (Figure 7c). Nonspecific bands were not observed. It should be noted that because of the limited size of the junctional region, it is extremely difficult to distinguish polyclonal from monoclonal rearrangements by running a simple polyacrylamide gel without performing a heteroduplex formation. Along this line, the analysis of PCR products by GeneScanning proved to be less straightforward (Figure 7c). While monoclonal rearrangements were clearly identified, the polyclonal rearrangement pattern had an oligoclonal aspect due to the limited junctional diversity. The interpretation was more difficult, particularly to distinguish polyclonal cases from those with a minor clonal B-cell population in a background of polyclonal B cells. We therefore

recommend heteroduplex analysis as the method of choice to analyze *IGL* gene rearrangements.

The sensitivity of the assay, performed on several cases, proved to be about 5% (2.5–10%) when dilution of tumor DNA was carried out in PB-MNC and about 10% (5–20%) when diluted in lymph node DNA.

### Results of general testing phase

The single-tube *IGL* PCR assay was evaluated on the series of 90 Southern blot defined lymphoid proliferations. This testing was carried out by nine laboratories, four with heteroduplex analysis only, one with GeneScanning only, and four using both techniques. Clonal *IGL* gene rearrangements were detected in 19 cases. In 15 of them more than 70% concordance was obtained within the nine laboratories. In four cases less than 70% concordance was obtained, which could be explained by minor clonal *IGL* gene rearrangements in three of them (ES-12, GB-10, and FR-10). This discordance in the fourth case (PT-11) remained unexplained, particularly because no *IGL* gene rearrangements were detected by Southern blotting. As concluded from the initial testing, interpretation of GeneScanning was more difficult than heteroduplex analysis, especially in the case of minor clonal populations. Of these 19 clonal *IGL* gene cases, 17 were B-cell proliferations (16 mature and one precursor B-cell). One case (ES-12) corresponded to Hodgkin's disease and another (FR-10) to a T-NHL. Both had only a minor clonal *IGL* gene rearrangement, and FR-10 also displayed a clonal *IGK* gene rearrangement.

Comparison with Southern blot data showed some discrepancies. Six cases with clonal *IGL* gene rearrangements by PCR appeared as polyclonal by Southern blot analysis. Three of them (PT-6, ES-12, and FR-10) concerned minor clonal populations, which may have been below the sensitivity level of the Southern blot technique. In the three other cases (NL-19, ES-1, and PT-11), a clonally rearranged band may have been missed by the

fairly complex rearrangement pattern of the *IGL* locus on Southern blot.<sup>26,81</sup> Conversely, the PCR assay failed to detect clonal rearrangements that were seen by Southern blot analysis in two cases (GBS-6 and FR-5). However, these were FCLs in which a high degree of somatic hypermutations may have prevented annealing of the *IGL* gene primers.

## Conclusion

In conclusion, the single-tube PCR assay for the detection of *IGL* gene rearrangements contains only three primers (Figure 7b), but is expected to detect the vast majority of *IGL* gene rearrangements (*V*λ1, *V*λ2, and *V*λ3 gene rearrangements). A study designed to evaluate the added value of a second PCR tube for a separate amplification of rearrangements using *V*λ4–*V*λ10 genes is currently being performed. When tested on the series of 90 Southern blot-defined cases, it did not result in the detection of any additional clonal *IGL* gene rearrangement. Finally, heteroduplex analysis is the preferred analytic method, although GeneScanning can be used, but maximal caution is recommended to avoid overinterpretation of clonality due to the limited junctional diversity.

## SECTION 5. *TCRB* gene rearrangements: *V*β–*J*β, *D*β–*J*β

M Brüggemann<sup>1</sup>, J Droese<sup>1</sup>, FL Lavender<sup>2</sup>, PJTA Groenen<sup>3</sup>, KI Mills<sup>4</sup>, E Hodges<sup>2</sup>, A Takla<sup>1</sup>, M Spaargaren<sup>5</sup>, B Martinez<sup>6</sup>, B Jasani<sup>4</sup>, PAS Evans<sup>7</sup>, GI Carter<sup>8</sup>, M Hummel<sup>9</sup>, C Bastard<sup>10</sup> and M Kneba<sup>1</sup>

<sup>1</sup>II Medizinische Klinik des Universitätsklinikums Schleswig-Holstein, Campus Kiel, Germany; <sup>2</sup>Wessex Immunology Service, Molecular Pathology Unit, Southampton University Hospitals, UK; <sup>3</sup>Department of Pathology, University Medical Center Nijmegen, The Netherlands; <sup>4</sup>Department of Haematology and Pathology, University of Wales College of Medicine, Cardiff, UK; <sup>5</sup>Department of Pathology, Academic Medical Center, Amsterdam, The Netherlands; <sup>6</sup>Molecular Pathology Program, Centro Nacional de Investigaciones Oncológicas, Madrid, Spain; <sup>7</sup>Academic Unit of Haematology and Oncology, University of Leeds, Leeds, UK; <sup>8</sup>Department of Molecular Diagnostics and Histopathology, Nottingham City Hospital, UK; <sup>9</sup>Institute of Pathology, Free University Berlin, Germany; and <sup>10</sup>Laboratoire de Genetique Oncologique, Centre Henri Becquerel, Rouen, France

## Background

Molecular analysis of the *TCRB* genes is an important tool for the assessment of clonality in suspect T-cell proliferations. *TCRB* gene rearrangements occur not only in almost all mature T-cell malignancies, but also in about 80% of the CD3<sup>+</sup> T-cell ALLs (T-ALL) and 95% of the CD3<sup>+</sup> T-ALL.<sup>28</sup> *TCRB* rearrangements are not restricted to T-lineage malignancies as about one-third of precursor B-ALL harbor rearranged *TCRB* genes.<sup>30</sup> Their frequency is much lower (0–7%) in mature B-cell proliferations.<sup>21</sup>

The human *TCRB* locus is located on the long arm of chromosome 7, at band 7q34 and spans a region of 685 kb. In contrast to the *TCRG* and *TCRD* loci, the V region gene cluster of the *TCRB* locus is far more complex (Figure 8a).<sup>1</sup> It contains

about 65 *V*β gene elements for which two different nomenclatures are used: the one summarized by Arden *et al*<sup>84</sup> follows the gene designation of Wei *et al*<sup>85</sup> and groups the *V*β genes into 34 families. The alternative nomenclature proposed by Rowen *et al*<sup>86</sup> subdivides 30 *V*β gene subgroups and was later adopted by IMGT, the international ImMunoGeneTics database <http://imgt.cines.fr> (initiator and coordinator: Marie-Paule Lefranc, Montpellier, France).<sup>62,63</sup> The largest families, *V*β5, *V*β6, *V*β8, and *V*β13 (Arden nomenclature) reach a size of seven, nine, five, and eight members, respectively. In all, 12 *V*β families contain only a single member. In general, the families are clearly demarcated from each other.<sup>84</sup> In this report, we follow the Arden nomenclature.<sup>84</sup>

Of the *V*β gene elements, 39–47 are qualified as functional and belong to 23 families. Seven to nine of the nonfunctional *V*β elements have an open-reading frame, but contain alterations in the splice sites, recombination signals, and/or regulatory elements. In all, 10–16 are classified as pseudogenes. In addition, a cluster of six nonfunctional orphan *V*β genes have been reported that are localized at the short arm of chromosome 9 (9p21).<sup>87,88</sup> They are not detected in transcripts.<sup>84,86</sup> All but one *V*β genes are located upstream of two *D*β–*J*β–*C*β clusters. Figure 8a illustrates that both *C*β gene segments (*C*β1 and *C*β2) are preceded by a *D*β gene (*D*β1 and *D*β2) and a *J*β cluster, which comprises six (*J*β1.1–*J*β1.6) and seven (*J*β2.1–*J*β2.7) functional *J*β segments. *J*β region loci are classified into two families according to their genomic localization, not to sequence similarity.<sup>85,86,89</sup>

Owing to the large germline-encoded repertoire, the combinatorial diversity of *TCRB* gene rearrangements is extensive compared to the *TCRG* and *TCRD* rearrangements. The primary repertoire of the *TCR*β molecules is further extended by an addition of an average of 3.6 (*V*β–*D*β junction) and 4.6 (*D*β–*J*β junction) nucleotides and deletion of an average of 3.6 (*V*β), 3.8 (5' of *D*β), 3.7 (3' of *D*β), and 4.1 (*J*β) nucleotides.<sup>86</sup> The complete hypervariable region resulting from the junction of the *V*β, *D*β, and *J*β segments comprises characteristically nine or 10 codons. Size variation is limited, as seven to 12 residues account for more than 80% of all functional rearrangements in contrast to the broad-length repertoire of the *IGH* CDR3 region.<sup>90</sup>

During early T-cell development, the rearrangement of the *TCRB* gene consists of two consecutive steps: *D*β to *J*β rearrangement and *V*β to *D*–*J*β rearrangement with an interval of 1–2 days between these two processes.<sup>91</sup> The *D*β1 gene segment may join either *J*β1 or *J*β2 gene segments, but the *D*β2 gene segment generally joins only *J*β2 gene segments because of its position in the *TCRB* gene locus.<sup>28,86</sup> Owing to the presence of two consecutive *TCRB* *D*–*J* clusters, it is also possible that two rearrangements are detectable on one allele: an incomplete *TCRB* *D*β2–*J*β2 rearrangement in addition to a complete or incomplete rearrangement in the *TCRB* *D*β1–*J*β1 region.<sup>1</sup>

In *TCRB* gene rearrangements, a nonrandom distribution of gene segment usage is seen. In healthy individuals, some *V*β families predominate in the PB T-cell repertoire (eg *V*β1–*V*β5), while others are only rarely used (eg *V*β11, *V*β16, *V*β18, and *V*β23). Mean values of the *V*β repertoire seem to be stable during aging, although the standard deviation increase in the elderly.<sup>13,92</sup> Also in the human thymus some *V*β gene segments dominate: the most prevalent seven *V*β genes (*V*β3-1, *V*β4-1, *V*β5-1, *V*β6-7, *V*β7-2, *V*β8-2, and *V*β13-2) cover nearly half of the entire functional *TCRB* repertoire.<sup>93</sup> The representation of *J* segments is also far from even. The *J*β2 family is used more frequently than the *J*β1 family (72 vs 28% of *TCRB* rearrangements).<sup>94</sup> In particular, the proportion of *J*β2.1 is higher than

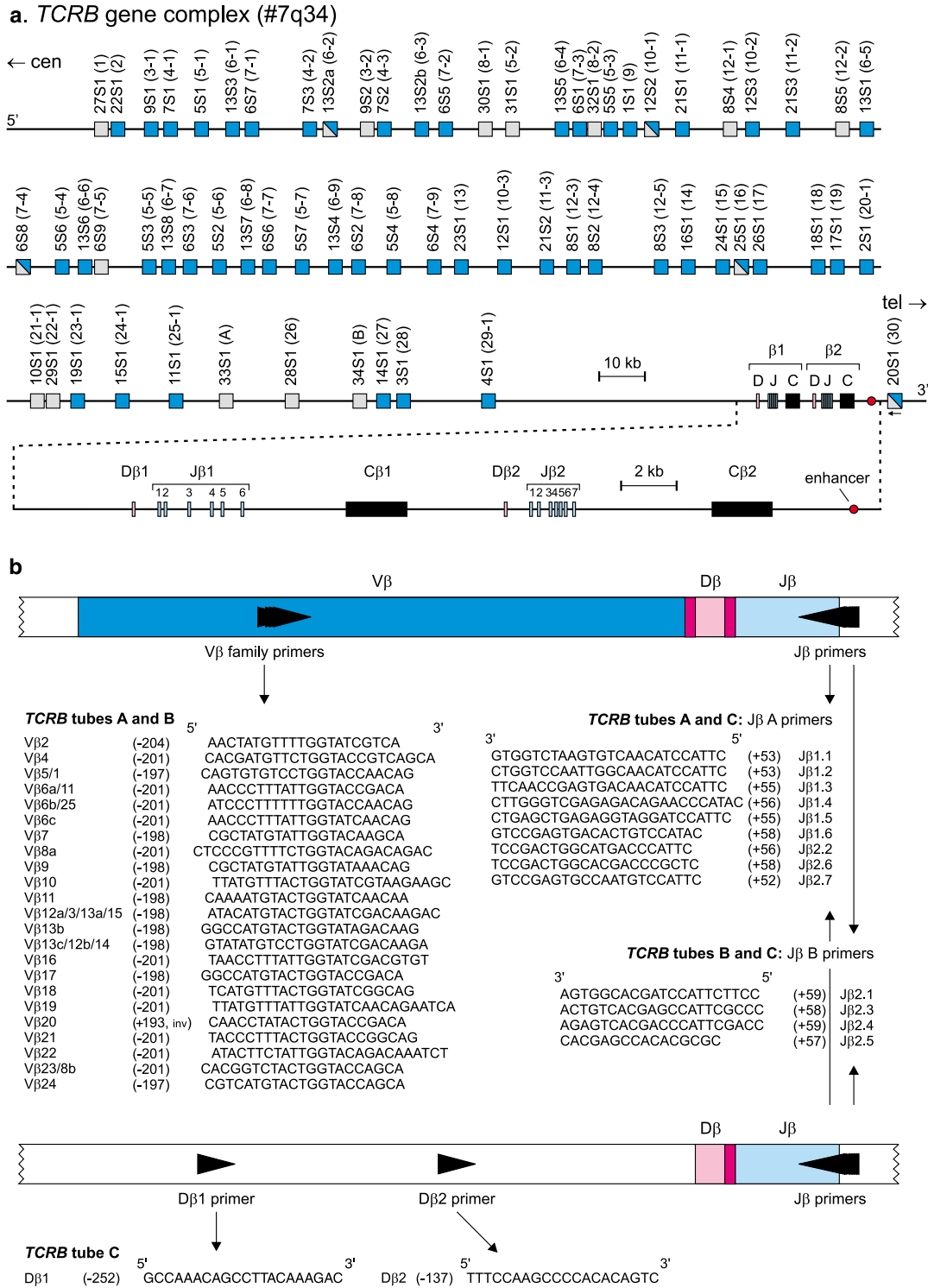
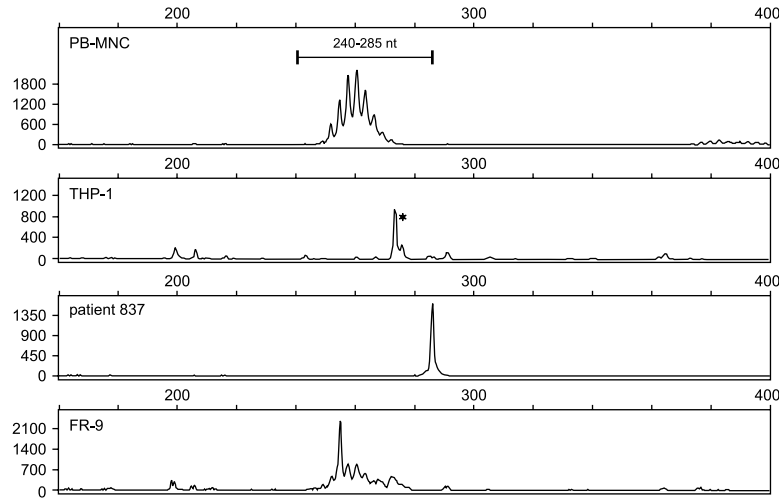
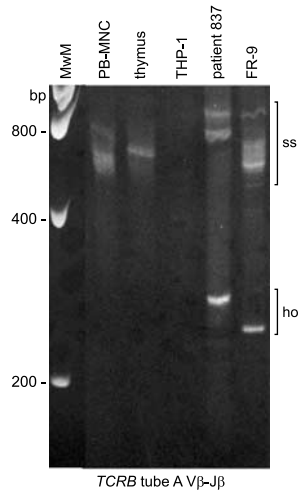
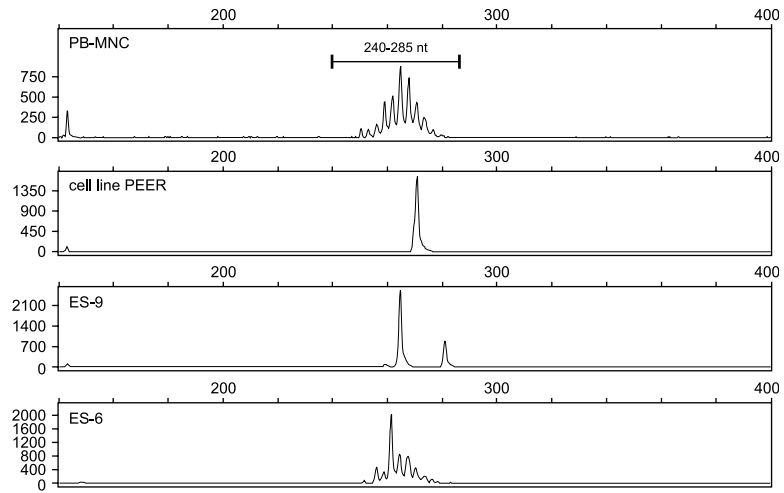
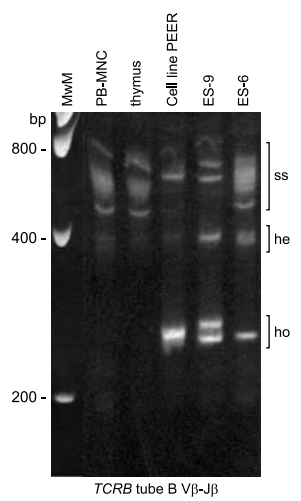


**Figure 8** PCR analysis of *TCRB* gene rearrangements. (a) Schematic diagram of the human *TCRB* locus. The gene segment designation is according to Arden *et al*<sup>64</sup> with the designation according to Rowen *et al*<sup>66</sup> and Lefranc *et al*<sup>62,63</sup> in parentheses. The figure is adapted from the international ImMunoGeneTics database.<sup>62,63</sup> Rearrangeable pseudogenes are depicted in gray, potential pseudogenes in half blue/half grey, and the remaining *Vβ* gene segments in blue. (b) Schematic diagram of *Vβ*–*Jβ* and *Dβ*–*Jβ* rearrangements. The 23 *Vβ* primers, 13 *Jβ* primers, and two *Dβ* primers are combined in three tubes: tube A with 23 *Vβ* primers and nine *Jβ* primers, tube B with 23 *Vβ* primers and four *Jβ* primers, and tube C with two *Dβ* primers and 13 *Jβ* primers. The 23 *Vβ* primers and the 13 *Jβ* primers are aligned in order to obtain comparably sized PCR products (see c and d). The *Vβ* primers cover approximately 90% of all *Vβ* gene segments. The relative position of the *Vβ*, *Dβ*, and *Jβ* primers is given according to their most 5' nucleotide upstream (–) or downstream (+) of the involved RSS. (c, d, and e) Heteroduplex analysis and GeneScanning of the same polyclonal and monoclonal cell populations, showing the typical heteroduplex smears and homoduplex bands (left panels) and the typical polyclonal Gaussian curves and monoclonal peaks (right panels). The approximate distribution of the polyclonal Gaussian curves is indicated in nt.

**c. TCRB tube A V $\beta$ -J $\beta$**



**d. TCRB tube B V $\beta$ -J $\beta$**



**e. TCRB tube C D $\beta$ -J $\beta$**

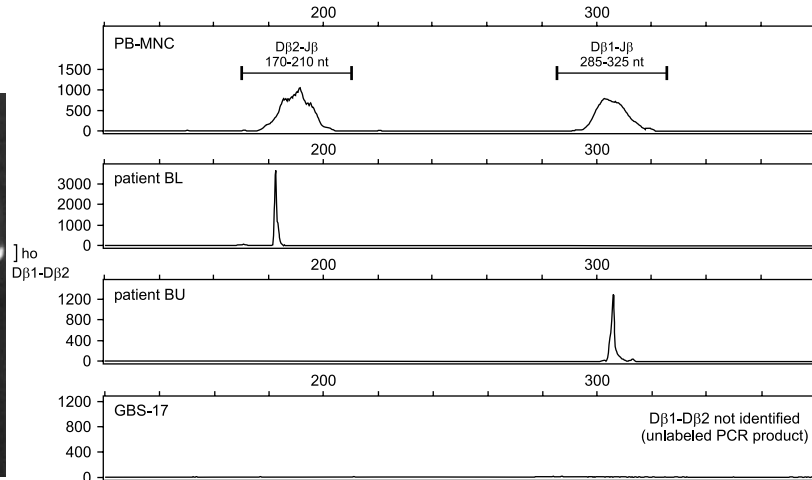
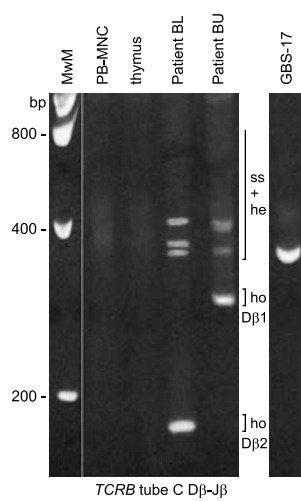


**Figure 8** Continued.

expected (24%) followed by J $\beta$ 2.2 (11%) and J $\beta$ 2.3 and J $\beta$ 2.5 (10% each).<sup>93</sup>

*TCRB* gene rearrangement patterns differ between categories of T-cell malignancies. Complete *TCRB* V $\beta$ –J $\beta$ 1 rearrangements and incompletely rearranged alleles in the *TCRB* D $\beta$ –J $\beta$ 2 cluster are seen more frequently in TCR $\alpha\beta$ <sup>+</sup> T-ALL as compared to CD3<sup>+</sup> T-ALL and TCR $\gamma\delta$ <sup>+</sup> T-ALL.<sup>28</sup> In the total group of T-ALL, the *TCRB* D $\beta$ –J $\beta$ 1 region is relatively frequently involved in rearrangements in contrast to crosslineage *TCRB* gene rearrangements in precursor-B-ALL, which exclusively involve the *TCRB* D $\beta$ –J $\beta$ 2 region.<sup>30,67</sup>

The development of monoclonal antibodies against most V $\beta$  domains has helped to identify V $\beta$  family expansions.<sup>13</sup> However, TCR gene rearrangement analysis is essential for clonality assessment in T-cell lymphoproliferative disorders. As the restricted germline-encoded repertoire of the *TCRG* and *TCRD* loci facilitates DNA-based PCR approaches, various PCR methods have been established for the detection of *TCRG* and *TCRD* gene rearrangements.<sup>95–97</sup> Nevertheless, the limited junctional diversity of *TCRG* rearrangements leads to a high background amplification of similar rearrangements in normal T cells (Section 6). The *TCRD* gene on the other hand is deleted in most mature T-cell malignancies.<sup>1</sup> Therefore, DNA-based *TCRB* PCR techniques are needed for clonality assessment. In addition, *TCRB* rearrangements are of great interest for follow-up studies of lymphoproliferative disorders, because the extensive combinatorial repertoire of *TCRB* rearrangements and the large hypervariable region enables a highly specific detection of clinically occult residual tumor cells. However, the extensive germline-encoded repertoire renders PCR assays more difficult. Some published PCR approaches use the time-consuming procedure of multiple tube approaches with a panel of family- or subfamily-specific primers.<sup>94,98</sup> Usage of highly degenerated consensus primers limits the number of detectable rearrangements that are theoretically covered by the primers because there is no single common sequence of sufficient identity to allow a reliable amplification of all possible rearrangements.<sup>42,99,100</sup> Some published assays use a nested PCR requiring an additional PCR reaction.<sup>42,100</sup> Other assays focus on the analysis of the *TCRB* V $\beta$ –D $\beta$ –J $\beta$ –C $\beta$  transcripts to limit the number of primers needed.<sup>16,98,101</sup> However, a major drawback of these mRNA-based approaches is the need for fresh or frozen material and a reverse transcription step before the PCR amplification.

We tried to overcome these limitations by creating a completely new and convenient DNA-based *TCRB* PCR. We designed multiple V $\beta$  and J $\beta$  primers, theoretically covering all functional V $\beta$  and J $\beta$  gene segments and being suitable for combination in multiplex PCR reactions. In addition, the assay should be applicable for heteroduplex analysis and GeneScanning and should also detect the incomplete *TCRB* D $\beta$ –J $\beta$  rearrangements with the same set of J $\beta$  primers. In order to avoid problems due to crosspriming, we decided to design all V $\beta$  and J $\beta$  primers at the same conserved region of each gene segment.

### Primer design

Initially, a total of 23 V $\beta$ , two D $\beta$  (D $\beta$ 1 and D $\beta$ 2) and 13 J $\beta$  (J $\beta$ 1.1–1.6 and J $\beta$ 2.1–2.7) primers were designed with all the V $\beta$  and J $\beta$  primers positioned in the same conserved region of each V $\beta$  and J $\beta$  gene segment so that the effects of cross-annealing in a multiplex reaction could be neglected. In

addition, rare polyclonal *TCRB* V $\beta$ –J $\beta$  rearrangements would not be mistaken for a clonal rearrangement even if they do not produce a fully polyclonal Gaussian peak pattern, because PCR products of all possible rearrangements are situated in the same size range.

For primer design, the rearrangeable pseudogenes or open-reading frame genes with alterations in splicing sites, recombination signals, and/or regulatory elements or changes of conserved amino acids were taken into consideration whenever possible. However, the main objective was to cover all functional V $\beta$  genes. The PE of each V $\beta$  primer was checked for every V $\beta$  gene using OLIGO 6.2 software. This led to primers that were not strictly V $\beta$  family specific. Consequently, some of the primers covered V $\beta$  gene segments of more than one family (Table 16). Primer dimerization made it necessary to split the J $\beta$  primers into two tubes. Initially, it was planned to use the primers in four sets of multiplex reactions as follows: all 23 V $\beta$  primers in combination with the six J $\beta$ 1 family primers (240–285 bp), all 23 V $\beta$  primers with the seven J $\beta$ 2 family primers (240–285 bp), D $\beta$ 1 (280–320 bp) with the six J $\beta$ 1 primers, and D $\beta$ 1 (285–325 bp) plus D $\beta$ 2 (170–210 bp) with the seven J $\beta$ 2 family primers.

### Results of initial testing phase

Initial monoplex testing of each possible primer combination was carried out using samples with known monoclonal *TCRB* rearrangements and polyclonal controls. PCR products of the expected size range were generated with differences in product intensity and signal profile for polyclonal samples depending on the frequency of usage of distinct V $\beta$  and J $\beta$  gene segments. However, when the primers were combined in a multiplex reaction, some J $\beta$ 2 rearrangements in particular were missed and nonspecific products in the tubes B and D were observed. In addition, cross-priming between the J $\beta$ 1 and J $\beta$ 2 primers resulted in interpretation problems. As a consequence, the J $\beta$ 2 primers had to be redesigned and the primer combinations in the different tubes had to be rearranged: J $\beta$  primers J $\beta$ 2.2, 2.6, and 2.7 were slightly modified and added to tube A. The localization of the primers J $\beta$ 2.1, 2.3, 2.4, and 2.5 was shifted by 4 bp downstream to avoid primer dimerization and crosspriming with the remaining J $\beta$  primers. Only nonspecific bands with varying intensity outside the expected size range persisted in tube B (bands: 150 bp, 221 bp) and tube C (128 bp, 337 bp) using specific template DNA. As these nonspecific amplification products were outside the size ranges of the *TCRB*-specific products, they did not affect interpretation and were considered not to be a problem. However, using nonspecific template controls one additional 273 bp nonspecific peak in tube A was inconsistently visible by GeneScanning. This product is completely suppressed when the DNA contains enough clonal or polyclonal *TCRB* rearrangements, but can appear in samples comprising low numbers of lymphoid cells. In the initial testing phase, relatively faint V $\beta$ –D $\beta$ –J $\beta$  PCR products were generated. Thus, we optimized PCR conditions for complete V $\beta$ –D $\beta$ –J $\beta$  rearrangements by increasing MgCl<sub>2</sub> concentration and the amount of *Taq* polymerase. Also usage of highly purified primers and application of ABI Buffer II instead of ABI Gold Buffer turned out to be extremely important. For the detection of the incomplete D $\beta$ –J $\beta$  rearrangements, it was finally possible to mix all J $\beta$  primers into one tube without the loss of sensitivity or informativity. Consequently, the total number of multiplex reactions needed was reduced to three tubes.

**Table 16** TCRBV primers, the recognized TCRBV genes segments, and their position relative to the RSS

Primer <sup>a</sup>	Covered gene segments			Primer <sup>a</sup>	Covered gene segments			Primer <sup>a</sup>	Covered gene segments		
	Arden	IMGT	Position <sup>b</sup>		Arden	IMGT	Position <sup>b</sup>		Arden	IMGT	Position <sup>b</sup>
V $\beta$ 2	BV2S1	20-1	-204	V $\beta$ 7	BV7S1	4-1	-198	V $\beta$ 13b	BV13S5	6-4	-198
V $\beta$ 4	BV4S1	29-1	-201		BV7S2	4-3	-198		BV13S4	6-9	-198
					BV7S3	4-2	-198	V $\beta$ 12b/ 13c/14	BV12S2	10-1	-198
V $\beta$ 1/5	BV1S1	9	-197	V $\beta$ 8a	BV8S1	12-3	-201		BV12S3	10-2	-198
	BV5S1	5-1	-197		BV8S2	12-4	-201		BV13S1	6-5	-198
	BV5S2	5-6	-197		BV8S3	12-5	-201		BV13S4	6-9	-198
	BV5S3	5-5	-197		BV8S4	12-1	-201		BV13S7	6-8	-195
	BV5S4	5-8	-197	V $\beta$ 9	BV9S1	3-1	-198		BV14S1	27	-200
	BV5S5	5-3	-197		BV9S2	3-2	-198	V $\beta$ 16	BV16S1	14	-201
	BV5S6	5-4	-197	V $\beta$ 10	BV10S1	21-1	-201	V $\beta$ 17	BV17S1	19	-198
	BV5S7	5-7	-197					V $\beta$ 18	BV18S1	18	-201
V $\beta$ 6a/11	BV6S1	7-3	-202	V $\beta$ 11	BV11S1	25-1	-198	V $\beta$ 19	BV19S1	23-1	-201
	BV6S3	7-6	-201					V $\beta$ 20	BV20S1	30	+193 (inv)
	BV6S4	7-9	-201	V $\beta$ 3/12a/ 13a/15	BV3S1	28	-199	V $\beta$ 21	BV21S1	11-1	-201
	BV6S5	7-2	-201		BV12S1	10-3	-198		BV21S2	11-3	-191
	BV6S7	7-1	-201		BV13S2a	6-2	-198		BV21S3	11-2	-201
	BV6S8	7-4	-201		BV13S2b	6-3	-198	V $\beta$ 22	BV22S1	2	-201
	BV6S9	7-5	-199		BV13S3	6-1	-198	V $\beta$ 23/8b	BV8S5	12-2	-201
V $\beta$ 6b/25	BV6S2	7-8	-201		BV13S6	6-6	-198		BV23S1	13	-201
	BV25S1	16	-201					V $\beta$ 24	BV24S1	15	-197
V $\beta$ 6c	BV6S6	7-7	-201		BV13S8	6-7	-198				
					BV15S1	24-1	-199				

<sup>a</sup>The nomenclature of the primers corresponds to the nomenclature by Arden *et al.*<sup>84</sup><sup>b</sup>Position of the primer according to the most 5' nucleotide upstream (–) of the involved RSS.

The finally approved primer set is (Figure 8b):

- Tube A:** 23 V $\beta$  primers and nine J $\beta$  primers: J $\beta$ 1.1–1.6, 2.2, 2.6, and 2.7.
- Tube B:** 23 V $\beta$  primers and four J $\beta$  primers: J $\beta$ 2.1, 2.3, 2.4, and 2.5.
- Tube C:** D $\beta$ 1, D $\beta$ 2, and all 13 J $\beta$  primers.

As tubes A and C contain J $\beta$ 1 and J $\beta$ 2 primers, differential labeling of J $\beta$ 1 and J $\beta$ 2 primers with different dyes (TET for J $\beta$ 1.1–1.6 and FAM for J $\beta$ 2.1–2.7 primers) allows GeneScanning discrimination of J $\beta$ 1 or J $\beta$ 2 usage in tubes A and C reactions (see Discussion).

Sensitivity testing was performed via dilution experiments with various cell lines and patient samples with clonally rearranged *TCRB* genes in MNC. Single PCR dilution experiments generally reached sensitivity levels of at least 0.1–1%. As expected, the sensitivity decreased in multiplex testing, probably due to an increase of background amplification. Especially in GeneScanning this background hampered interpretation due to the relative small length variation of the *TCRB* PCR products. Nevertheless, in 33 of 36 positive controls tested, a sensitivity of at least 1–10% was reached using heteroduplex analysis or GeneScanning (Table 17).

### Results of general testing phase

In all, 11 groups participated in the analysis of DNA from a series of 90 Southern blot-defined malignant and reactive lymphoproliferative disorders using the *TCRB* multiplex protocol (Figure 8c–e). Every sample was analyzed by heteroduplex analysis in two laboratories and in six labs using GeneScanning. Another three laboratories used both techniques for PCR

analysis. This testing phase as well as experience from use of these *TCRB* PCR assays in Work Package 2 of the BIOMED-2 project raised some general issues about the protocol that were in part already described in the initial testing phase: (1) The limited length variation of the *TCRB* PCR products may hamper GeneScanning detection of clonal signals within a polyclonal background. (2) Only bands/peaks within the expected size range represent clonal *TCRB* gene rearrangements. Especially for tube A, a nonspecific control DNA must be included to define the nonspecific 273 bp peak that may occur in situations without competition (Figure 8c). (3) It is extremely important to use highly purified primers and ABI Buffer II (and not ABI Gold Buffer) for good PCR results as well as the recommended PCR product preparation protocol for heteroduplex analysis.

Of the 90 Southern blot-defined cases submitted for Work Package 1, 29 were Southern blot positive for monoclonal *TCRB* rearrangements. Of these cases, 25 (86%) displayed dominant PCR products after heteroduplex analysis and 23 (79%) after GeneScanning, indicating the presence of clonal *TCRB* gene rearrangements. One of the GeneScanning-negative heteroduplex analysis-positive cases (FR-9) was interpreted as monoclonal on GeneScanning by four of the nine laboratories involved in the general testing phase (Figure 8c). However, due to a significant polyclonal background, interpretation of the GeneScanning patterns was difficult in this particular case. The other GeneScanning-negative heteroduplex analysis-positive case displayed an atypical PCR product in tube C with a size of about 400 bp (Figure 8e). The PCR product was clearly visible in agarose gels and heteroduplex analysis but not by GeneScanning. After DNA sequencing of this fragment, a *TCRB* D $\beta$ 1–D $\beta$ 2 amplification product was identified explaining the unlabelled PCR product. Four Southern blot-positive cases (NL-15, NL-16, GBN-2, and FR-6) were neither detected by GeneScanning nor

**Table 17** Sensitivity of the detection of clonal *TCRB* rearrangements

<i>TCRB</i> tube	Involved primer pair		Clonal Control	Size of PCR product	Sensitivity of detection	
	V	J			Single PCR (%) <sup>a</sup>	Multiplex PCR (%)
Tube A	V $\beta$ 2	J $\beta$ 1.2	Patient	261 nt	1–5	5
	V $\beta$ 2	J $\beta$ 1.3	Patient	267 nt	5	5
	V $\beta$ 2	J $\beta$ 1.6	Patient	267 nt		<5
	V $\beta$ 7	J $\beta$ 2.2	Patient	254 nt		10
	V $\beta$ 8a	J $\beta$ 1.2	JURKAT	267 nt	0.1	0.5–1
	V $\beta$ 8a	J $\beta$ 2.7	Patient	264 nt		10
	V $\beta$ 10	J $\beta$ 2.7	PEER	263 nt		20
	V $\beta$ 3/12a/13a/15	J $\beta$ 1.6	Patient	278 nt	<5	5
	V $\beta$ 3/12a/13a/15	J $\beta$ 2.7	Patient	286 nt		10
	V $\beta$ 17	J $\beta$ 2.7	RPMLI-8402	260 nt		10
	V $\beta$ 17	J $\beta$ 1.1	Patient	260 nt	1	10
	V $\beta$ 18	J $\beta$ 1.2	DND-41	261 nt	1	10
	V $\beta$ 22	J $\beta$ 1.1	Patient	265 nt	0.1	10
	V $\beta$ 8b/23	J $\beta$ 1.2	HUT78 (H9)	257 nt	0.1	0.5
	V $\beta$ 24	J $\beta$ 1.5	RPMLI-8402	264 nt	0.5	10
Tube B	V $\beta$ 2	J $\beta$ 2.1	MOLT-4	267 nt	5	5
	V $\beta$ 1/5	J $\beta$ 2.1	Patient	266 nt	5	1–5
	V $\beta$ 6a/11	J $\beta$ 2.1	Patient	265 nt	1	5
	V $\beta$ 6a/11	J $\beta$ 2.5	Patient	258 nt		5
	V $\beta$ 7	J $\beta$ 2.3	PEER	271 nt		<5
	V $\beta$ 8a	J $\beta$ 2.1	Patient	293 nt	0.1	1
	V $\beta$ 3/12a/13a/15	J $\beta$ 2.1	Patient	258 nt	5	10
	V $\beta$ 3/12a/13a/15	J $\beta$ 2.3	Patient	258 nt		<5
	V $\beta$ 16	J $\beta$ 2.1	Patient	258 nt	0.5	10
	V $\beta$ 17	J $\beta$ 2.5	CML-T1	270 nt	0.1–1	1
	V $\beta$ 21	J $\beta$ 2.3	Patient	282 nt	0.5	<10
Tube C	D $\beta$ 1	J $\beta$ 1.1	Patient	304 nt	0.10	<5
	D $\beta$ 1	J $\beta$ 1.2	Patient	306 nt	5	5
	D $\beta$ 1	J $\beta$ 1.4	Patient	310 nt		5–10
	D $\beta$ 1	J $\beta$ 1.6	Patient	320 nt		20
	D $\beta$ 1	J $\beta$ 2.1	Patient	309 nt	5	20
	D $\beta$ 1	J $\beta$ 2.7	Patient	307 nt		<5
	D $\beta$ 1	J $\beta$ 2.5	Patient	310 nt		<1
	D $\beta$ 2	J $\beta$ 1.4	Patient	182 nt		<1
	D $\beta$ 2	J $\beta$ 2.1	Patient	185 nt	1	<5
	D $\beta$ 2	J $\beta$ 2.5	Patient	191 nt		5

<sup>a</sup>The dilution experiment for assessing the sensitivity of the single PCR was not performed in each case.

by heteroduplex analysis, all of them with an underlying B lymphoid malignancy. Possibly these Southern blot detected *TCRB* gene rearrangements in B-cell malignancies involve non-functional V $\beta$  gene segments that are partially not recognized by the V $\beta$  primer set. Alternative explanations for this failure are atypical rearrangements (eg incomplete V $\beta$ –D $\beta$  rearrangements),<sup>28,102</sup> sequence variations of the rearranged V $\beta$  gene segments<sup>86</sup> or a lack of sensitivity for particular rearrangements.

Of the WP1 samples, 61 were considered to be polyclonal by Southern blot. For 60 (98%) of these cases PCR results were concordant with at least one method of analysis, for 56 (92%) cases results were concordant using both methods. The one Southern blot-negative sample (ES-14) found to be monoclonal by heteroduplex analysis and GeneScanning analysis showed an incomplete D $\beta$ 2 rearrangement. For four samples nonuniform results were obtained: one sample was considered to be clonal by GeneScanning, but only by 50% of the labs analyzing the PCR products by heteroduplex analysis (GBS-4). Three samples were found to produce weak clonal signals only by heteroduplex analysis (ES-6, (see Figure 8d), GBS-9, and DE-2). *TCRB* rearranged subclones being too small to be detected by Southern blot analysis may only be seen by the more sensitive PCR methodology. In B-cell malignancies, the detected rearrangements may also represent clonal or oligoclonal expan-

sions of residual T cells.<sup>103</sup> In this case, these weak clonal PCR products should not be regarded as an evidence of a clonal T-cell disorder. This stresses the importance of the interpretation of the PCR results in context with other diagnostic tests and the clinical picture of the patients. Optimal PCR assessment of *TCRB* rearrangements is obtained by the combined use of heteroduplex analysis and GeneScanning. Sensitivity may differ between the two detection methods as a function of clonal PCR product size compared to the polyclonal size distribution: on the one hand, heteroduplex analysis disperses the polyclonal background from the clonal products and on the other PCR products outside the main size range allow a more sensitive GeneScanning detection. Also the risk of false-positive results is reduced in the combined use of heteroduplex analysis and GeneScanning. Furthermore, heteroduplex analysis allows the detection of some additional atypical *TCRB* D $\beta$ 1–D $\beta$ 2 rearrangements that cannot be detected by GeneScanning of the PCR product as no labeled primer is involved in amplification. However, GeneScanning is in general the more informative method for samples with a high tumor load because the exact size of the monoclonal PCR product is indicated, which may be used for monitoring purposes and differentially labeled J $\beta$  primers provide additional information about J $\beta$  gene usage.



## Conclusion

In conclusion, the three-tube *TCRB* multiplex PCR system provides a new and convenient assay for clonality assessment in suspect T-cell proliferations with an unprecedentedly high clonality detection rate.

## SECTION 6. *TCRG* gene rearrangements

K Beldjord<sup>1</sup>, E Delabesse<sup>1</sup>, J Droese<sup>2</sup>, PAS Evans<sup>3</sup>, R García Sanz<sup>4</sup>, AW Langerak<sup>5</sup>, R Villuendas<sup>6</sup>, FL Lavender<sup>7</sup>, L Foroni<sup>8</sup>, BJ Milner<sup>9</sup>, D Bloxham<sup>10</sup>, M Hummel<sup>11</sup>, L Trümper<sup>12</sup>, M-H Delfau-Larue<sup>13</sup> and EA Macintyre<sup>1</sup>

<sup>1</sup>Laboratoire d'Hématologie and INSERM EMI 210, Hôpital Necker-Enfants Malades, Paris, France; <sup>2</sup>II Medizinische Klinik der Universität, Kiel, Germany; <sup>3</sup>Academic Unit of Haematology and Oncology, University of Leeds, UK; <sup>4</sup>Servicio de Hematología, Hospital Universitario de Salamanca, Spain; <sup>5</sup>Department of Immunology, Erasmus MC, Rotterdam, The Netherlands; <sup>6</sup>Molecular Pathology Program, Centro Nacional de Investigaciones Oncológicas, Madrid, Spain; <sup>7</sup>Wessex Immunology Service, Molecular Pathology Unit, Southampton University Hospitals, UK; <sup>8</sup>Department of Haematology, Royal Free Hospital, London, UK; <sup>9</sup>Department of Medicine and Therapeutics, University of Aberdeen, UK; <sup>10</sup>Department of Clinical Haematology, Addenbrooke's NHS Trust Hospital, Cambridge, UK; <sup>11</sup>Institute of Pathology, Free University Berlin, Germany; <sup>12</sup>Department of Internal Medicine, Georg August Universität, Göttingen, Germany; and <sup>13</sup>Service d'Immunologie Biologique, Hôpital Henri Mondor, Creteil, France

## Background

*TCRG* gene rearrangements have long been used for DNA PCR detection of lymphoid clonality and represent the 'prototype' of restricted repertoire targets. It is a preferential target for clonality analyses since it is rearranged at an early stage of T lymphoid development, probably just after *TCRD*,<sup>104</sup> in both *TCRαβ* and *TCRγδ* lineage precursors. It is rearranged in greater than 90% of T-ALL, T-large granular lymphocyte (LGL), and T-PLL, in 50–75% of peripheral T-NHL and mycosis fungoides but not in true NK cell proliferations. It is also rearranged in a major part of B-lineage ALLs, but much less so in B-NHL.<sup>1,30,67</sup> Unlike several other Ig/TCR loci, the complete genomic structure has been known for many years. It contains a limited number of *Vγ* and *Jγ* segments. The amplification of all major *Vγ*–*Jγ* combinations is possible with four *Vγ* and three *Jγ* primers.

The human *TCRG* locus on chromosome 7p14 contains 14 *Vγ* segments, only 10 of which have been shown to undergo rearrangement (Figure 9a). The expressed *Vγ* repertoire includes only six *Vγ* genes (*Vγ*2, *Vγ*3, *Vγ*4, *Vγ*5, *Vγ*8, and *Vγ*9), but rearrangement also occurs with the *ψVγ*7, *ψVγ*10, and *ψVγ*11 segments.<sup>105,106</sup> Rearrangement of *ψVγ*B (also known as *ψVγ*12)<sup>105</sup> is so exceptional that it is rarely used in diagnostic PCR strategies. Rearranging *Vγ* segments can be subdivided into those belonging to the *Vγ*l family (*Vγ*fl: *Vγ*2, *Vγ*3, *Vγ*4, *Vγ*5, *ψVγ*7, and *Vγ*8; overall homology >90% and highest between *Vγ*2 and *Vγ*4 and between *Vγ*3 and *Vγ*5) and the single member *Vγ*9, *ψVγ*10, and *ψVγ*11 families. The *TCRG* locus contains five *Jγ* segments: *Jγ*1.1 (*Jγ*P1), *Jγ*1.2 (*Jγ*P), *Jγ*1.3 (*Jγ*1), *Jγ*2.1 (*Jγ*P2), and

*Jγ*2.3 (*Jγ*2), of which *Jγ*1.3 and *Jγ*2.3 are highly homologous, as are *Jγ*1.1 and *Jγ*2.1.<sup>107,108</sup>

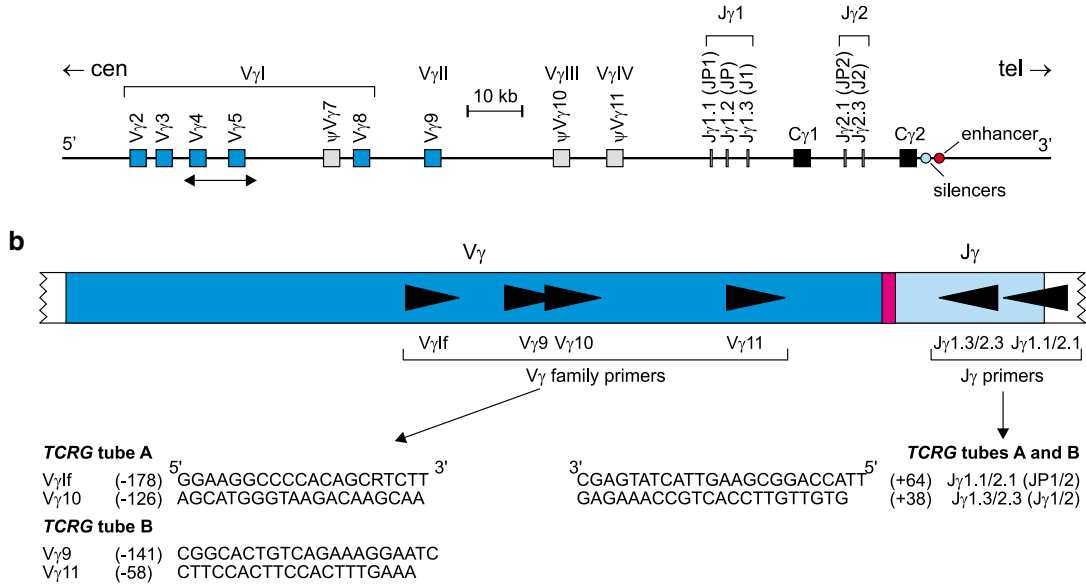
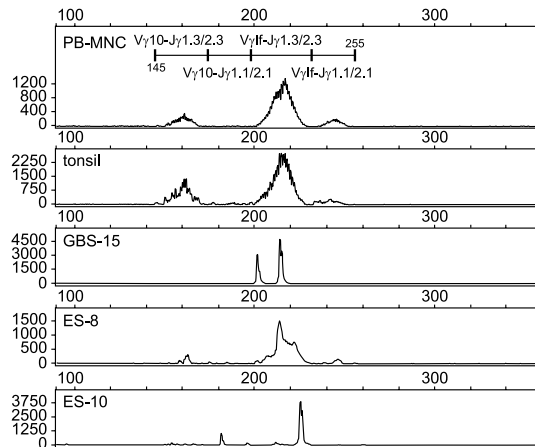
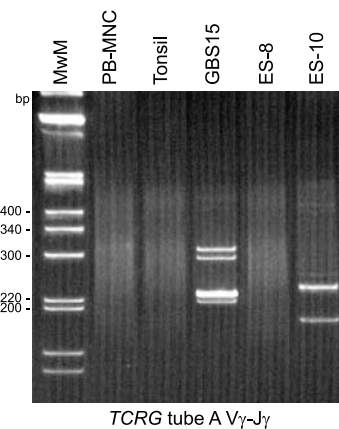
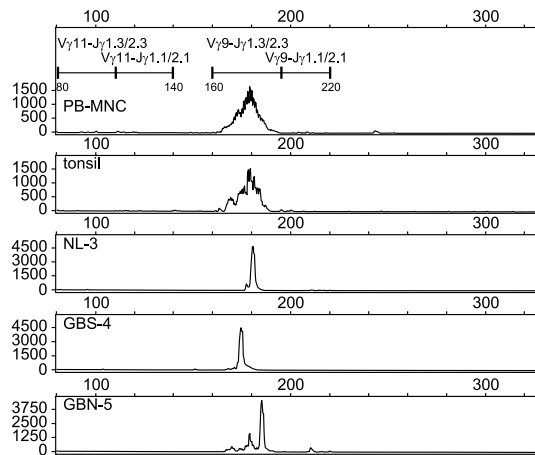
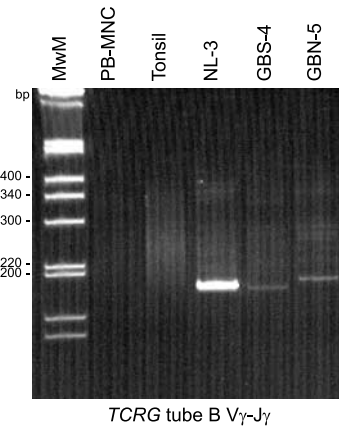
While the restricted *TCRG* germline repertoire facilitates PCR amplification, the limited junctional diversity of *TCRG* rearrangements complicates distinction between clonal and polyclonal PCR products. The *TCRG* locus does not contain D segments and demonstrates relatively limited nucleotide additions. *TCRG* V–J junctional length therefore varies by 20–30 bp, compared to approximately 60 bp for *IGH* and *TCRD*. The capacity to distinguish clonal from polyclonal *TCRG* rearrangements depends on the complexity of the polyclonal repertoire. In general, minor clonal populations using frequent *Vγ*–*Jγ* rearrangements such as *Vγ*fl–*Jγ*1.3/2.3 are at risk of being lost amidst the polyclonal repertoire, whereas rare combinations will be detected with greater sensitivity. However, occasional polyclonal T-lymphocytes demonstrating rare *Vγ*–*Jγ* rearrangements may be mistaken for a clonal rearrangement, due to the absence of a polyclonal background for that type of rearrangement. A further possible source of minor clonal populations results from the presence of *TCRγδ*-expressing T-lymphocytes demonstrating 'canonical' *TCRG* rearrangements, which do not demonstrate N nucleotide additions. The most commonly recognized human canonical *TCRG* rearrangement involves the *Vγ*9–*Jγ*1.2 segments and occurs in approximately 1% of blood T-lymphocytes.<sup>109,110</sup> It is therefore extremely important to analyze *TCRG* PCR products using high-resolution electrophoretic techniques or to separate PCR products on criteria other than purely on size, in order to reduce the risk of false-positive results. It is also important to be aware of the profile of canonical rearrangements and the situations in which they most commonly occur. Canonical *Vγ*9–*Jγ*1.2 rearrangements, for example, are found predominantly in PB and increase in frequency with age, since they result from accumulation of *TCRγδ*<sup>+</sup> T-lymphocytes.<sup>19</sup>

Unlike *TCRD*, *TCRG* is not deleted in *TCRαβ* lineage cells. Since *TCRG* rearrangements occur in both *TCRαβ* and *TCRγδ* lineage precursors, their identification cannot be used for the determination of the type of T-cell lineage. Similarly, *TCRG* rearrangements occur in 60% of B-lineage ALLs,<sup>30</sup> implying that they cannot be used for the assessment of B- vs T-cell lineage in immature proliferations. However, they occur much less frequently in mature B lymphoproliferative disorders, including the majority of B-NHL,<sup>1</sup> and might therefore be used, in combination with clinical and immunophenotypic data, to determine lineage involvement in mature lymphoproliferative disorders.

The limited germline repertoire allows determination of *Vγ* and *Jγ* segment utilization, either by Southern blot or PCR analysis. Approximate relative use of the different *Vγ* and *Jγ* segments in precursor B-ALL, T-ALL, and T-NHL is shown in Table 18.<sup>1,30,111,112</sup> The identification of *Vγ* and *Jγ* usage is not of purely academic interest, since specific amplification is required for MRD analysis.<sup>113</sup>

We undertook to develop a minimal number of multiplex *TCRG* strategies that would maintain optimal sensitivity and informativity, minimize the risk of false-positive results, and allow simple *Vγ* and *Jγ* identification, including by heteroduplex analysis or monofluorescent GeneScanning strategies. We chose to include *Vγ* primers detecting all rearranging segments other than *ψVγ*B (*ψVγ*12), given its rarity. In order to reduce the risk of falsely identifying canonical rearrangements as clonal products, we excluded the *Jγ*1.2 primer, since it is rarely involved in lymphoid neoplasms (Table 18) and is usually, although not always, associated with a *TCRG* rearrangement on the other allele.<sup>111</sup>

## a. TCRG gene complex (#7p14)

c. TCRG tube A V<sub>γ</sub>-J<sub>γ</sub>d. TCRG tube B V<sub>γ</sub>-J<sub>γ</sub>

**Figure 9** PCR analysis of TCRG gene rearrangements. (a) Schematic diagram of the human TCRG locus on chromosome band 7p14. Only the rearrangeable V<sub>γ</sub> gene segments are depicted in blue (functional V<sub>γ</sub>) or in gray (nonfunctional V<sub>γ</sub>). For the J<sub>γ</sub> gene segments, both nomenclatures are used.<sup>62,63,108</sup> (b) Schematic diagram of TCRG V<sub>γ</sub>-J<sub>γ</sub> rearrangement with four V<sub>γ</sub> primers and two J<sub>γ</sub> primers, which are divided over two tubes. The relative position of the V<sub>γ</sub> and J<sub>γ</sub> primers is indicated according to their most 5' nucleotide upstream (−) or downstream (+) of the involved RSS. (c and d) Heteroduplex analysis and GeneScanning of the same polyclonal and monoclonal cell populations, showing the typical heteroduplex smears and homoduplex bands (left panels) and the typical polyclonal Gaussian curves and monoclonal peaks (right panels). The approximate distribution of the polyclonal Gaussian curves is indicated in nt (see also Table 18).

### Primer design

We initially developed three V $\gamma$  and two J $\gamma$  primers, to be used in two multiplex reactions, as follows: one tube with J $\gamma$ 1.3/2.3 with V $\gamma$ 9-specific (160–190 bp), V $\gamma$ fl consensus (200–230 bp), and V $\gamma$ 10/11 consensus (220–250 bp) and a second tube with J $\gamma$ 1.1/2.1 with V $\gamma$ 9-specific (190–220 bp), V $\gamma$ fl consensus (230–260 bp), and V $\gamma$ 10/11 consensus (250–280 bp).

V $\gamma$  usage was to be identified by PCR product size by heteroduplex analysis. No distinction between J $\gamma$ 1.3 and J $\gamma$ 2.3 or J $\gamma$ 1.1 and J $\gamma$ 2.1 was attempted.

### Results of initial testing phase

While all V $\gamma$ –J $\gamma$  combinations gave the expected profiles on single PCR amplification, multiplex amplification led to the competition of larger PCR products, with preferential amplification of smaller fragments, and failure to detect some V $\gamma$ fl and V $\gamma$ 10/11 rearrangements. This was further complicated by a significant primer dimer formation between the V $\gamma$ 10/11 consensus and the V $\gamma$ fl primers. Competition between differently sized fragments and primer dimer formation led to unsatisfactory sensitivity and informativity, and this strategy was therefore abandoned.

We reasoned that competition would be minimized by separating the most frequently used V $\gamma$  primers (V $\gamma$ fl and V $\gamma$ 9) and combining them with V $\gamma$ 10- and V $\gamma$ 11-specific primers, respectively. The latter rearrangements are rarely used and therefore minimize competition for the predominant repertoires (Table 18). The V $\gamma$ 10/11 consensus primer was therefore replaced by two specific V $\gamma$  primers, which generated smaller PCR products (Figure 9b). By mixing J $\gamma$ 1.3/2.3 and J $\gamma$ 1.1/2.1, it was possible to maintain a two-tube multiplex that allows approximate identification on the basis of product size of V $\gamma$  usage by heteroduplex analysis, and of both J $\gamma$  and V $\gamma$  usage by GeneScanning (Table 18).

The approved set of multiplex TCRG PCR tubes with four V $\gamma$  and two J $\gamma$  primers includes:

Tube A: V $\gamma$ fl + V $\gamma$ 10 + J $\gamma$ 1.1/2.1 + J $\gamma$ 1.3/2.3.  
Tube B: V $\gamma$ 9 + V $\gamma$ 11 + J $\gamma$ 1.1/2.1 + J $\gamma$ 1.3/2.3.

The position and the sequence of the primers are shown in Figure 9b. These primers gave satisfactory amplification in both single and multiplex PCR formats and allowed the detection of virtually all known V $\gamma$ –J $\gamma$  combinations. The competition of

larger PCR fragments was no longer seen, although it cannot be excluded that some competition of V $\gamma$ 9 or V $\gamma$ fl rearrangements may occur if these are present in a minority population. Sensitivity of detection varied between 1 and 10%, as a function of the complexity of the polyclonal repertoire and the position of the clonal rearrangement relative to the polyclonal Gaussian peak.<sup>112</sup> Interpretation of  $\psi$ V $\gamma$ 11 rearrangements can be difficult, since the normal repertoire is extremely restricted and since these primitive rearrangements are often present in subclones.

As the V $\gamma$ 4 segment is approximately 40 bp longer than the other V $\gamma$ fl members and V $\gamma$ 4 rearrangements are relatively common in both physiological and pathological lymphoid cells, the polyclonal repertoire can be skewed towards larger sized fragments, and clonal V $\gamma$ 4–J $\gamma$ 1.3/2.3 rearrangements could theoretically be mistaken for V $\gamma$ fl–J $\gamma$ 1.1/2.1 rearrangements. The proximity of the different repertoires also makes V $\gamma$  and J $\gamma$  identification much more reliable if differently labeled J $\gamma$  primers are used. For example, the use of a TET-labeled J $\gamma$ 1.1/2.1 and a FAM-labeled J $\gamma$ 1.3/2.3 was tested in a single center and was shown to give satisfactory results (see Discussion). It is, however, possible to estimate V $\gamma$  and J $\gamma$  usage following GeneScanning on the basis of size alone (Figure 9c and d).

### Interstitial deletion of V $\gamma$ 2

Interstitial deletion of approximately 170 bp at the 3'-end of the V $\gamma$ 2 segment has been described in several T-ALL cases, where it has been estimated to represent approximately 5% of rearrangements. It occurs at the site of a cryptic internal heptamer.<sup>111,114,115</sup> Since this heptamer is situated at position 130, the V $\gamma$ fl primer will fail to amplify these rearrangements (Figure 9b). This was confirmed to be the case with two ALL patient, demonstrating such an internal V $\gamma$ 2 deletion. Failure to detect these rearrangements is not, however, a significant problem, since they are rare (<1% of all TCRG rearrangements) and are associated with rearrangement on the other TCRG allele.

### Positive controls

The amplification of PB-MNC represents the simplest way to verify that all primers are functional, although this can only be effectively assessed by GeneScanning. This also allows the assessment of the reproducibility and absence of competition.

**Table 18** Approximate sizes of TCRG PCR products, positive controls, and frequencies of rearrangements

TCRG tube	Type of TCRG rearrangement	Size of PCR product	Clonal controls	Frequencies of rearrangements			
				PB-MNC	PTCL <sup>a</sup>	T-ALL <sup>b</sup>	Prec.-B-ALL <sup>c</sup>
Tube A	V $\gamma$ 10–J $\gamma$ 1.3/2.3	145–175 nt	RPMI-8402 (159 nt)	+	Rare	7%	Rare
	V $\gamma$ 10–J $\gamma$ 1.1/2.1	175–195 nt	Patient	Rare	Rare	1%	Rare
	V $\gamma$ fl–J $\gamma$ 1.3/2.3	195–230 nt	PEER (212 nt)	+++	50%	60%	55%
	V $\gamma$ fl–J $\gamma$ 1.1/2.1	230–255 nt	MOLT-13 (235 nt)	++	30%	13%	18%
Tube B	V $\gamma$ 11–J $\gamma$ 1.3/2.3	80–110 nt	JURKAT (115 nt)	Rare	Rare	4%	5%
	V $\gamma$ 11–J $\gamma$ 1.1/2.1	110–140 nt	Patient	Neg	Rare	1%	2%
	V $\gamma$ 9–J $\gamma$ 1.3/2.3	160–195 nt	PEER (170 nt)	++	16%	10%	16%
	V $\gamma$ 9–J $\gamma$ 1.1/2.1	195–220 nt	Patient	Rare	Rare	Rare	2%

<sup>a</sup>Data derived from van Dongen et al.<sup>5,12,21,198</sup>

<sup>b</sup>Data derived from Szczepański et al.<sup>111</sup>

<sup>c</sup>Data derived from Szczepański et al.<sup>30</sup>

As shown in Table 18, the  $V\gamma 1\text{f1-J}\gamma 1.3/2.3$ ,  $V\gamma 1\text{f1-J}\gamma 1.1/2.1$ ,  $V\gamma 9\text{f1-J}\gamma 1.3/2.3$ , and  $V\gamma 10\text{f1-J}\gamma 1.3/2.3$  repertoires should all be detectable, to variable extents. The polyclonal  $V\gamma 9\text{f1-J}\gamma 1.1/2.1$ ,  $V\gamma 10\text{f1-J}\gamma 1.1/2.1$ , and  $V\gamma 11\text{f1-J}\gamma 1.3/2.3$  repertoires are much less complete and, by consequence, a Gaussian distribution is rare (Figure 9c and d). Polyclonal  $V\gamma 11\text{f1-J}\gamma 1.1/2.1$  rearrangements are not seen. The assessment of sensitivity is commonly performed using cell lines diluted into polyclonal lymphocytes. The type and size of representative rearrangements in common T-cell lines is shown in Table 18; patient material can obviously also be used.

### Results of general testing phase

Given the limited germline *TCRG* repertoire and the restricted junctional diversity, reactive T-lymphocytes that have undergone *TCRG* rearrangements using a single  $V\gamma$  and  $J\gamma$  segment with variable CDR3 sequences that are of uniform length, will migrate as an apparent clonal population by GeneScanning. Heteroduplex analysis formation will disperse these rearrangements more easily and will therefore prevent their erroneous interpretation as evidence of lymphoid clonality. In contrast, GeneScanning provides improved resolution and sensitivity compared to heteroduplex analysis. For these reasons, optimal assessment of *TCRG* rearrangements requires both heteroduplex analysis and GeneScanning analysis. If this is not possible, heteroduplex analysis alone is probably preferable, since it might be associated with a risk of false-negative results, whereas GeneScanning alone will increase the risk of false-positive results.

Of the 18 *TCRG* rearrangements detected by Southern blotting in the 90 cases (Table 8), 16 were also detected by PCR. The minor  $V\gamma 1\text{f1-J}\gamma 1.3/2.3$  rearrangement detected by Southern blot analysis in the NL-1 oligoclonal case was only detected by PCR in a proportion of laboratories performing GeneScanning. A major  $V\gamma 9\text{f1-J}\gamma 1.3/2.3$  rearrangement detected in GBS-6 was found to be polyclonal by both heteroduplex analysis and GeneScanning in all laboratories and, as such, probably represents a false-negative PCR result or polyclonal  $V\gamma 9\text{f1-J}\gamma 1.3/2.3$  rearrangements, falsely detected as clonal by Southern blotting.

Comparison of allele identification showed that, for all alleles identified by Southern blotting, PCR  $V\gamma$  and  $J\gamma$  identification on the basis of size gave concordant results. Seven rearrangements were detected by Southern blotting, but precise allele identification was not possible. Six of these were due to  $J\gamma 1.1/2.1$  usage, suggesting that PCR allows preferential detection of this type of rearrangement.

In all, 72 samples were considered to be polyclonal by Southern blotting. Of these, 16 (22%) demonstrated a total of 24 rearrangements by *TCRG* PCR. Of these, 13 (81%) were B lymphoid proliferations. Of the 24 clonal rearrangements, 16 were minor, with 15 only being detected by GeneScanning in the majority of laboratories. It is worth noting that, of these minor rearrangements, nine (39%) involved the  $\psi V\gamma 10$  segment and eight (33%)  $V\gamma 9$ .  $\psi V\gamma 11$  rearrangements were not detected. No  $\psi V\gamma 10$  rearrangements were detected by Southern blot analysis. PCR therefore allowed more sensitive detection of minor clonal  $\psi V\gamma 10$  rearrangements, particularly by GeneScanning. It is likely that these rearrangements represent residual, predominantly  $TCR\alpha\beta$  lineage, T-lymphocytes with a restricted repertoire, which may or may not be related to the underlying B lymphoid malignancy. These minor peaks should obviously not be interpreted as an evidence of a clonal T-cell disorder. They emphasize the importance of understanding the nature of *TCRG*

rearrangements before using this locus as a PCR target in the lymphoid clonality diagnostic setting. Consequently, it is also extremely important to interpret *TCRG* gene results within their clinical context.

### Conclusion

In conclusion, the two *TCRG* multiplex tubes allow the detection of the vast majority of clonal *TCRG* rearrangements. The potential risk of false-positive results due to overinterpretation of minor clonal peaks can be minimized by the combined use of heteroduplex analysis and GeneScanning and by interpreting results within their clinical context, particularly when the apparent clonality involves the  $\psi V\gamma 10$  and  $\psi V\gamma 11$  segments. The relative merits of *TCRG* compared to *TCRB* analysis for the detection of clonal T lymphoproliferative disorders should be studied prospectively. They are likely to represent complementary strategies.

### SECTION 7. *TCRD* gene rearrangements: $V\delta\text{-D}\delta\text{-J}\delta$ , $D\delta\text{-D}\delta$ , $V\delta\text{-D}\delta$ , and $D\delta\text{-J}\delta$

FL Lavender<sup>1</sup>, E Hodges<sup>1</sup>, KI Mills<sup>2</sup>, HE White<sup>1</sup>, T Flohr<sup>3</sup>, M Nakao<sup>3</sup>, AW Langerak<sup>4</sup>, PJTA Groenen<sup>5</sup>, R Villuendas<sup>6</sup>, BA Jennings<sup>7</sup>, BJ Milner<sup>8</sup>, D Bloxham<sup>9</sup>, J Droese<sup>10</sup>, EA Macintyre<sup>11</sup>, K Beldjord<sup>11</sup>, F Davi<sup>12</sup> and JL Smith<sup>1</sup>

<sup>1</sup>Wessex Immunology Service, Molecular Pathology Unit, Southampton University Hospitals NHS Trust, UK; <sup>2</sup>Department of Haematology, University of Wales College of Medicine, Cardiff, UK; <sup>3</sup>Institute of Human Genetics, University of Heidelberg, Germany; <sup>4</sup>Department of Immunology, Erasmus MC, Rotterdam, The Netherlands; <sup>5</sup>Department of Pathology, University Medical Center Nijmegen, The Netherlands; <sup>6</sup>Molecular Pathology Program, Centro Nacional de Investigaciones Oncológicas, Madrid, Spain; <sup>7</sup>Department of Medicine, Health Policy and Practise, University of East Anglia, Norwich, UK; <sup>8</sup>Department of Medicine and Therapeutics, University of Aberdeen, UK; <sup>9</sup>Department of Clinical Haematology, Addenbrooke's NHS Trust Hospital, Cambridge, UK; <sup>10</sup>II Medizinische Klinik der Universität, Kiel, Germany; <sup>11</sup>Laboratoire d'Hématologie and INSERM EMI 210, Hôpital Necker-Enfants Malades, Paris, France; and <sup>12</sup>Department of Hematology, Hôpital Pitié-Salpêtrière, Paris, France

### Background

The human *TCRD* gene locus is located on chromosome 14q11.2 between the  $V\alpha$  and  $J\alpha$  gene segments. The major part of the *TCRD* locus ( $D\delta\text{-J}\delta\text{-C}\delta$ ) is flanked by *TCRD*-deleting elements,  $\psi J\alpha$  and  $\delta\text{REC}$  such that rearrangement of the deleting elements to each other or rearrangement of  $V\alpha$  to  $J\alpha$  gene segments causes deletion of the intermediate *TCRD* gene locus (Figure 10a). The germline-encoded *TCRD* locus consists of  $8V\delta$ ,  $4J\delta$ , and  $3D\delta$  gene segments, of which at least five of the eight  $V\delta$  gene segments can also rearrange to  $J\alpha$  gene segments.<sup>116</sup> Other  $V\alpha$  gene segments may also be utilized in *TCRD* gene rearrangements in rare cases. The WHO-IUIS nomenclature<sup>117</sup> for TCR gene segments uses a different numbering system for those V genes used mainly or exclusively in  $TCR\delta$  chains from those that can be used in either  $TCR\alpha$  or

TCR $\delta$  chains. Thus, *TCRDV101S1* (V $\delta$ 1), *TCRDV102S1* (V $\delta$ 2), and *TCRDV103S1* (V $\delta$ 3) are used almost exclusively in *TCRD* rearrangements, whereas *TCRADV6S1* (V $\delta$ 4), *TCRADV21S1* (V $\delta$ 5), and *TCRADV17S1* (V $\delta$ 6) can be used in either TCR $\delta$  or  $\alpha$  chains. *TCRADV28S1* (V $\delta$ 7) and *TCRADV14S1* (V $\delta$ 8) are used extremely rarely in *TCRD* rearrangements.

The germline-encoded repertoire of the TCR $\gamma\delta^+$  T cells is small compared to the TCR $\alpha\beta^+$  T cells and the combinatorial repertoire is even more limited due to preferential recombination in PB and thymocyte TCR $\gamma\delta^+$  T cells. At birth, the repertoire of cord blood TCR $\gamma\delta^+$  T cells is broad, with no apparent restriction or preferred expression of particular V $\gamma$ /V $\delta$  combinations. During childhood, however, the PB TCR $\gamma\delta^+$  T-cell repertoire is strikingly shaped so that V $\gamma$ 9/V $\delta$ 2 cells clearly dominate in adults.<sup>118</sup> Studies have shown that V $\delta$ 1 and V $\delta$ 2 repertoires become restricted with age leading to the appearance of oligoclonal V $\delta$ 1<sup>+</sup> and V $\delta$ 2<sup>+</sup> cells in blood and intestine.<sup>119</sup> TCR $\gamma\delta^+$  T cells are evenly distributed throughout human lymphoid tissues, but there is preferential expression of particular V $\delta$  segments in specified anatomical localizations. Notably, most intraepithelial TCR $\gamma\delta$  T cells occurring in the small intestine and in the colon express V $\delta$ 1. Similarly, V $\delta$ 1 is expressed by normal spleen TCR $\gamma\delta^+$  T cells, but TCR $\gamma\delta^+$  T cells in the skin express the V $\delta$ 2 gene.<sup>120–123</sup>

Although the small number of V, D, and J gene segments available for recombination limits the potential combinatorial diversity, the CDR3 or junctional diversity is extensive due to the addition of N regions, P regions, and random deletion of nucleotides by recombinases. This diversity is also extended by the recombination of up to three D $\delta$  segments and therefore up to four N regions within the rearranged *TCRD* locus. This limited germline diversity encoded at the *TCRD* locus in conjunction with extensive junctional diversity results in a useful target for PCR analysis and *TCRD* recombination events have been used most extensively as clonal markers in both T- and B-cell ALL.<sup>124,125</sup> The *TCRD* locus is the first of all TCR loci to rearrange during T-cell ontogeny. The first event is a D $\delta$ 2–D $\delta$ 3 rearrangement, followed by a V $\delta$ 2–(D $\delta$ 1–D $\delta$ 2)–D $\delta$ 3 rearrangement, and finally V $\delta$ –D $\delta$ –J $\delta$  rearrangement. Immature rearrangements (V $\delta$ 2–D $\delta$ 3 or D $\delta$ 2–D $\delta$ 3) occur in 70% of precursor B-ALL (and are therefore nonlineage restricted),<sup>30</sup> while there is a predominance of mature rearrangements comprising incomplete D $\delta$ 2–J $\delta$ 1 and complete V $\delta$ 1, V $\delta$ 2, V $\delta$ 3 to J $\delta$ 1 found in T-ALL.<sup>23,126</sup> Thus, specific primer sets can be used to identify different types of complete and incomplete rearrangements corresponding to different types of ALL (Table 19).<sup>127</sup>

TCR $\gamma\delta^+$  T-ALL form a relatively small subgroup of ALL, representing 10–15% of T-ALL, but still only constitute 2% of all ALL. V $\delta$ 1–J $\delta$ 1 rearrangements predominate in TCR $\gamma\delta^+$  T ALL; interestingly, V $\delta$ 1 is never found in combination with J $\delta$  segments other than J $\delta$ 1.<sup>15,20</sup> Other recombinations occur in less than 25% of alleles. Furthermore, V $\delta$ 1–J $\delta$ 1–C $\delta$  chains are almost always disulfide linked to either V $\gamma$ 1 or V $\gamma$ 11 gene families recombined to J $\gamma$ 2.3–C $\gamma$ 2. Such gene usage is consistent with the immature thymic origin of these leukemic cells.

Most T-cell lymphomas express TCR $\alpha\beta$ , while the minority express TCR $\gamma\delta$  and comprise of several distinct entities. Peripheral T-cell lymphomas (PTCL)-expressing TCR $\gamma\delta$  comprise 8–13% of all PTCL, and V $\delta$ 1–J $\delta$ 1 as well as other V $\delta$  to J $\delta$ 1 recombinations have been documented (Table 19).<sup>128,129</sup> Hepatosplenic  $\gamma\delta$  T-cell lymphoma is derived from splenic TCR $\gamma\delta$  T cells that normally express V $\delta$ 1. It is an uncommon entity that exhibits distinctive clinicopathologic features, and gene usage analysis has indicated clonal V $\delta$ 1–J $\delta$ 1 rearrangements associated with these lymphomas.<sup>130</sup> Furthermore, the

rare type of cutaneous TCR $\gamma\delta^+$  T-cell lymphomas express V $\delta$ 2 and therefore appear to represent a clonal expansion of TCR $\gamma\delta^+$  T cells that normally reside in the skin.<sup>131</sup> Other clonal TCR $\gamma\delta$  proliferations include CD3<sup>+</sup> TCR $\gamma\delta^+$  LGL proliferations that comprise about 5% of all CD3<sup>+</sup> LGL and often show V $\delta$ 1–J $\delta$ 1 rearrangements (Table 19).<sup>132</sup>

The development of monoclonal antibodies towards FR regions of TCR $\gamma\delta$  and more recently to specific V $\delta$  gene segments has helped identify TCR $\gamma\delta^+$  T-cell populations by flow cytometric analysis,<sup>15</sup> but PCR clonality studies are still required to identify whether these populations represent clonal or polyclonal expansions.<sup>133</sup>

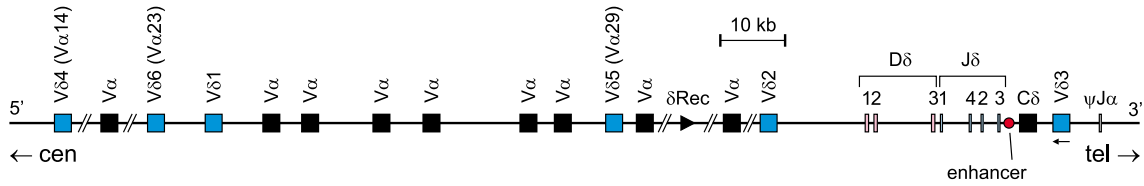
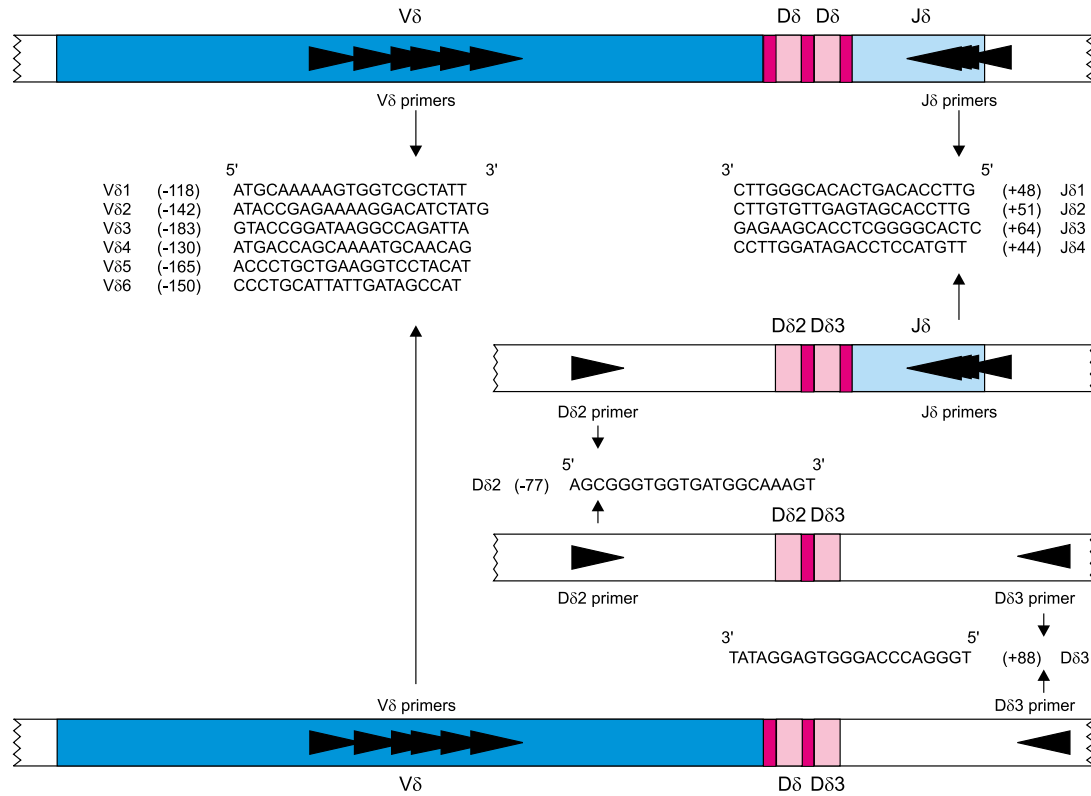
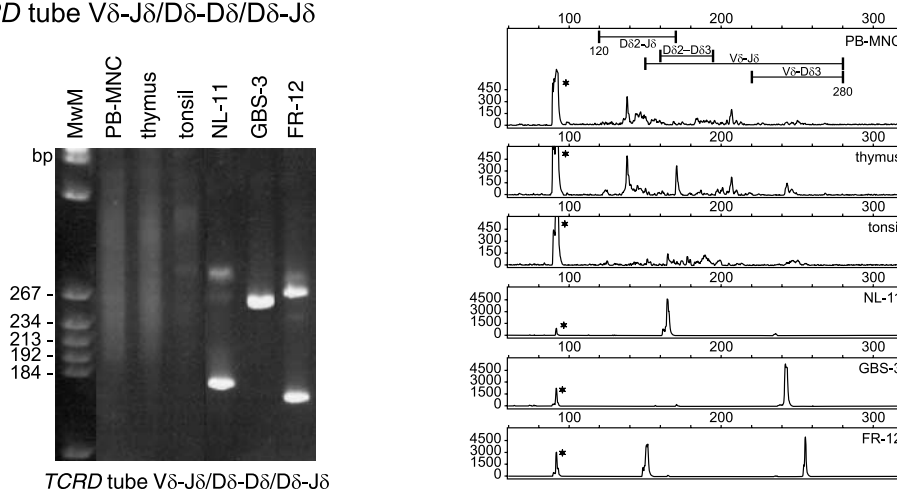
### Primer design

The *TCRD* gene segments, consisting of eight V $\delta$ , four J $\delta$ , and three D $\delta$  gene segments, show little or no homology to each other and so segment-specific primers were designed that would not crossanneal with other gene segments. Usage of V $\delta$ 7 and V $\delta$ 8 gene segments was considered too rare to justify inclusion of primers for these segments and so, following the general BIOMED-2 guidelines for primer design, a total of 16 primers were designed: six V $\delta$ , four J $\delta$ , and 5' and 3' of the three D $\delta$  gene segments (Figure 10b, Table 20). All primers were designed to multiplex together in any combination, but originally it was planned to have one tube (A) with all V and all J primers that would amplify all the complete V(D)J rearrangements, and a second tube (B) with V $\delta$ 2, D $\delta$ 2–5', D $\delta$ 3–3', and J $\delta$ 1 primers to amplify the major partial rearrangements (V $\delta$ 2–D $\delta$ 3, D $\delta$ 2–D $\delta$ 3, and D $\delta$ 2–J $\delta$ 1). Together these tubes should amplify 95% of known rearrangements. The other primers (D $\delta$ 1–5', D $\delta$ 3–5', D $\delta$ 1–3', and D $\delta$ 2–3') could be used to amplify other D $\delta$ –J $\delta$ , V $\delta$ –D $\delta$ , or D $\delta$ –D $\delta$  rearrangements, but were always intended to be optional.

### Results of initial testing phase

All primer pair combinations were tested using polyclonal DNA (tonsil and MNC).<sup>134,135</sup> Most gave products of the expected size, but some (D $\delta$ 1–5', D $\delta$ 1–3', and D $\delta$ 2–3') gave no visible product in combination with any other primer. Rearrangements involving these primer regions are likely to be extremely rare and so these, and D $\delta$ 3–5', were excluded from subsequent testing. Clonal cases for the six main rearrangements (V $\delta$ 1–J $\delta$ 1, V $\delta$ 2–J $\delta$ 1, V $\delta$ 3–J $\delta$ 1, D $\delta$ 2–D $\delta$ 3, V $\delta$ 2–D $\delta$ 3, and D $\delta$ 2–J $\delta$ 1) were tested initially in monoplex PCR and then in multiplex tubes A and B (see above). Serial dilutions of clonal DNA in polyclonal DNA (tonsil or MNC) showed detection sensitivities of at least 5% in all cases. However, in clonal cases with biallelic rearrangements, which were clearly detected in single PCR reactions, the second, usually larger, allele often failed to amplify on multiplexing. In addition, it was found, using a different set of clonal cases that several of the V $\delta$ 2–J $\delta$ 1 rearrangements failed to amplify. A polymorphic site was subsequently identified at the position of the original V $\delta$ 2 primer;<sup>136</sup> the frequency of this polymorphism in the general population is unknown, and so this primer was redesigned to a new region of the V $\delta$ 2 gene segment, retested and found to amplify all cases. The problem with the failure to amplify the second allele was overcome by increasing the MgCl<sub>2</sub> concentration from 1.5 to 2.0 mM.

We also tested the possibility of combining the two tubes into a single multiplex reaction. In total, 12 clonal cases were tested, which had a total of 21 gene rearrangements between them. A

**a. TCRD gene complex (#14q11.2)****b****c. TCRD tube Vδ-Jδ/Dδ-Dδ/Dδ-Jδ**

**Figure 10** PCR analysis of *TCRD* gene rearrangements. (a) Schematic diagram of human *TCRD* locus on chromosome band 14q11.2. The six 'classical' *Vδ* gene segments are indicated in blue, scattered between the *Vα* gene segments in black. Since *Vδ4*, *Vδ5*, and *Vδ6* are also recognized as *Vα* gene segments, their *Vα* gene code is given in parentheses. (b) Schematic diagram of *Vδ-Jδ*, *Dδ2-Jδ*, *Dδ2-Dδ3*, and *Vδ-Dδ3* rearrangements, showing the positioning of six *Vδ*, four *Jδ*, and two *Dδ* primers, all combined in a single tube. The relative position of the *Vδ*, *Dδ*, and *Jδ* primers is indicated according to their most 5' nucleotide upstream (–) or downstream (+) of the involved RSS. (c) Heteroduplex analysis (left panel) and GeneScanning (right panel) of the same polyclonal and monoclonal cell populations. The polyclonal cell populations show a vague smear in heteroduplex analysis and a complex and broad peak pattern in GeneScanning. The monoclonal bands and peaks are clearly visible. The approximate position of the PCR products of the different types of rearrangements is indicated (see also Table 20).

**Table 19** *TCRD* gene rearrangements in T-cell malignancies

<i>T-cell malignancy</i>	<i>Biallelic TCRD deletions (%)</i>	<i>At least one TCRD allele rearranged (%)</i>	<i>Dominant types of rearrangements</i>
<i>Thymic derived</i>			
CD3 <sup>-</sup> T-ALL (T-LBL)	10	80	V $\delta$ -J $\delta$ 1/D $\delta$ 2-J $\delta$ 1 V $\delta$ 2-D $\delta$ 3/D $\delta$ 2-D $\delta$ 3
TCR $\gamma$ $\delta$ <sup>+</sup> T-ALL (T-LBL)	0	100	V $\delta$ -J $\delta$ 1/D $\delta$ 2-J $\delta$ 1
TCR $\alpha$ $\beta$ <sup>+</sup> T-ALL (T-LBL)	65	35	Various
<i>Post-thymic</i>			
ATLL, CTLL, T-PLL	75-90	10-25	Various
TCR $\alpha$ $\beta$ <sup>+</sup> T-LGL	>75	<25	Various
TCR $\gamma$ $\delta$ <sup>+</sup> T-LGL	0	100	V $\delta$ 1-J $\delta$ 1/D $\delta$ 2-J $\delta$ 1
T-NHL	>75	<25	Various

**Table 20** Approximate sizes of PCR products with *TCRD* primers

	<i>J<math>\delta</math>1</i>	<i>J<math>\delta</math>2</i>	<i>J<math>\delta</math>3</i>	<i>J<math>\delta</math>4</i>	<i>D<math>\delta</math>3-3'</i>
V $\delta$ 1	170-210 nt	170-210 nt	180-220 nt	160-200 nt	~220 nt
V $\delta$ 2	200-240 nt	200-240 nt	200-240 nt	190-230 nt	~240 nt
V $\delta$ 3	230-270 nt	230-270 nt	240-280 nt	220-260 nt	~280 nt
V $\delta$ 4	180-220 nt	180-220 nt	190-230 nt	170-210 nt	~230 nt
V $\delta$ 5	220-260 nt	220-260 nt	230-270 nt	210-250 nt	~270 nt
V $\delta$ 6	200-240 nt	200-240 nt	210-250 nt	190-230 nt	~250 nt
D $\delta$ 2-5'	~130 nt	~140 nt	~150 nt	~130 nt	~190 nt

single multiplex tube containing 12 primers (six V $\delta$ , four J $\delta$ , D $\delta$ 2-5', and D $\delta$ 3-3') was used with ABI Gold Buffer and 2.0 mM MgCl<sub>2</sub> to amplify all the cases. All gene rearrangements were indeed detected with a sensitivity of 0.5-10% by heteroduplex analysis when diluted in polyclonal MNC DNA (Table 21). The only problem with combining all *TCRD* primers in a single tube was the appearance of a nonspecific band at about 90 bp in all amplifications, which was not present when the two separate multiplex tubes were used. Since the band was outside the size range of the *TCRD* products and did not interfere with interpretation, it was not considered to be a problem.

### Results of general testing phase

The testing of the 90 Southern blot-defined samples for Work Package 1 in 10 laboratories raised some general issues about the *TCRD* protocol:

- Interpretation of some GeneScanning results was difficult. Owing to the large size range of products for the *TCRD* locus, there is no classical Gaussian distribution for polyclonal samples (see Figure 10c), and this coupled with the low usage of *TCRD* in many samples meant that in some cases it was hard to determine whether a sample was polyclonal or clonal. The same problem did not arise with heteroduplex analysis and so the recommendation is that GeneScanning should only be used for *TCRD* with extreme care and awareness of the potential problems.
- The 90 bp nonspecific band was quite intense in some laboratories, but less so in others. It appeared to be weaker when using Buffer II rather than Gold Buffer (confirmed by subsequent testing) and is also sensitive to MgCl<sub>2</sub> concentration, becoming more intense as MgCl<sub>2</sub> concentration increases. This product has now been sequenced and

found to be an unrelated gene utilizing the D $\delta$ 2 and J $\delta$ 3 primers.

The results of the general testing of the 90 Southern blot-defined samples showed that the overall concordance of all the PCR groups doing the testing was very high (95%). Of the 90 cases, six were Southern blot positive for *TCRD* clonal rearrangements, five of which were found to be clonal by PCR. The remaining case (DE-10, a T-ALL with high tumor load) was found to be polyclonal by all labs. Of the 84 Southern blot-negative cases, 75 were found to be polyclonal by PCR, four were found to be clonal, and the remaining five cases showed discordance between the GeneScanning and heteroduplex analysis results. Of the clonal cases, two (DE-2 and GBS-9) were T-rich B-NHLs with presumably low tumor load and so the results may reflect the increased sensitivity of PCR over Southern blotting. The other two clonal cases (GBS-15 and ES-7) had high tumor load. Of the five cases, which showed discrepancy between the GeneScanning and heteroduplex analysis results, one (NL-1) was a difficult oligoclonal case, which caused problems for several other loci. The remaining four were found to be polyclonal by heteroduplex analysis and clonal by GeneScanning. In three of the cases (NL-13, NL-15, and NL-18) this may reflect the greater sensitivity of GeneScanning over heteroduplex analysis, but the remaining case (PT-1, a reactive lymph node) may be attributed to 'pseudoclonality' on GeneScanning because of the limited repertoire of *TCRD* usage in some samples.

### Conclusion

In conclusion, the recommended protocol for the detection of *TCRD* gene rearrangements (as indicated in Table 4) is a single-tube assay containing 12 primers for the detection of all major V $\delta$ (D) $\delta$ , V $\delta$ -D $\delta$ , D $\delta$ -D $\delta$ , and D $\delta$ -J $\delta$  rearrangements using Buffer

**Table 21** Sensitivity of detection of clonal *TCRD* gene rearrangements in single tube multiplex PCR

<i>TCRD</i> rearrangement	Clonal control sample (approximate size)	Sensitivity of detection by heteroduplex (%)
V $\delta$ 1-J $\delta$ 1	Patient (200 nt)	5
	Patient (190 nt)	1-5
	Patient (200 nt)	5
V $\delta$ 2-J $\delta$ 1	Patient (200 nt)	5
	Patient (220 nt)	5
	Patient (210 nt)	5
V $\delta$ 2-J $\delta$ 3	Patient (220 nt)	5
V $\delta$ 3-J $\delta$ 1	Patient (270 nt)	5
V $\delta$ 6-J $\delta$ 2	Loucy (210 nt)	0.5
	Patient (210 nt)	10
D $\delta$ 2-J $\delta$ 1	Loucy (150 nt)	0.2
	Patient (160 nt)	0.5
	Patient (135 nt)	0.5
D $\delta$ 2-J $\delta$ 3	Patient (150 nt)	5
D $\delta$ 2-D $\delta$ 3	NALM-16 (170 nt)	1
	Patient (200 nt)	1
	Patient (190 nt)	0.5
	Patient (170 nt)	0.5
V $\delta$ 2-D $\delta$ 3	REH (240 nt)	5-10
	NALM-16 (230 nt)	1-5
	Patient (250 nt)	5

II and 2.0 mM MgCl<sub>2</sub> to ensure maximum specificity and detection. The preferred analysis method is heteroduplex analysis, but GeneScanning may be used with care if consideration is given to the problems of pseudoclonality caused by the limited usage of *TCRD* in some samples. However, the use of multicolor GeneScanning (see Discussion) can be helpful in the rapid recognition of the different types of complete and incomplete *TCRD* rearrangements in the different types of ALL. With these limitations in mind, *TCRD* can nevertheless be a valuable PCR target for clonality studies in the more immature T-cell leukemias as well as TCR $\gamma$  $\delta$ <sup>+</sup> T-cell proliferations.

## SECTION 8. t(11;14) with *BCL1-IGH* rearrangement

P Wijers-Koster<sup>1</sup>, J Droese<sup>2</sup>, E Delabesse<sup>3</sup>, M Spaargaren<sup>4</sup>, L Hermosin<sup>5</sup>, TC Diss<sup>6</sup>, KI Mills<sup>7</sup>, BA Jennings<sup>8</sup>, BJ Milner<sup>9</sup>, D Bloxham<sup>10</sup>, TM Al Saati<sup>11</sup>, L Bassegio<sup>12</sup>, PhM Kluin<sup>1,13</sup> and E Schuurin<sup>1,13</sup>

<sup>1</sup>Department of Pathology, Leiden University Medical Center, The Netherlands; <sup>2</sup>II Medizinische Klinik der Universität Kiel, Germany; <sup>3</sup>Laboratoire d'Hématologie and INSERM EMI 210, Hôpital Necker-Enfants Malades, Paris, France; <sup>4</sup>Department of Pathology, Academic Medical Center, Amsterdam, The Netherlands; <sup>5</sup>Hematologia, Jerez de la Frontera, Spain; <sup>6</sup>Department of Histopathology, Royal Free and UCL Medical School, London, UK; <sup>7</sup>Department of Haematology, University of Wales College of Medicine, Cardiff, UK; <sup>8</sup>Department of Medicine, Health Policy and Practice, University of East Anglia, Norwich, UK; <sup>9</sup>Department of Medicine and Therapeutics, University of Aberdeen, UK; <sup>10</sup>Department of Clinical Haematology, Adden-

brooke's NHS Trust Hospital, Cambridge, UK; <sup>11</sup>Unité de Physiopathologie Cellulaire et Moléculaire, Toulouse, France; <sup>12</sup>Department of Hematology, Centre Hospitalier Lyon-Sud, Pierre-Benite, France; and <sup>13</sup>Department of Pathology, University Medical Center Groningen, The Netherlands

## Background

The t(11;14)(q13;q32) is characteristic for MCL because this cytogenetic reciprocal translocation was observed in 60-70% of MCL cases and only sporadically in other B-cell NHL.<sup>137</sup> The breakpoint region was originally cloned by Tsujimoto *et al*<sup>138</sup> and referred to as the *BCL1* region. However, in only few cases with a cytogenetic t(11;14) a genomic breakpoint in the *BCL1* region was identified. Using fiber and interphase FISH with probes covering the approximately 750 kb 11q13-*BCL1* region, in almost all MCL (33 out of 34) a breakpoint was observed and all breakpoints were confined to a region of 360 kb 5' of the cyclin D1 (*CCND1*) gene.<sup>139,140</sup> In nearly half of MCL cases (41%), the breakpoints were clustered within an 85 bp region that was referred to as the major translocation cluster region, *BCL1-MTC*.<sup>137,141,142</sup> In most, if not all, cases of MCL the break at the *IGH* locus located at 14q32 involves the JH genes juxtaposing the *IGH-E $\mu$*  enhancer to chromosome 11q13 sequences, and consequently resulting in the transcriptional activation of the cyclin D1 gene.<sup>143</sup> Cyclin D1 together with CDK4 phosphorylates (and inactivates) pRB and allows for progression through the G1 phase of the cell cycle. As cyclin D1 is silent in B-lymphocytes and B-cell NHL other than MCL, and the presence of this translocation correlates well with cyclin D1 expression, this gene is considered to be the biological relevant target in MCL.<sup>143</sup> Both expression of cyclin D1 and/or the presence of t(11;14)(q13;q32) is used as an additional tool in the differential diagnosis of NHL.<sup>2</sup> The gold standard detection strategy for the presence of the t(11;14) that will identify almost all breakpoints is interphase FISH using breakpoint-flanking probes in fresh or frozen material<sup>140</sup> as well as in archival specimens.<sup>144</sup> However, a PCR-based detection strategy for the t(11;14) might be useful for residual disease monitoring. Many groups have developed PCR-based assays to detect the *BCL1/JH* breakpoints, in general using a consensus JH primer in combination with primers in the *BCL1-MTC* region that were all located in a region of 392 bp.<sup>145,146</sup> Breaks within the *BCL1-MTC* region can occur up to 2 kb downstream of the MTC region, but the majority of breakpoints are tightly clustered within an 85 bp segment, immediately downstream of the reported most 3' primer ('primer B' in Pott *et al*<sup>141</sup> Williams *et al*<sup>145</sup>). As breaks in this *BCL1-MTC* region account for only part of the breakpoints in the 11q13-*BCL1* region in MCL cases (41%), the PCR-based strategy for t(11;14) seriously impairs the diagnostic capability with an high rate of false-negative results as compared to FISH.

The t(11;14)(q13;q32) has also been reported to be observed in several other B-cell proliferative diseases such as multiple myeloma (20%), SLVL (30%), B-PLL (33%), and B-CLL (8%).<sup>137,147,148</sup> One reason for the presence of the t(11;14) in B-CLL in some studies might be due to the incorrect classification of B-CLL.<sup>137</sup> In myeloma, the breakpoints are quite different from those in MCL because (i) the frequency is much lower; (ii) most breaks involve switch-class recombination sites; and (iii) although all tested cases are located in the same 360 kb *BCL1* region, there seems to be no preferential clustering within the *BCL1-MTC* region. On the other hand, in all cases with a break, the cyclin D1 gene is activated. Of note, in a subgroup of



multiple myelomas with a *IGH* switch-break *MYEOV*, an additional gene in the 11q13-*BCL1* region, is involved.<sup>147</sup>

### Primer design

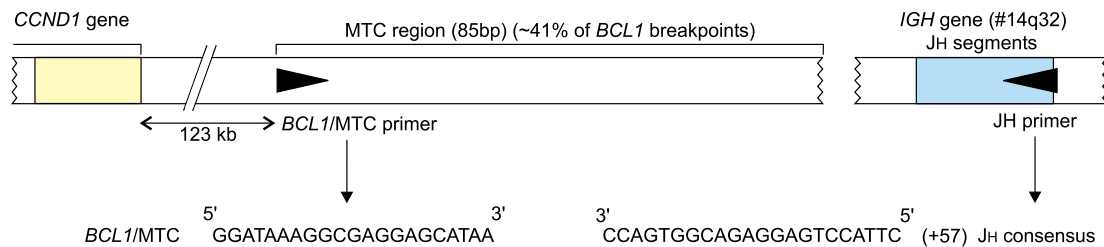
Based on the location of the reported most-far 5' breakpoint and available nucleotide sequences from the *BCL1*-MTC region (GenBank accession no. S77049), we designed a single *BCL1* primer (5'-GGATAAAGGCGAGGAGCATAA-3') in the 472-bp region 5' of this breakpoint by using the primer design program OLIGO6.2 relative to the consensus BIOMED-2-JH primer (Figure 11a).

### Results of initial testing phase

Using the consensus JH primer in combination with the single *BCL1*-MTC primer on a small series of MCL ( $n=5$ ) previously identified as positive with an in-house *BCL1*-JH PCR using a similar consensus JH18 primer<sup>149</sup> and 5'-GCACTGTCTGGATG-CACCGC-3' as *BCL1*-MTC primer, we initially compared both assays in parallel. In contrast to the analysis of Ig/TCR gene rearrangements via GeneScanning and/or heteroduplex analysis, the *BCL1*-JH PCR products (as for *BCL2*-JH products) are identified via agarose-gel electrophoresis using ethidium bro-

mid staining only. The results on the five positive and two negative samples were identical except that the BIOMED-2 PCR products were significantly weaker. To evaluate whether we could increase the sensitivity of the BIOMED-2 PCR, we determined the effect of different concentrations of MgCl<sub>2</sub> and primers, and different temperatures in a Stratagene-Robocycler PCR-machine (all other PCR were performed on ABI-480 or ABI-9700). Most intriguing was the variation due to small changes in MgCl<sub>2</sub> concentration. At 2.0 mM a weak nonspecific product of 550 bp became apparent, whereas at 2.5 mM and higher this nonspecific product was very prominent in all DNAs including nontemplate DNA controls. At lower concentrations (less than 1.5 mM) no nonspecific fragments were observed, but the expected specific products were very weak. Hybridizations with a *BCL1*-MTC internal oligoprobe (5'-ACCGAATATG-CAGTGCAGC-3') did not show hybridization to this 550 bp product. PCRs with each of the primers separately revealed that the 550 bp product could be generated by using the BIOMED-2-JH consensus primer only. In some MCL cases, in addition to the PCR products ranging from 150 to 350 bp (Figure 11b), larger specific PCR products might be apparent due to the annealing of the consensus JH primer to downstream JH5 and JH6 segments as described for *BCL2*/JH.<sup>149</sup> From the initial testing phase, the most optimal conditions for the BIOMED-2 *BCL1*-MTC/JH PCR were: annealing temperature of 60°C, 2.0 mM MgCl<sub>2</sub>, and 10 pmol of each primer (for 35 PCR cycles in the PE-9700).

#### a. *BCL1* locus (#11q13)



#### b. t(11;14) tube *BCL1* MTC-JH

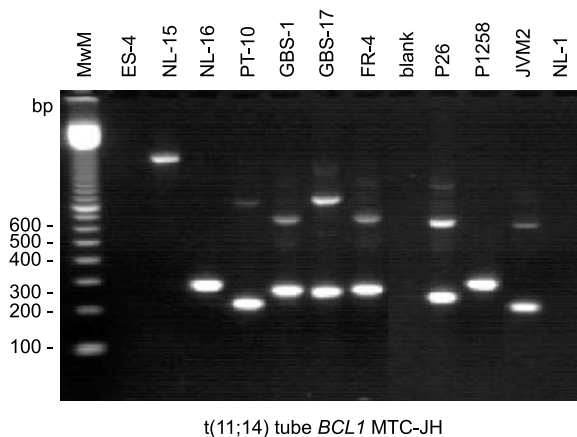


**Figure 11** Detection of *BCL1*-*IGH* rearrangements. (a) Schematic diagram of the *CCND1* gene and the *BCL1* breakpoint region MTC on chromosome band 11q13 as well as the JH gene segment on chromosome band 14q32. For the primer design in the *BCL1*-MTC region an artificial *BCL1*-MTC/JH4 junctional sequence was composed (as partially reported for JVM2<sup>150</sup>): the first 50 nucleotides as reported by Williams<sup>145</sup> were linked to nucleotides 1–439 from MTC sequence present at NCBI (accession number S77049<sup>146</sup>); the N region 'GCCC' of JVM2<sup>150</sup> was added followed by nucleotides 1921–3182 representing the JH4–JH6 genomic region (accession number J00256). (b) Agarose-gel electrophoresis of a series of *BCL1*-*IGH* PCR products from different MCL patients and the positive control cell line JVM2. The PCR products differ in size, indicating different positions of the *BCL1*-MTC breakpoints. The larger bands of lower density represent PCR products that extend to the next downstream germline JH gene segment.

To evaluate the specificity of the BIOMED-2 PCR on a larger series of cases, the *BCL1*-MTC/JH PCR was performed in three laboratories on DNA from a total of 25 cases MCL that were all previously identified as positive with in-house *BCL1*/JH PCR, and from 18 negative controls. None of the negative cases revealed a PCR product, whereas 22 of 25 positive cases showed products of the expected size. In the three cases that did not reveal a product on agarose gel, a product was detected with GeneScanning suggesting that the sensitivity is lower when compared to in-house PCR (see next paragraph).

The sensitivity of the PCR was evaluated by amplifying DNA dilutions of an MCL in normal tonsillar DNA. Sensitivity between  $10^{-3}$  and  $10^{-4}$  was observed on agarose gel using the developed PCR primers. An in-house PCR performed in parallel on the same samples was at least  $\times 10$  more sensitive. Hybridizations with the in-house *BCL1*-MTC-oligoprobe revealed a  $\times 10$ –100 higher sensitivity of both PCRs. Dilutions with DNA of an established cell line JVM2 (available through DSMZ; <http://www.dsmz.de>) with a *BCL1*-MTC/JH4 breakpoint<sup>150</sup> is used as our standard positive control. As a negative control normal tonsillar tissue or PB cells might be used, but almost any non-MCL B-cell NHL should be suitable because of the very low frequency of this aberration.<sup>137</sup>

### Results of general testing phase

To evaluate interlaboratory variations for the detection of breakpoints at the *BCL1*-MTC region, 10 groups participated in the analysis of DNA from a series of 90 histologically defined malignant and reactive lymphoproliferations (see Table 8) using the *BCL1*-MTC/JH PCR protocol. All cases were defined for their status at the Ig and TCR loci using Southern hybridization techniques. Of the 90 cases, seven were histologically characterized as MCL. All seven MCL cases were shown to have a clonal *IGH* rearrangement by Southern hybridization. The assessment of rearrangements within the *BCL1*-MTC region at chromosome 11q13 by either Southern hybridization or FISH was not performed in all cases. In six of the seven MCL cases, the PCR product was identified in all 10 laboratories. In MCL case NL-15 in six of the laboratories the expected 1.8kb PCR product was identified. This particular case carries an exceptional breakpoint with an uncommon large PCR product (normally ranging from 150 to 350bp) and represents the 3'-most-far detectable *BCL1*-MTC breakpoint to our knowledge. In two of six labs, the PCR product was observed but initially considered as nonspecific because of its uncommon size. In ES-4, characterized histologically as MCL in none of the 10 labs, a PCR product could be detected, suggesting that this case carries a breakpoint outside the *BCL1*-MTC. It should be stressed that the MCL cases submitted to this series for the general testing phase were selected and thus are expected to carry breaks at the *BCL1*-MTC region at a higher incidence than normal. Importantly, except for one single case (FR-1), in all 83 other non-MCL cases including 16 cases that were histologically characterized as B-CLL, no *BCL1*/JH PCR product was detected in any laboratory. In case FR-1 histologically characterized as B-CLL, in three of the 10 labs a product was identified indicating that the number of cells with this break is low. The *IGH* status determined by Southern blot analysis revealed that this sample was composed of 90% clonal B cells in good agreement with the histological examination (see Table 8). PCR-based B-cell clonality analyses for *IGH* and *IGK* (sensitivity of approximately 1%) revealed a single clone and Southern blot analysis for *IGK* showed a single major *IGK* rearrangement only (see Table 8). In addition, Northern blot

analysis for expression of cyclin D1 did not show overexpression. All these data suggested that the very small number (less than 1%) of t(11;14)-positive cells represent either (i) a subclone derived from the B-CLL, (ii) an independent second B malignancy, or (iii) normal B-cells as described for t(14;18)-positive B-cells in normal individuals.<sup>149</sup> However, with the available data of this patient at present, we cannot discriminate between these three alternatives. In summary, the analysis by the 10 laboratories illustrates the high specificity of the *BCL1*/JH PCR strategy.

To evaluate the presence of possible false-negative cases due to the relative low sensitivity of the BIOMED-2 PCR, in one laboratory (LUMC, Leiden), the previously described in-house PCR (with about 10-fold higher sensitivity) was performed on DNA of all 90 cases and the PCR products of both assays were also hybridized with an internal-*BCL1*-MTC oligoprobe that increases the sensitivity another 10 to 100-fold. This analysis revealed no PCR products in other cases.

### Conclusion

We conclude that the sensitivity of the BIOMED-2 *BCL1*/JH-PCR (between  $10^{-3}$  and  $10^{-4}$ ) is sufficiently high for the detection of the *BCL1*/JH breakpoint in diagnostic material. The results of this approach are very encouraging and suggest that the definition of common approaches and reaction conditions can minimize erroneous results. However, it should be remembered that maximally 40–50% of the t(11;14) breakpoints in MCL will be detected by PCR only and that for diagnosis additional detection tools are necessary.

### SECTION 9. t(14;18) with *BCL2*-*IGH* rearrangement

PAS Evans<sup>1</sup>, C Bastard<sup>2</sup>, E Delabesse<sup>3</sup>, EA Macintyre<sup>3</sup>, P Wijers-Koster<sup>4</sup>, E Schuurin<sup>4,5</sup>, E Moreau<sup>6</sup>, D González<sup>7</sup>, KI Mills<sup>8</sup>, BA Jennings<sup>9</sup>, BJ Milner<sup>10</sup>, D Bloxham<sup>11</sup>, P Starostik<sup>12</sup>, M-H Delfaul-Larue<sup>13</sup>, M Ott<sup>14</sup>, G Salles<sup>15</sup> and GJ Morgan<sup>1</sup>

<sup>1</sup>Academic Unit of Haematology and Oncology, University of Leeds, Leeds, UK; <sup>2</sup>Laboratoire de Genetique Oncologique, Centre Henri Becquerel, Rouen, France; <sup>3</sup>Laboratoire d'Hematologie and INSERM EMI 210, Hôpital Necker-Enfants Malades, Paris, France; <sup>4</sup>Department of Pathology, Leiden University Medical Center, The Netherlands; <sup>5</sup>Department of Pathology, University Medical Center Groningen, The Netherlands; <sup>6</sup>Laboratory of Clinical Biology, H Hartziekenhuis, Roeselare, Belgium; <sup>7</sup>Servicio de Hematologia, Hospital Universitario de Salamanca, Spain; <sup>8</sup>Department of Haematology, University of Wales College of Medicine, Cardiff, UK; <sup>9</sup>Department of Medicine, Health Policy and Practise, University of East Anglia, Norwich, UK; <sup>10</sup>Department of Medicine and Therapeutics, University of Aberdeen, UK; <sup>11</sup>Department of Clinical Haematology, Addenbrooke's NHS Trust Hospital, Cambridge, UK; <sup>12</sup>Institute of Pathology, University of Würzburg, DE; <sup>13</sup>Service d'Immunologie Biologique, Hôpital Henri Mondor, Creteil, France; <sup>14</sup>Institute of Pathology, Luitpoldkrankenhaus, Würzburg, Germany; and <sup>15</sup>Department of Hematology, Centre Hospitalier Lyon-Sud, Pierre-Benite, France

### Background

The t(14;18) is one of the best characterized recurrent cytogenetic abnormalities in peripheral B-cell lymphoproliferative disease.<sup>151</sup> It is detectable in up to 90% of FCLs and 20% of

large-cell B-cell lymphomas depending upon the diagnostic test used.<sup>152</sup> As a consequence of the translocation the *BCL2* gene from 18q21 is placed under the control of the strong enhancers of the *IGH* locus resulting in the deregulation of its normal pattern of expression.<sup>153,154</sup> *BCL2* is located on the outer mitochondrial membrane and its normal function is to antagonize apoptosis and when deregulated it is intimately involved in the pathogenesis of the tumor.<sup>155–158</sup> As a consequence of this role in pathogenesis, the t(14;18) provides an ideal target for both diagnosis and molecular monitoring of residual disease.

The *IGH* locus is located at 14q32.3 with the VH regions lying telomeric and the DH, JH, and constant regions placed more centromeric. The transcriptional orientation is from telomere to centromere with enhancers located 5' of the V regions and between each of the constant regions. The most common form of the translocation involves the process of VDJ recombination and one of the six germline JH regions is closely opposed to *BCL2*. Most PCR-based detection strategies have utilized a consensus JH primer that will detect the majority of translocations.<sup>159,160</sup> In contrast to the *IGH* locus, the pattern of breaks in *BCL2* is more complicated. *BCL2* is located on chromosome 18q21 and is orientated 5'–3' from centromere to telomere. The majority of breakpoints fall within the 150 bp MBR located in the 3'-untranslated region of exon 3.<sup>161</sup> As a consequence of the translocation, the S $\mu$  enhancer located 3' of the JH regions is placed in close proximity to the *BCL2* gene leading to its deregulation. As more translocations have been investigated, it has become apparent that there are a number of other breakpoint regions that must be taken into account for an efficient PCR detection strategy. Positioned 4 kb downstream of the MBR is a further breakpoint region, the 3' MBR subcluster, encompassing a region of 3.8 kb.<sup>162</sup> The mcr is located 20 kb 3' of the MBR and covers a region of 500 bp.<sup>163</sup> However, although analogous to the MBR, the mcr is more extensive than was initially envisaged and a region 10 kb upstream of the mcr, the 5' mcr subcluster, has been described.<sup>164,165</sup> In addition to these classical breakpoints, a number of variant translocations are described where the breaks occur 5' of *BCL2*.<sup>166</sup> These are, however, rare and thus cannot be taken into account using a PCR-based detection strategy.

There is no single gold standard detection strategy for the t(14;18), and a combination of cytogenetics and Southern blotting have been generally used.<sup>167,168</sup> Interphase FISH detection strategies offer an applicable alternative that have the potential to pick up more translocations.<sup>169</sup> In contrast, DNA-based fiber FISH has been very informative for defining variant translocations, but is unsuitable for routine application.<sup>170</sup> For molecular diagnostic laboratories PCR-based detection strategies offer rapid results, are generally applicable, and can be used for residual disease monitoring. However, the primers commonly used have been derived on an *ad hoc* basis and have not been designed to take into account recent information on the molecular anatomy of the breakpoints. As a consequence when compared to gold standard approaches, PCR-based techniques only detect up to 60% of translocations, which seriously impairs the diagnostic capability of PCR. Compounding this high percentage of false-negative results is the problem of false-positive results arising from contamination from other samples and previously amplified PCR products.

### Primer design

We initially evaluated a two-tube multiplex system, one tube designed to detect breakpoints within the MBR and a second

tube used to identify breakpoints outside this region. The MBR strategy contained three primers MBR1, MBR2, and the consensus JH primer. The second multiplex reaction contained five primers, MCR1, MCR2, 5'mcr, 3'MBR1, and the consensus JH (Figure 12a) and was designed to detect breakpoints within the mcr, 5'mcr, and 3'MBR regions.

### Results of initial testing phase

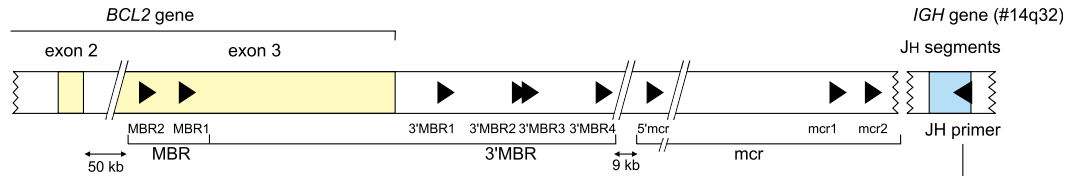
The evaluation of these primers was performed in three laboratories on DNA derived from a total of 124 cases of FCL known to carry a t(14;18). In all, 109 cases (88%) were identified with a *BCL2-IGH* fusion, 83/124 (67%) were positive using the MBR multiplex and 26/124 (21%) were positive using the non-MBR multiplex strategy. In 15/124 (12%) cases, there was no amplifiable PCR product. Further examination of the cases identified with the non-MBR multiplex showed that 11 (9%) had a breakpoint within the mcr, five cases (4%) within the 5'mcr, and 10/124 (8%) within the 3'MBR.

To further investigate the value of this set of primers for the detection of breakpoints within the 5'mcr and 3'MBR subcluster regions, a series of 32 cases of t(14;18)-positive FCLs known to be germline at the MBR and mcr by Southern hybridization were analyzed in one laboratory. Five of the cases had breakpoints within the 5'mcr (260–490 bp) and were amplified using both the 5'mcr primer in isolation and with the multiplex reaction. None of the remaining cases showed a positive result. Of the series of 32 cases, nine were already known to have breakpoints within the 3'MBR region and the multiplex approach was able to detect 5/9 of these cases.

In order to improve the sensitivity of the assay within this region, we designed three further primers that spanned the 3'MBR subcluster region: 3'MBR2, 3'MBR3, and 3'MBR4, and combined them with 3'MBR1 and the consensus JH in an additional multiplex reaction; 3'MBR multiplex (Figure 12a). This new approach confirmed that eight of the 32 cases were positive, but missed the ninth case. The primers were then used individually, and in this experiment 11 of the 32 cases were positive. The breakpoints were distributed as follows: 2/11 cases had a breakpoint present between primer 3'MBR1 and 3'MBR2, 3/11 cases between primers 3'MBR2 and 3'MBR3, 2/11 cases between primers 3'MBR3 and 3'MBR4, and the remaining four cases amplified using primer 3'MBR4, and were distributed 200–1000 bp 3' of this primer. In this series of cases, there were three false-negative results using the 3'MBR multiplex. One of the cases was a true false-negative where the break occurred in the middle of the 3'MBR, in proximity to an Alu repeat sequence. The translocation was detected using the 3'MBR3 primer when used in isolation and a product of 450 bp was generated, suggesting a reduced sensitivity of the multiplex. The remaining two false-negative cases generated products larger than 1000 bp with the 3'MBR4 primer, placing them in the far 3'MBR not fully covered by this approach. Further improvement in the sensitivity of the 3'MBR assay has been achieved following the general testing phase of this study. Substituting primer 3'MBR3 with a new downstream primer 5'-GGTGACA-GAGCAAAACATGAACA-3' (see Figure 12a) significantly improved both the sensitivity and specificity of the 3'MBR assay.

Based on this, the 3'MBR multiplex was incorporated into our diagnostic strategy. The analysis of the Southern blot defined cases was therefore carried out using the three-tube multiplex system presented in Figure 12a.

The sensitivity of the multiplex reactions was evaluated by amplifying DNA dilutions of the cell lines known to have

**a. *BCL-2* gene (#18q21)**

**t(14;18) tube A: MBR primers**

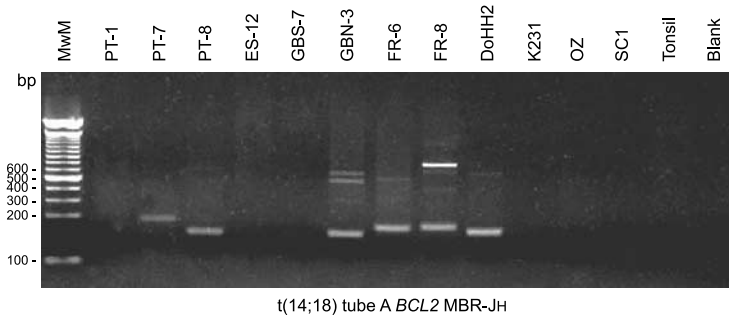
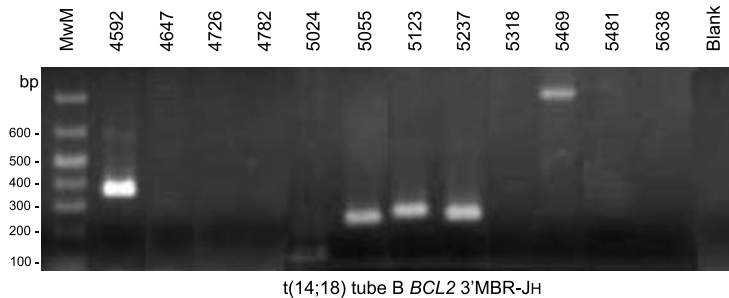
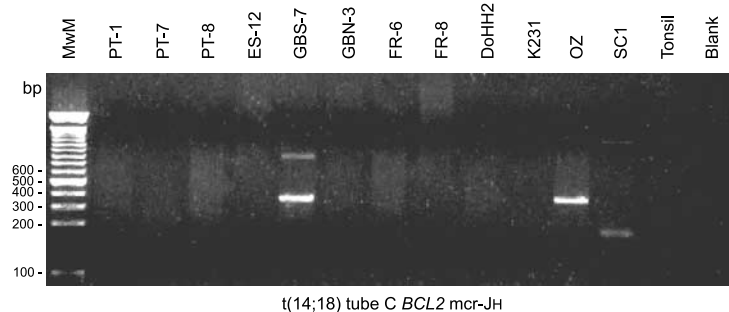
MBR1 (3' end of exon 3) (-3072)	5' GACCAGCAGATTCAAATCTATGG	3' CCAGTGGCAGAGGAGTCCATTC	5' t(14;18) tubes A, B, and C (+57)
MBR2 (3' end of exon 3) (-3575)	ACTCTGTGGCATTATTGCATTATAT		JH consensus

**t(14;18) tube B: 3'MBR primers**

3'MBR1 (3' end of exon 3) (+549)	GCACCTGCTGGATACAACACTG
3'MBR2 (3' end of exon 3) (+1224)	AAACTAGCAGGGTGTGGTGGC (replaced by +1362; GGTGACAGAGCAAAACATGAACA)
3'MBR3 (3' end of exon 3) (+1619)	GTAATGACTGGGGAGCAAAATCTT
3'MBR4 (3' end of exon 3) (+2550)	ACTGGTTGGCGTGTTTAGAGA

**t(14;18) tube C: mcr primers**

5'mcr (3' end of exon 3) (+15681)	CCTTCTGAAAGAAACGAAAGCA
mcr1 (file AF275873) (+1961)	TAGAGCAAGCGCCCAATAAATA
mcr2 (file AF275873) (+2407)	TGAATGCCATCTCAATCCAA

**b. t(14;18) tube A *BCL2* MBR-JH****c. t(14;18) tube B *BCL2* 3'MBR-JH****d. t(14;18) tube C *BCL2* mcr-JH**

**Figure 12** PCR detection of *BCL2*-*IGH* rearrangements. (a) Schematic diagram of the *BCL2* gene on chromosome band 18q21. The majority of the *BCL2* breakpoints cluster in three regions: MBR, 3' MBR, and mcr. Consequently, multiplex primers have been designed to cover the potential breakpoints in these three regions: two MBR primers, four 3' MBR primers, and three mcr primers. The relative position of the *BCL2* primers is indicated according to their most 5' nucleotide upstream (–) or downstream (+) to the 3'-end of *BCL2* exon 3 (according to NCBI accession no. AF325194S1), except for two *BCL2*-mcr primers; their position is indicated downstream of the first nucleotide of the AF275873 sequence. (b, c, and d) Agarose-gel electrophoresis of PCR products from different FCL patients and several positive control cell lines (DoHH2, K231, OZ, and SC1). (b) and (d) Contain the same samples and show complementarity in positivity, illustrating that tube C (mcr tube) has added value. The PCR products differ in size, related to different position of the *BCL2* breakpoints. The larger bands of lower density in the same lanes represent PCR products that extend to the next downstream germline JH gene segment or to the next upstream *BCL2* primer.

breakpoints within the four subcluster regions: DoHH2, SC1, Oz, and K231 in normal tonsil DNA.<sup>165</sup> A sensitivity of between  $3.3 \times 10^{-2}$  and  $10^{-3}$  was consistently achievable using the MBR and 5'mcr/mcr multiplex reactions. Sensitivity of the 3'MBR multiplex was assessed with the K231 cell line, and was determined as  $10^{-2}$ . This is lower than would be expected for the primers used in pairs, but this is more than adequate for diagnostic material.

### Results of general testing phase

Interlaboratory variations feature significantly in diagnostic PCR strategies. To evaluate this, 11 groups participated in an extensive external quality control exercise. DNA was extracted from a series of 90 histologically defined malignant and reactive lymphoproliferations were analyzed using the t(14;18) multiplex protocol (Figure 12b–d). All cases were defined for their status at the Ig and TCR loci using Southern hybridization techniques. Karyotypic confirmation of the t(14;18) was not available on this series. We therefore adopted an approach requiring greater than 70% concordance between members of the network for acceptance of the t(14;18). Of the 90 cases, 11 were characterized histologically as FCL. All 11 cases were shown to have a clonal *IGH* rearrangement by Southern hybridization. The assessment of rearrangements within the *BCL2* gene was also performed by Southern hybridization using specific probes to the MBR, mcr and 3'MBR in 10/11 cases. In all, 4/10 cases showed a rearrangement within the MBR that was concordant with the PCR result. A single case, GBS-7, shown to be mcr multiplex PCR positive, gave an inconclusive Southern blot result with the mcr probe. Immunophenotypically this case demonstrated two distinct clonal populations, representing approximately 5 and 15% of the original diagnostic material. The discrepancy between the two techniques in this case probably represents the reduced sensitivity of Southern blot compared with PCR. There was no evidence of a 3'MBR rearrangement in any of the remaining cases by Southern blot.

Of the six Southern blot-negative FCL cases, a single case, ES-7, showed a t(14;18) using the MBR multiplex. In all, 5/11 FCL cases showed no evidence of a t(14;18) by either Southern blot or PCR. A t(14;18) was detected in two further cases by PCR; FR-6, a case of DLBCL showed an MBR breakpoint and was identified by all 11 laboratories, this finding is compatible with previous studies that have detected a t(14;18) in 20–40% of DLBCL cases.<sup>171,172</sup> Using the 3'MBR multiplex, 10/11 laboratories reported a positive result for sample ES-12, this was a case of Hodgkin's disease that contained very few B cells. It is difficult to explain this result in the absence of an *IGH* rearrangement by Southern blotting. Contamination or incorrect labeling of the sample at source is the most likely explanation.

Overall there was excellent concordance throughout the network, although small numbers of both false-positive and false-negative results were encountered. Overall 12 false-positive results were identified, representing less than 0.4% (12/3036) of the total number of analyses. These were reported by five laboratories and involved six of the samples. The majority of the false positives (9/12) were found in three cases. Five false-negative results, representing a 6% (5/88) failure rate, were reported by three laboratories, ES-7 was not detected by two laboratories, three further groups within the network commented that this case had shown weak amplification signals with the MBR multiplex. The remaining three false-negative cases were reported in isolation by individual laboratories. The results of diagnoses using this approach are very encouraging

and suggest that the definition of common approaches and reaction conditions can minimize erroneous results.

### Conclusion

In conclusion, we have designed and evaluated a robust three-tube multiplex PCR in order to maximize the detection of the t(14;18). This strategy is capable of amplifying across the breakpoint region in the majority of cases of FCL with a cytogenetically defined translocation. Although the sensitivity of this strategy is lower than conventional single-round or nested PCR approaches, it is still perfectly acceptable for diagnostic procedures. The widespread adoption of standardized reagents and methodologies has helped to minimize inaccurate results within this large multicenter network. However, it is worth noting from the general testing phase (and subsequent examination of 109 Work Package 2 FCL cases) of this study that it is impossible to detect a t(14;18) in all cases. This is certainly influenced by additional molecular mechanisms capable of deregulating the *BCL2* gene.<sup>173,174</sup>

### SECTION 10. Use of BIOMED-2 protocols with DNA extracted from paraffin-embedded tissue biopsies and development of control gene primer set

HE White<sup>1</sup>, FL Lavender<sup>1</sup>, E Delabesse<sup>2</sup>, EA Macintyre<sup>2</sup>, S Harris<sup>1</sup>, E Hodges<sup>1</sup>, DB Jones<sup>1</sup> and JL Smith<sup>1</sup>

<sup>1</sup>Wessex Immunology Service, Molecular Pathology Unit, Southampton University Hospitals NHS Trust, Southampton, UK; and <sup>2</sup>Laboratoire d'Hématologie and INSERM EMI 210, Hôpital Necker-Enfants Malades, Paris, France

### Background

Fresh/frozen tissue is considered to be the ideal sample type for the extraction of DNA for use in PCR-based clonality analysis. However, fresh/frozen material is not always available to diagnostic laboratories and in many laboratories throughout Europe, paraffin-embedded tissue samples constitute the majority of diagnostic biopsies submitted for analysis. DNA extracted from paraffin-embedded material is often of poor quality and so PCR protocols need to be evaluated for use with these sample types before they can be widely used in diagnostic laboratories.

The integrity of DNA extracted from paraffin-embedded samples and its amplification by PCR are affected by a number of factors such as thickness of tissue, fixative type, fixative time, length of storage before analysis, DNA extraction procedures, and the coextraction of PCR inhibitors.<sup>175–182</sup> Neutral-buffered formalin (10% NBF) is the most commonly used fixative, although laboratories within the BIOMED-2 program also use a number of other fixatives, including unbuffered formalin and Bouins. The use of 10% NBF permits the amplification of DNA fragments of a wide range of sizes, whereas Bouins appears to be the least amenable for use in PCR analysis.<sup>177,178,181,183</sup> The integrity of DNA fragments extracted from paraffin-embedded samples also depends on the length of time the blocks have been stored with the best results usually obtained from blocks less than 2 years old, while blocks over 15 years old tend to yield very degraded fragments.<sup>184</sup>

The aim of this study was to evaluate the use of the BIOMED-2 primer sets with DNA isolated from paraffin-embedded tissue biopsies matched to the fresh/frozen tissue samples tested in Work Package 1. The design of a set of control gene PCR primers to assess the quality and amplifiability of DNA samples is also described for assessing the quality of the DNA isolated from the paraffin-embedded samples.

### Primer design

Initially, five pairs of control gene PCR primers were designed to amplify products of exactly 100, 200, 400, 600, and 1000 bp in order to assess the quality of DNA submitted for analysis in the BIOMED-2 program. The target genes were selected on the basis of having large exons with open-reading frames to reduce the risk of selecting polymorphic regions and the primers were designed for multiplex usage in the standardized BIOMED-2 protocols. The following target genes were selected: human thromboxane synthase gene (*TBXAS1*, exon 9; GenBank accession no. D34621), human recombination activating gene (*RAG1*, exon 2; GenBank accession no. M29474), human promyelocytic leukemia zinc-finger gene (*PLZF*, exon 1; GenBank accession no. AF060568), and human AF4 gene (exon 3; GenBank accession no. Z83679, and exon 11; GenBank accession no. Z83687).

### Results of initial testing phase

The primer pairs were tested in separate reactions and subsequently in multiplex reactions using high molecular weight DNA. Owing to the large size range of the products (100–1000 bp), it was necessary to vary the ratio of primer concentrations to obtain bands of equal intensities in the multiplex reactions. However, it proved extremely difficult to be able to amplify all the bands reproducibly and it was decided that the 1000 bp product was probably unnecessary, since all the BIOMED-2 PCR protocols give products of less than 600 bp. It was therefore decided to exclude the 1000 bp product in order to improve the reproducibility of the assay. By increasing the  $MgCl_2$  concentration to 2 mM and adding the primers in a 1:1:1:2 ratio, it was possible to reproducibly amplify four bands (100, 200, 400, and 600 bp) of equal intensity from high molecular weight DNA samples. However, for DNA extracted from paraffin blocks, it was thought that an extra size marker at 300 bp would be extremely informative and that the 600 bp marker might not be necessary. Using the gene sequence for the 1000 bp marker (*PLZF*), primers were redesigned to generate a 300 bp product. These were tested successfully both in monoplex reactions and in multiplex reactions combining the 100, 200, 300, 400, and 600 bp primers (see Figure 13a).

Thus, two primer sets are available for assessing the quality of DNA for amplification:

1. The 100, 200, 300, and 400 bp primers used at 2.5 pmol each can be used for assessing DNA from paraffin-embedded tissues.
2. The addition of the 600 bp primers at 5 pmol allows this set to be used to check the quality of any DNA sample for use with the BIOMED-2 primers and protocols.

Both primer sets are used with ABI Buffer II and 2.0 mM  $MgCl_2$  under standardized BIOMED-2 amplification conditions (see Table 4). Products can be analyzed on 6% PAGE or 2% agarose (see Figure 13b).

### Results of general testing phase

In all, 45 paraffin-embedded biopsies were collected corresponding to 30 of the B-cell malignancies, eight of the T-cell malignancies, and seven of the reactive lymphoproliferations submitted as fresh/frozen tissue samples for Work Package 1 (DE-1, 2, and 5; ES-4, 5, 6, and 7; FR-4, 5, 6, 7, 8, and 9; PT-1, 4, 5, 6, 7, 9, and 10; NL-2, 3, 4, 5, 6, 11, 12, 14, 15, and 16; GBS-1, 2, 3, 4, 8, 11, and 12; GBN-1, 2, 3, 4, 5, 7, and 9). The age of the paraffin blocks as well as the methods of fixation and embedding of the samples varied between National Networks. The ES samples were submitted as precut sections, NL-14, 15, and 16 were submitted as DNA samples and the remaining biopsies were submitted as paraffin blocks. Five sections (10  $\mu$ m each) were cut from the paraffin blocks and DNA was extracted using the QIAamp DNA Mini Kit (QIAGEN) following the manufacturer's protocol for isolation of genomic DNA from paraffin-embedded tissue. This method of DNA extraction was chosen since the kit can be used to rapidly extract good quality DNA from blood, fresh/frozen tissue, and paraffin-embedded tissue, and thus enables the parallel processing of a variety of sample types with assured quality control. Numerous protocols for the extraction of DNA from paraffin-embedded tissue for PCR analysis have been published.<sup>181,182,185–187</sup> Many of these aim to reduce DNA degradation and the coextraction of PCR inhibitors, but many of these methods require prolonged extraction procedures and can be unsuitable for use in the routine diagnostic laboratory.<sup>176,177,188,189</sup>

DNA sample concentration and integrity were estimated by spectrophotometry and by comparison of sample DNA with known standards on agarose-gel electrophoresis. DNA samples (100 ng) were then analyzed for integrity and amplifiability using the control gene PCR primers (100–400 bp) and assessed for clonality at all target loci using the BIOMED-2 PCR protocols.

In the control gene PCR reaction of 24/45 cases, the amplified products were at least 300 bp, whereas in the remaining 21 samples the amplified products were 200 bp or less. No clear correlation between the quality of the DNA and the age of the block or fixation method could be demonstrated. Therefore, it is likely that a combination of factors is responsible for the DNA quality in these samples.

The DNA samples were evaluated for clonality using the 18 BIOMED-2 multiplex PCR reactions and were analyzed by both heteroduplex analysis and GeneScanning in the Southampton laboratory. The number of paraffin samples showing clonality and translocations at the nine target loci were compared with the corresponding fresh/frozen sample data (Table 22). In samples with control gene PCR products of up to 200 bp, the overall detection of clonality at the nine target loci was 9/55 (16%). Of the 46 missed rearrangements, 45 could be explained by the fact that the expected clonal PCR products had a molecular weight higher than the maximum size amplified by the sample in the control gene PCR. The remaining sample (PT-9) amplified to 100 bp in the control gene PCR, but the expected 81 bp *TCRG* clonal product was not detected. In samples with control gene PCR products of at least 300 bp, the overall detection of clonality at the nine target loci was 42/55 (76%). Of the 13 missed rearrangements, five could again be explained by the fact that the expected clonal PCR products were larger than the maximum size amplified by the sample in the control gene PCR. The remaining eight missed rearrangements could not be explained directly by the quality of the DNA. One false-positive clonal result (GBN-9; *IGL*) was detected in a reactive lymph node that may represent pseudoclonality.



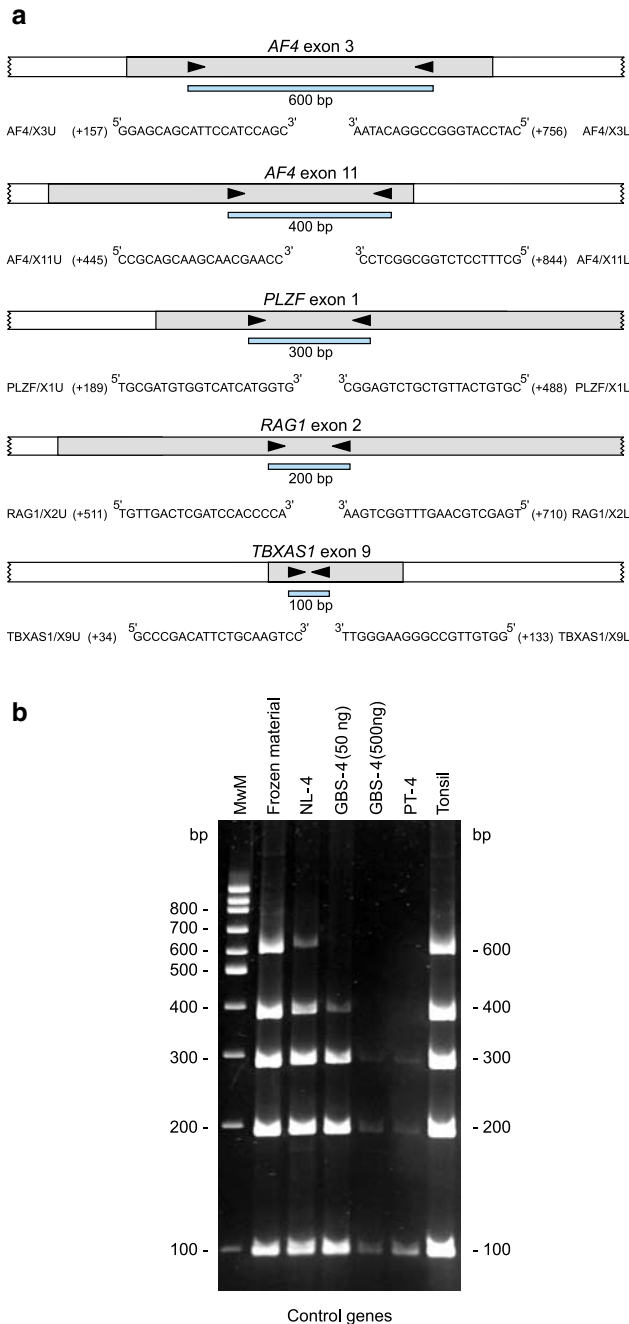


**Figure 13** Control gene PCR for the assessment of amplifiability and integrity of DNA samples. (a) Schematic diagram of five control genes exons and the five primer sets for obtaining PCR products of 600, 400, 300, 200, and 100 bp. The relative position of the control gene primers is given according to their most 5' nucleotide downstream of the 5' splice site of the involved control gene exon. (b) Control gene PCR products of six DNA samples separated in a 6% polyacrylamide gel. Two control samples contained high molecular weight DNA (outer lanes) and four DNA samples were obtained from paraffin-embedded tissue samples, showing reduced amplifiability (eg GBS-4 50 ng vs GBS-4 500 ng) or reduced integrity of the DNA (PT-4).

PCR inhibitors are known to be present in DNA extracted from paraffin samples. Dilution of the DNA sample may reduce the concentration of these inhibitors to levels that allow successful amplification to occur. To investigate the effect of diluting DNA samples on the efficiency of amplification, four different concentrations of DNA were tested in the control gene

PCR reaction: 5, 50, 100, and 500 ng. The results in Table 23 show that dilution of the DNA samples has a significant effect on the size of the PCR products in the control gene PCR. Overall, 24/45 cases (53%) showed an increased efficiency of amplification when diluted from 100 to 50 ng. The optimal DNA concentration appears to be between 50 and 100 ng, whereas the use of 500 ng appears to inhibit the amplification of large products (300 bp or above). Although the use of 5 ng of DNA gives acceptable results with the control gene PCR, this can lead to false positivity in PCR-based clonality assays due to the low representation of total lymphoid cell DNA.<sup>190,191</sup> More importantly, 5 ng of DNA has no advantage over a dilution to 50 ng of DNA.

To assess whether the use of 50 ng of DNA would also increase the detection of clonality, all the samples were retested at the *IGH* V-J locus using this DNA concentration. The number of clonal rearrangements detected in the three *IGH* V-J tubes using 100 ng of DNA was 12, compared with 23 using the corresponding fresh/frozen samples. The overall detection of clonality at this locus increased to 17 out of 23 when 50 ng of DNA was used, with an additional nine FR1, six FR2, and four FR3 clonal products being detected. Thus the dilution of the DNA can increase the detection of clonal products, presumably because of dilution of PCR inhibitors. Logically, dilution of DNA is only likely to improve both control gene PCR results and the detection of clonality, if PCR inhibitors are present, not if the DNA sample is highly degraded. Therefore, it is recommended that at least two dilutions of DNA are tested using the control gene PCR and that the dilution that gives the better result is used in subsequent clonality analysis.

Nine clonal rearrangements (ie one with amplified products up to 100 bp and eight products of at least 300 bp) remained undetected after initial analysis, which could not be explained by DNA quality (*TCRG* in PT-9 and NL-11; *TCRB* in GBS-4; *TCRD* in NL-15; *IGK* in GBN-4, NL-4, and NL-5; *IGH* V-JH in GBS-6, and GBS-8). These samples were retested using 50 ng of DNA, but only one sample (GBS-8; *IGH*) showed improved detection, suggesting that other, unknown, factors can prevent the amplification of specific targets in a small number of cases. However, it should be noted that for seven of these samples (NL-11, GBS-4, NL-15, GBN-4, NL-5, GBS-6, and GBS-8) clonal products were detected in at least one other locus. This demonstrates that testing for clonality at multiple target loci increases the likelihood of detecting clonal lymphocyte populations.

## Conclusion

In conclusion, the BIOMED-2 protocols work well with DNA extracted from paraffin-embedded material provided that the DNA can amplify products of 300 bp or more in the control gene PCR. Two concentrations of DNA should be tested in the control gene PCR and the more 'amplifiable' concentration should be used in further testing, although with the proviso that concentrations of DNA less than 20 ng may contribute to the detection of pseudoclone due to the low representation of target lymphoid DNA.<sup>190,191</sup> Overall, the data show that the assessment of DNA quality using the control gene PCR provides a good indication of the suitability of the DNA for clonality analysis using the BIOMED-2 protocols. It is also important to note that the control gene PCR will give no indication of the amount of lymphoid cell DNA present in the sample and therefore good quality DNA may still produce false-negative results for clonality analysis. To ensure monoclonal results are

**Table 22** Number of clonal rearrangements detected in paraffin samples compared with number of clonal rearrangements detected in matched fresh/frozen sample

Maximal size of control gene PCR product	No. of clonal rearrangements in paraffin samples per no. of clonal rearrangements in fresh or frozen samples									
	IGH V-J	IGH D-J	IGK	IGL	TCRB	TCRG	TCRD	t(11;14) BCL1-IGH	t(14;18) BCL2-IGH	All loci
100 or 200 bp	3/11 (27%)	2/5 (40%)	2/10 (20%)	1/3 (33%)	0/9 (0%)	1/9 (11%)	0/3 (0%)	0/3 (0%)	0/2 (0%)	9/55 (16%)
300 or 400 bp	9/12 (75%)	5/7 (71%)	12/15 (80%)	4/4 (100%)	4/5 (80%)	3/5 (60%)	1/2 (50%)	1/2 (50%)	3/3 (100%)	42/55 (76%)

**Table 23** Effect of amount of DNA on the maximal size of control gene PCR products in 45 samples

Maximal size of PCR products	Number of cases according to maximal size of PCR products			
	500 ng	100 ng	50 ng	5 ng
100 bp	20 (44%)	19 (42%)	5 (11%)	14 (31%)
200 bp	23 (51%)	2 (4%)	13 (29%)	7 (16%)
300 bp	2 (4%)	18 (40%)	12 (27%)	11 (24%)
400 bp	0 (0%)	6 (13%)	15 (33%)	13 (29%)

reproducible (and to avoid potential pseudoclonality), all clonality assays, particularly using paraffin-extracted DNA, should be performed in duplicate and evaluated by heteroduplex analysis and GeneScanning, whenever possible. Recent further modifications of the PCR conditions (M Hummel *c.s.*) showed a further increase in the clonality detection rate.

It should be noted that 67% of the paraffin biopsies submitted for this study had a diagnosis of B-cell malignancy, 18% presented with T-cell malignancy, and 15% had a reactive lesion. Therefore, the Ig gene primer sets have been more extensively evaluated than the TCR gene primer sets. Further evaluation of all primer sets will be undertaken by analyzing paraffin biopsy samples matched to fresh tissue samples submitted for Work Package 2.

## General discussion

The main aim of the BIOMED-2 Concerted Action BMH4-CT98-3936 study presented here was to develop standardized multiplex PCR tubes and PCR protocols for reliable and easy detection of clonality in suspect lymphoproliferations. To reach this challenging aim, two main problems had to be solved: (1) Prevention of false-negative results, mainly caused by inappropriate primer annealing (each gene segment not being optimally recognized or mismatches caused by somatic hypermutation). (2) Prevention of false-positive results, mainly caused by inappropriate discrimination between monoclonal and polyclonal rearrangements.

The first problem was addressed by the design of multiple primers for each Ig/TCR locus in order to cover as many gene segments as possible as well as by the inclusion of virtually all types of Ig/TCR gene rearrangements. Particularly for circumventing the somatic mutation problems in follicular and postfollicular B-cell malignancies, multiple Ig gene targets were included: in addition to three multiplex tubes for *IGH* VH-JH gene rearrangements, two multiplex tubes for incomplete *IGH* DH-JH, two for *IGK*, and one for *IGL* rearrangements were

designed. One tube for t(11;14) (*BCL1-IGH*) and three tubes for t(14;18) (*BCL2-IGH*) were also included. For clonality testing in different types of T-cell malignancies, three *TCRB* multiplex tubes were developed (two for V $\beta$ -J $\beta$  and one for D $\beta$ -J $\beta$ ), as well as two for *TCRG* and one for *TCRD* gene rearrangements. In particular, the three *TCRB* tubes appeared to be highly powerful, because they cover the vast majority of functional V $\beta$  gene segments (23 V $\beta$  primers), both D $\beta$  gene segments, and all 13 J $\beta$  gene segments.

In total, 18 multiplex tubes were designed containing combinations of 107 different primers. Several primers are used in more than one tube. For example, the JH consensus primer is used in nine different tubes and the V $\kappa$ , V $\beta$ , J $\beta$ , and J $\gamma$  primers are used in two different tubes.

The second problem was addressed by the use of two different techniques for discrimination between monoclonal and polyclonal Ig and TCR gene rearrangements: (1) Heteroduplex analysis of double-stranded PCR products, with separation according to the composition and length of the junctional regions. (2) GeneScanning of fluorescently labeled single-stranded PCR products, based on accurate separation according to the length of the junctional regions.

## PCR protocol, PCR conditions, and positive controls

The same standardized BIOMED-2 PCR protocol can be used for all multiplex tubes (Table 4). Also the reaction conditions are comparable with some limited variations. Two types of buffers were evaluated during the two testing phases: ABI Gold Buffer and ABI Buffer II. Some tubes gave better results with ABI Gold Buffer whereas for other tubes ABI Buffer II was preferred (Table 24). In principle, 1 U of Ampli Taq Gold can be used except for the two *TCRB* V $\beta$ -J $\beta$  tubes, which contain many primers that might result in extra PCR products and extra enzyme consumption, particularly if high frequencies of T-lymphocytes are present in the tested sample. Finally, the standard MgCl<sub>2</sub> concentration is recommended to be 1.5 mM, but varied between 1.5 and 3.0 mM (see Table 24).



**Table 24** Conditions and control samples for multiplex PCR analysis of Ig/TCR gene rearrangements and translocations t(11;14) and t(14;18)

Multiplex PCR	Tubes	PCR conditions			Positive controls (examples)	
		Buffer	TaqGold (U)	MgCl <sub>2</sub> (mM)	Polyclonal	Monoclonal <sup>a</sup>
<i>IGH</i> VH-JH	A/B/C	Gold/II	1	1.5	Tonsil	A: NALM-6; SU-DHL-6; EHEB B: NALM-6; SU-DHL-6; EHEB C: NALM-6; SU-DHL-6; EHEB
<i>IGH</i> DH-JH	D/E	Gold	1	1.5	Tonsil	D: KCA; ROS-15 E: HSB-2, HPB-ALL
<i>IGK</i>	A/B	Gold/II	1	1.5	Tonsil	A: KCA; ROS-15 B: ROS-15, 380
<i>IGL</i>	A	Gold/II	1	2.5	Tonsil	A: CLL-1; EB-4B; KCA
<i>TCRB</i>	A/B/C	II	2 (A, B) <sup>b</sup> 1 (C)	3.0 (A, B) 1.5 (C)	PB-MNC <sup>c</sup>	A: RPMI-8402; JURKAT; PEER; DND-41 B: PEER; CML-T1, MOLT-3 C: JURKAT
<i>TCRG</i>	A/B	II	1	1.5	PB-MNC <sup>c</sup>	A: MOLT-3; RPMI-8402; JURKAT; PEER B: JURKAT; PEER
<i>TCRD</i>	A	II	1	2.0	PB-MNC <sup>c</sup>	A: PEER, REH, NALM-16
<i>BCL1-IGH</i>	A	II	1	2.0	NA <sup>c</sup>	A: JVM 2
<i>BCL2-IGH</i>	A/B/C	II	1	1.5	NA <sup>c</sup>	A: DoHH2; SU-DHL-6 B: K231 <sup>d</sup> C: OZ; SC1 <sup>d</sup> ; SU-DHL-16

<sup>a</sup>Most clonal cell line controls can be obtained via the Deutsche Sammlung von Mikroorganismen und Zellkulturen GmbH; contact person: Dr HG Drexler (address: Department of Human and Animal Cell Cultures, Mascheroder Weg 1B, 38124 Braunschweig, Germany).<sup>192,193</sup>

<sup>b</sup>In most BIOMED-2 multiplex tubes only 1 U TaqGold is needed, but 2 U TaqGold are needed in *TCRB* tubes A and B because they contain > 15 different primers.

<sup>c</sup>PB-MNC, mononuclear cells from peripheral blood; NA, not applicable.

<sup>d</sup>The t(14;18)-positive cell lines K231, OZ, and SC1 were kindly provided by Professor Martin Dyer, University of Leicester, Leicester, UK.

The recommended positive controls include polyclonal controls and monoclonal cell line controls for each Ig/TCR gene tube, and specific cell line controls for the *BCL1-IGH* and *BCL2-IGH* tubes. For most tubes, at least two well-known cell line controls could be selected, most of them being available via the Deutsche Sammlung von Mikroorganismen und Zellkulturen GmbH (contact person: Dr HG Drexler, Department of Human and Animal Cell Cultures, Mascheroder Weg 1B, 38124 Braunschweig, Germany, Tel: +49 -531 -2616 -160; Fax: +49 531 2616 150, E-mail: hdr@dsMZ.de).<sup>192,193</sup> The polyclonal controls particularly concerned tonsil samples (generally containing 50–60% B-lymphocytes) for Ig gene targets and MNC samples (generally containing 60–70% T-lymphocytes) for TCR gene targets.

#### PCR product analysis: size ranges, nonspecific bands, and preferred technique

Based on the experience obtained by the 30 PCR laboratories during the initial and general testing phases, all relevant background information per multiplex tube has been summarized in Table 25. Per tube the size ranges of the monoclonal and polyclonal PCR products are given as well as the potential nonspecific bands.

GeneScanning and heteroduplex analysis are equally suited for the analysis of *IGH* VH-JH and *TCRB* PCR products, which contain large and highly diverse junctional regions. However, heteroduplex analysis is slightly preferred in case of *IGH* DH-JH, *IGK*, and *TCRG* PCR products, mainly because of the

smaller junctional regions and the consequently limited variation in the sizes of the PCR products, which may hamper easy interpretation of GeneScanning results. For the analysis of *IGL* and *TCRD* PCR products heteroduplex analysis is clearly preferred, although multicolor GeneScanning of *TCRD* PCR products can be highly informative for the identification of the type of *TCRD* gene rearrangement (see below).

*BCL1-IGH* and *BCL2-IGH* PCR products should be analyzed in agarose gels. GeneScanning and heteroduplex analysis are not optimally suited for these two PCR targets, because of the large variation in the sizes of the PCR products.

#### Interpretation of Ig/TCR gene results

Correct interpretation of the heteroduplex and GeneScanning results needs insight into the polyclonal Ig/TCR gene rearrangement patterns, the sensitivity of detecting clonal PCR products, the occurrence of nonspecific bands, and the occurrence of large PCR products.

**Polyclonal Ig/TCR gene rearrangements: smears and Gaussian curves:** In heteroduplex analysis of PCR products, polyclonal Ig/TCR gene rearrangements appear as a smear (= heteroduplexes), positioned between homoduplexes and single-strand molecules. This applies to all Ig/TCR gene rearrangements. In GeneScanning of PCR products, typical Gaussian curves with triplet spacing of peaks are found in case of polyclonal *IGH* VH-JH and *TCRB* V $\beta$ -J $\beta$  rearrangements, fully in line with the high frequency of in-frame VH-JH

**Table 25** Size ranges, nonspecific bands, and detection method in multiplex PCR analysis of Ig/TCR gene rearrangements and chromosome aberrations t(11;14) and t(14;18)

Multiplex PCR	Size range (nt)	Nonspecific bands (nt)	Preferred method of analysis	GeneScanning running time: gel/capillary
IGH VH-JH	Tube A: 310–360	Tube A: ~85	GeneScanning and heteroduplex analysis equally suitable	3–3.5 h/45 min
	Tube B: 250–295 Tube C: 100–170	Tube B: — Tube C: —		
IGH DH-JH	Tube D: 110–290 (DH1/2/4/5/6-JH) +390–420 (DH3-JH)	Tube D: 350 <sup>a</sup>	Heteroduplex analysis slightly preferred over GeneScanning (variation of product sizes hampers GeneScanning)	3–3.5 h/45 min
	Tube E: 100–130	Tube E: 211 <sup>b</sup>		
IGK	Tube A: 120–160 (Vκ1f/6/Vκ7-Jκ) +190–210 (Vκ3f-Jκ) +260–300 (Vκ2f/Vκ4/Vκ5-Jκ)	Tube A: —	Heteroduplex analysis slightly preferred over GeneScanning (small junction size+variation of product sizes hampers GeneScanning)	3–3.5 h/45 min
	Tube B: 210–250 Vκ1f/6/Vκ7-Kde +270–300 (Vκ3f/intron-Kde) +350–390 (Vκ2f/Vκ4/Vκ5-Kde)	Tube B: ~404		
IGL	Tube A: 140–165	Tube A: —	Heteroduplex analysis clearly preferred over GeneScanning (small junction size hampers GeneScanning)	2 h/45 min
TCRB	Tube A: 240–285	Tube A: (273) <sup>c</sup>	GeneScanning and heteroduplex analysis equally suitable	2 h/45 min
	Tube B: 240–285	Tube B: <150, 221 <sup>d</sup>		
	Tube C: 170–210 (Dβ2) +285–325 (Dβ1)	Tube C: 128, 337 <sup>d</sup>		
TCRG	Tube A: 145–255	Tube A: —	Heteroduplex analysis slightly preferred over GeneScanning (limited repertoire, particularly in case of ψVγ10 and ψVγ11 usage)	2 h/45 min
	Tube B: 80–220	Tube B: —		
TCRD	Tube A: 120–280	Tube A: ~90	Heteroduplex analysis clearly preferred over GeneScanning (low amount of template+variation of product sizes hampers GeneScanning)	2 h/45 min
BCL1-IGH	Tube A: 150–2000	Tube A: ~550 (weak)	Agarose	NA <sup>e</sup>
BCL2-IGH	Tube A: variable Tube B: variable Tube C: variable	Tube A: — Tube B: — Tube C: —	Agarose	NA <sup>e</sup>

<sup>a</sup>The nonspecific 350 bp band is the result of crossannealing of the DH2 primer to a sequence in the region upstream of JH4. In GeneScanning, this nonspecific band does not comigrate with D–J products (see Figure 5b).

<sup>b</sup>The 211 bp PCR product represents the smallest background band derived from the germline DH7–JH1 region. When the PCR amplification is very efficient, also longer PCR products might be obtained because of primer annealing to downstream JH gene rearrangements; for example, 419 bp (DH7–JH2), 1031 bp (DH7–JH3), etc.

<sup>c</sup>The 273 bp band (mainly visible by GeneScanning) is particularly seen in samples with low numbers of contaminating lymphoid cells.

<sup>d</sup>Intensity of nonspecific band depends on primer quality.

<sup>e</sup>NA, not applicable.

rearrangements in mature B-lymphocytes and in-frame Vβ–Jβ rearrangements in mature T-lymphocytes. In most other BIOMED-2 multiplex tubes, the Gaussian curves do not show these typical triplet-spaced peaks, because of incomplete

rearrangements (DH–JH and Dβ–Jβ), high frequency of out-of-frame rearrangements (IGK-Kde and TCRG Vγ–Jγ), relatively short junctional regions (Vκ–Jκ and Vλ–Jλ), and/or the scattered position of some primers (DH, Vκ, and Vδ).

**Sensitivity of heteroduplex analysis and GeneScanning:** Heteroduplex analysis of Ig/TCR gene rearrangements generally gives reliable results for clonality assessment. However, one should be aware that small clones (<10%) might be missed because of the limited sensitivity (1–10%). In particular, in cell samples with high frequencies of reactive B- or T-lymphocytes, it might be difficult to detect a small B- or T-cell clone, respectively, because during the duplex formation step the PCR products of the polyclonal rearrangements ‘consume’ the PCR products of the monoclonal rearrangements.<sup>40,41</sup> GeneScanning is somewhat more sensitive (0.5–5%), because the clonal peaks are generally easily visible on top of the polyclonal Gaussian curve. Nevertheless, one should realize that both heteroduplex analysis and GeneScanning have been developed for classical Ig/TCR clonality studies with clonal cell populations of >10%, not for the detection of minor subclones.

**Nonspecific bands:** In several multiplex tubes, a nonspecific band might be seen. Virtually all nonspecific bands are located outside the size range of the normal PCR products and can therefore easily be recognized (Table 24). For convenience of the readership, they are marked with an asterisk in all relevant GeneScanning figures. Most nonspecific PCR products are caused by nonspecific annealing of primers or by the amplification of a germline fragment, such as in case of the 211 bp DH7–27–JH1 germline product in *IGH* tube E.

**Occurrence of large clonal PCR products:** Additional clonal PCR products of large size can be obtained in case of *IGH*, *IGK*, and *TCRB* gene rearrangements, generally caused by J primer annealing to the next downstream (germline) J gene segment. For example, the six JH gene segments are clustered in a small region of ~2.3 kb and are all recognized by the same JH consensus primer. The five J $\kappa$  gene segments are clustered in a region of ~1.4 kb and are recognized by two homologous J $\kappa$  primers. Finally, the seven J $\beta$ 2 gene segments are clustered in a ~1.1 kb region and recognized by seven homologous J $\beta$  primers. In the *IGH* and *IGK* tubes, the larger (extended) clonal PCR product will generally be found in combination with the corresponding smaller PCR product, unless the actually rearranged JH or J $\kappa$  gene segment is not recognized properly because of somatic mutations or extensive nucleotide deletion. However, in case of the *TCRB* V $\beta$ –J $\beta$  tubes, the larger and corresponding smaller PCR products might be found in separate tubes, because the J $\beta$ 2.2, J $\beta$ 2.6, and J $\beta$ 2.7 primers are in tube A, whereas the other J $\beta$ 2 primers are in tube B. Consequently, a V $\beta$ –J $\beta$ 2.5 rearrangement can give a small PCR product (~250 bp) in tube B and the same but larger (extended) V $\beta$ –J $\beta$ 2.5–J $\beta$ 2.6 PCR product in tube A.

#### Detection rate of Ig/TCR gene clonality: complementarity of PCR targets

For assessing the detection rate of clonal rearrangements by the various multiplex PCR tubes, a large series of 90 DNA samples was used, including 49 B-cell malignancies, 18 T-cell malignancies, 15 reactive samples, and eight samples of miscellaneous origin (see Table 8). All patient samples were evaluated in detail by Southern blotting for the detection of *IGH*, *IGK*, *IGL*, *TCRB*, *TCRG*, and *TCRD* gene rearrangements, assuming that Southern blotting can be regarded as the gold standard for the detection of virtually all Ig/TCR gene rearrangements with a sensitivity of at least 10%.

**Detection rate of clonal Ig gene rearrangements in B-cell malignancies:** A remarkably high concordance was found between the PCR and Southern blotting results for the individual Ig gene rearrangements in the B-cell malignancies (Table 26). Overall, only 10–20% of the Southern blotting detected Ig rearrangements were missed by PCR analysis of the individual loci, mainly in germinal center and postgerminal center B-cell malignancies.

The combined usage of the three *IGH* VH–JH multiplex tubes had a clear added value (82% detection rate), which was further increased by use of the *IGH* DH–JH tubes, resulting in a total detection rate of 92% (Table 27). Apparently, the three VH–JH primer tubes compensate each other in annealing to mutated VH gene segments somatically. The virtually complete absence of somatic mutations in incomplete DH–JH rearrangements probably explains the added value of the DH–JH tubes, despite the lower frequency of these rearrangements (40–70%).

The clonality detection rate could be further increased to maximal levels (98–100%) by inclusion of the two *IGK* multiplex tubes. The combined *IGK* V $\kappa$ –J $\kappa$  and *IGK*–K $\delta$  tubes had a high clonality detection rate of 80–90% (Table 27). This high detection rate is particularly based on the fact that ~30% of Ig $\kappa$ <sup>+</sup> B-cell malignancies and all Ig $\lambda$ <sup>+</sup> B-cell malignancies contain *IGK*–K $\delta$  rearrangements, which are rarely somatically mutated.<sup>69,194</sup> It was remarkable to see that the *IGL* tube had virtually no added value on top of the *IGH* and *IGK* tubes, even not in Ig $\lambda$ <sup>+</sup> B-cell malignancies (not shown). This can be explained by the presence of *IGK*–K $\delta$  rearrangements in all Ig $\lambda$ <sup>+</sup> B-cell malignancies. Our current studies in several categories of WHO-defined B-cell malignancies confirm the strong added value of the *IGH* DH–JH and *IGK* tubes.

**Detection rate of clonal TCR gene rearrangements in T-cell malignancies:** A remarkably high concordance was also found in T-cell malignancies between PCR and Southern blotting results for the individual TCR gene rearrangements (Table 26). Although only 18 cases were studied, it was clear that only a few TCR gene rearrangements were missed by PCR analysis.

Traditionally, the *TCRG* gene rearrangements have been used as PCR targets for clonality studies. Now *TCRB* gene rearrangements can be exploited as highly reliable PCR targets (Table 28); they represent attractive targets because of their extensive junctional regions. The combined usage of the *TCRB* and *TCRG* multiplex tubes has an unprecedentedly high clonality detection rate in T-cell malignancies. This is explained by the fact that virtually all T-cell malignancies have *TCRG* gene rearrangements and that the vast majority has *TCRB* gene rearrangements. This is confirmed by our current studies in several categories of WHO-classified T-cell malignancies. Logically, *TCRD* gene rearrangements are useful PCR targets in immature (lymphoblastic) T-cell malignancies and in T-cell malignancies of the TCR $\gamma\delta$  lineage.

#### Detection of t(11;14) (*BCL1*–*IGH*) and t(14;18) (*BCL2*–*IGH*)

In MCL patients with t(11;14) (*BCL1*–*IGH*), the *BCL1* breakpoints are scattered over a large region of more than 200 kb, thereby precluding a high detection rate in routine PCR analysis. Also the here presented *BCL1*–*IGH* tube only detects approximately 40% of *BCL1* translocations in MCL, which is comparable to the literature.

**Table 26** Concordance between multiplex PCR results and Southern blot analysis results (PCR/SB) on Ig/TCR gene rearrangements per (sub)category of included frozen samples

Diagnosis	<i>IGH</i> <sup>a</sup>	<i>IGK</i>	<i>IGL</i>	<i>TCRB</i>	<i>TCRG</i>	<i>TCRD</i>
Prefollicular ( <i>n</i> = 8)	C <sup>b</sup> : 8/8 P <sup>b</sup> : 0/0	C: 8/8 P: 0/0	C: 4/4 P: 4/4	C: 2/4 <sup>c</sup> P: 4/4	C: 0/0 P: 8/8	C: 0/0 P: 8/8 <sup>e</sup>
B-CLL ( <i>n</i> = 16)	C: 15/16 P: 0/0	C: 16/16 P: 0/0	C: 5/5 P: 9/11	C: 1/1 P: 15/15	C: 0/0 P: 16/16	C: 2/2 P: 14/14
(Post)follicular ( <i>n</i> = 25)	C: 22/25 <sup>c</sup> P: 0/0	C: 19/24 <sup>d</sup> P: 0/1	C: 3/5 P: 19/20	C: 2/4 P: 21/21 <sup>e,f</sup>	C: 0/1 P: 22/24	C: 0/0 P: 24/25 <sup>f</sup>
All B-cell malignancies ( <i>n</i> = 49)	C: 45/49 P: 0/0	C: 43/48 P: 0/1	C: 12/14 P: 32/35	C: 5/9 P: 40/40	C: 0/1 P: 46/48	C: 2/2 P: 46/47
T-cell malignancies ( <i>n</i> = 18)	C: 2/2 P: 15/16 <sup>f</sup>	C: 0/0 P: 17/18	C: 0/0 P: 17/18	C: 17/17 <sup>d</sup> P: 1/1	C: 15/16 <sup>c</sup> P: 1/2	C: 2/3 P: 14/15 <sup>f</sup>
Reactive samples ( <i>n</i> = 15)	C: 0/0 P: 15/15	C: 0/0 P: 15/15	C: 0/0 P: 15/15	C: 0/0 P: 14/15	C: 0/0 P: 15/15	C: 0/0 P: 15/15
Miscellaneous ( <i>n</i> = 8)	C: 3/3 P: 3/5	C: 2/2 P: 4/6	C: 0/0 P: 6/8	C: 3/3 P: 5/5 <sup>e</sup>	C: 1/1 P: 6/7	C: 1/1 P: 5/7
All samples ( <i>n</i> = 90)	C: 50/54 P: 33/36	C: 45/50 P: 36/40	C: 12/14 P: 70/76	C: 25/29 P: 60/61	C: 16/18 P: 68/72	C: 5/6 P: 80/84

<sup>a</sup>Includes both VH–JH and DH–JH PCR analysis.<sup>b</sup>C, clonal rearrangements; P, polyclonal rearrangements.<sup>c</sup>In one sample clonality in GeneScanning only.<sup>d</sup>In one sample clonality in heteroduplex analysis only.<sup>e</sup>In one sample polyclonality in GeneScanning only.<sup>f</sup>In one sample polyclonality in heteroduplex analysis only.

In contrast, knowledge about the clustering of the breakpoints in the downstream *BCL2* region allowed the design of three *BCL2-IGH* multiplex tubes that reached a total detection rate of >80%, which is an unprecedentedly high frequency as compared to the literature.

### Choice of targets and choice of technique for PCR-based clonality diagnostics

Based on the above summarized data and the current experience of the participants of the BIOMED-2 Concerted Action BMH4-CT98-3936, it is possible to design stepwise strategies for PCR-based clonality diagnostics in suspect B-cell or T-cell proliferations. For example, in case of a suspect B-cell proliferation the three *IGH* VH–JH tubes and the two *IGK* tubes (Vκ–Jκ and Kde) can be used as five first-choice multiplex tubes (Table 27). If no clonal PCR products are obtained, extra PCR analyses can be performed by use of the *IGH* DH–JH and *IGL* tubes (three extra tubes). Alternative strategies can be designed, for example, by choosing two *IGH* VH–JH multiplex tubes (eg VH–FR1 and VH–FR2 primers), one *IGH* DH–JH (tube D) and the two *IGK* multiplex tubes. These five multiplex tubes can detect clonality in virtually all B-cell malignancies.

Logically, if the lymphoproliferation is suspected to be an MCL or FCL, the t(11;14) (*BCL1-IGH*) and t(14;18) (*BCL2-IGH*) tubes should also be included, respectively.

For clonality diagnostics in suspect T-cell proliferations, the choice of PCR targets is relatively simple: three multiplex *TCRB* tubes (two Vβ–Jβ and one Dβ–Jβ) as well as two multiplex *TCRG* tubes. These five TCR multiplex tubes should be able to detect clonality in the vast majority of T-cell malignancies (Table 28). In immature T-cell malignancies or TCRγδ<sup>+</sup> T-cell proliferations, the *TCRD* gene rearrangements should also be studied.

As heteroduplex analysis separates PCR products according to length and composition of the junctional region, this technique can be used for all Ig/TCR targets, also for rearrangements with short junctional regions (*IGH* DH–JH and *IGK*). However, a low tumor load and small subclones (<10%) might be missed. GeneScanning separates PCR products according to length of the junctional regions only. Therefore, GeneScanning works perfectly for *IGH* VH–JH and *TCRB* gene targets, but also for *TCRG* gene targets, with a good sensitivity of 0.5–5%. However, GeneScanning of *IGH* DH–JH and *IGK* PCR products might be difficult, particularly in case of a low tumor load or small subclones.

Consequently, the choice of PCR targets and the choice of technique will be influenced by the diagnostic problem such as the type and the estimated relative size of the suspect lymphoproliferation.

### Control gene primer sets for quality assessment of DNA from paraffin-embedded tissue samples

DNA extracted from paraffin-embedded tissue samples frequently is of moderate to poor quality and might contain PCR inhibitors. Consequently, it is essential to evaluate the integrity and amplifiability of DNA extracted from paraffin-embedded tissues. The multiplex BIOMED-2 Control Gene tube (PCR products of 100, 200, 300, 400, and 600 bp) has proven to be informative for such evaluation. For reliable Ig/TCR assays on DNA from paraffin-embedded tissue samples, the control gene PCR tube should result in PCR products of at least 300 bp (sufficient DNA integrity) and at least two concentrations of DNA should be tested, for example, 100 and 50 ng (dilution of PCR inhibitors). The better amplifiable DNA concentration should be used for duplicate PCR-based clonality studies in

**Table 27** Complementarity of different Ig multiplex PCR targets for clonality detection in Southern blot-defined B-cell malignancies

Multiplex PCR tubes	Diagnosis <sup>a</sup>			
	Pregerminal center B (n = 8)	B-CLL (n = 16)	(Post)germinal center B (n = 25)	All B-cell malignancies (n = 49)
IGH VH-JH FR1	8/8 <sup>b</sup> (100%)	14/16 <sup>c</sup> (88%)	15/25 <sup>b</sup> (60%)	37/49 (76%)
IGH VH-JH FR2	8/8 (100%)	15/16 (94%)	14/25 <sup>b</sup> (56%)	37/49 (76%)
IGH VH-JH FR3	8/8 (100%)	14/16 (88%)	11/25 <sup>c</sup> (44%)	33/49 (67%)
IGH VH-JH all FR	8/8 (100%)	15/16 (94%)	17/25 (68%)	40/49 (82%)
IGH DH-JH	0/8 (0%)	11/16 (69%)	11/25 (44%)	22/49 (45%)
IGH VH-JH+IGH DH-JH	8/8 (100%)	15/16 (94%)	22/25 (88%)	45/49 (92%)
IGK	8/8 (100%)	16/16 (100%)	21/25 <sup>d</sup> (84%)	45/49 (92%)
IGL	4/8 (50%)	7/16 <sup>e</sup> (44%)	4/25 <sup>f</sup> (16%)	15/49 (31%)
IGH VH-JH+IGK	8/8 (100%)	16/16 (100%)	21/25 (84%)	45/49 (92%)
IGH VH-JH+IGL	8/8 (100%)	15/16 (94%)	17/25 (68%)	40/49 (82%)
IGH VH-JH+IGH DH-JH+IGK	8/8 (100%)	16/16 (100%)	24/25 (96%)	48/49 (98%)
IGH VH-JH+IGH DH-JH+IGK+IGL	8/8 (100%)	16/16 (100%)	24/25 (96%)	48/49 (98%)

<sup>a</sup>All samples have clonal gene rearrangements in at least the *IGH* locus as determined by Southern blot analysis.

<sup>b</sup>Two cases showed clonal products in GeneScanning, but polyclonal products in heteroduplex analysis.

<sup>c</sup>One case showed clonal products in GeneScanning, but polyclonal products in heteroduplex analysis.

<sup>d</sup>Including case 25-NL-4 with weak clonal *IGH*, but polyclonal *IGK* gene rearrangements in Southern blot analysis.

<sup>e</sup>Including cases 11-NL-19 and 12-ES-1 with clonal *IGH+IGK*, but polyclonal *IGL* gene rearrangements in Southern blot analysis.

<sup>f</sup>Including case 39-PT-11 with clonal *IGH+IGK*, but polyclonal *IGL* gene rearrangements in Southern blot analysis.

order to aim for a high detection rate of clonal rearrangements (see Section 10 for details).

Although the Control Gene tube can be helpful in estimating the success rate of the BIOMED-2 multiplex tubes for clonality studies in paraffin-embedded material, it should be emphasized that usage of fresh or frozen tissue samples is preferred for PCR-based clonality diagnostics.

### Availability of BIOMED-2 multiplex PCR tubes

The production, vialing and quality control testing of the 18 BIOMED-2 multiplex PCR tubes and the Control Gene tube is time-consuming and not easy to perform by a single or a few laboratories. Therefore, it was decided to make the BIOMED-2 primers commercially available via InVivoScribe Technologies (Carlsbad, CA, USA; [www.invivoscribe.com](http://www.invivoscribe.com)). The quality control testing of each new batch of BIOMED-2 multiplex tubes will be performed by a group of 13 BIOMED-2 laboratories on a rotation basis.

### Multicolor GeneScanning

GeneScanning allows the application of up to three or four different fluorochrome-conjugated primers in a single tube. Such differential labeling of primers is only relevant if this results in extra discrimination between different types of Ig or TCR gene rearrangements.

Differential labeling of V primers generally has no added value, but differential labeling of downstream primers might support the rapid and easy identification of the type of Ig/TCR gene rearrangement, which is useful for PCR-based detection of MRD.<sup>195,196</sup> Labeling of J primers is not regarded to be informative for *IGH* (VH-JH or DH-JH), *IGK* (Vκ-Jκ), or *IGL* (Vλ-Jλ). For rapid identification of *IGK*-Kde rearrangements, it might be interesting to discriminate between Vκ-Kde and intronRSS-Kde rearrangements by differential labeling of the Kde and intronRSS primers (see Figure 6b).

The most informative multicolor GeneScanning can be designed for TCR gene rearrangements, facilitating the rapid recognition of the different types of *TCRB*, *TCRG*, and *TCRD* gene rearrangements. For example, Dr M Brüggemann and colleagues (Kiel, Germany) showed that differential labeling of the Jβ1 and Jβ2 primers in *TCRB* tube A (see Figure 8b) allows the easy identification of the polyclonal and monoclonal Vβ-Jβ1 vs Vβ-Jβ2 rearrangements (Figure 14a). Dr EA Macintyre and co-workers (Paris, France) introduced differential labeling of the Jγ1.3/2.3 and Jγ1.1/2.1 primers (Figure 9b), which results in the easy identification of the different types of *TCRG* gene rearrangements (Figure 14b). Finally, Dr FL Lavender and co-workers (Southampton, UK) designed a multicolor *TCRD* tube with differential labeling of the Jδ primers, Dδ2 primer, and Dδ3 primer (Figure 10b). This results in the easy identification of the most relevant *TCRD* gene rearrangements, such as Dδ2-Jδ, Vδ-Jδ, Dδ2-Dδ3, and Vδ2-Dδ3 rearrangements (Figure 14c).

The multicolor BIOMED-2 multiplex tubes have not extensively been tested by all 30 PCR laboratories, but it appears in practice that multicolor GeneScanning is easy and convenient.

**Table 28** Complementarity of different TCR multiplex PCR targets for clonality detection in Southern blot-defined T-cell malignancies

	TCRG	TCRB	TCRD	TCRG+TCRB	TCRG+TCRB+TCRD
T-cell malignancies (n = 18) <sup>a</sup>	16/18 <sup>b</sup> (89%)	17/18 (94%)	2/18 (11%)	18/18 (100%)	18/18 (100%)

<sup>a</sup>All samples have clonal gene rearrangements in the *TCRB* and/or *TCRG* locus as determined by Southern blot analysis, but only three cases had clonal *TCRD* gene rearrangements.

<sup>b</sup>Including case 56-ES-10 with clonal *TCRB*, but polyclonal *TCRG* gene rearrangements in Southern blot analysis.

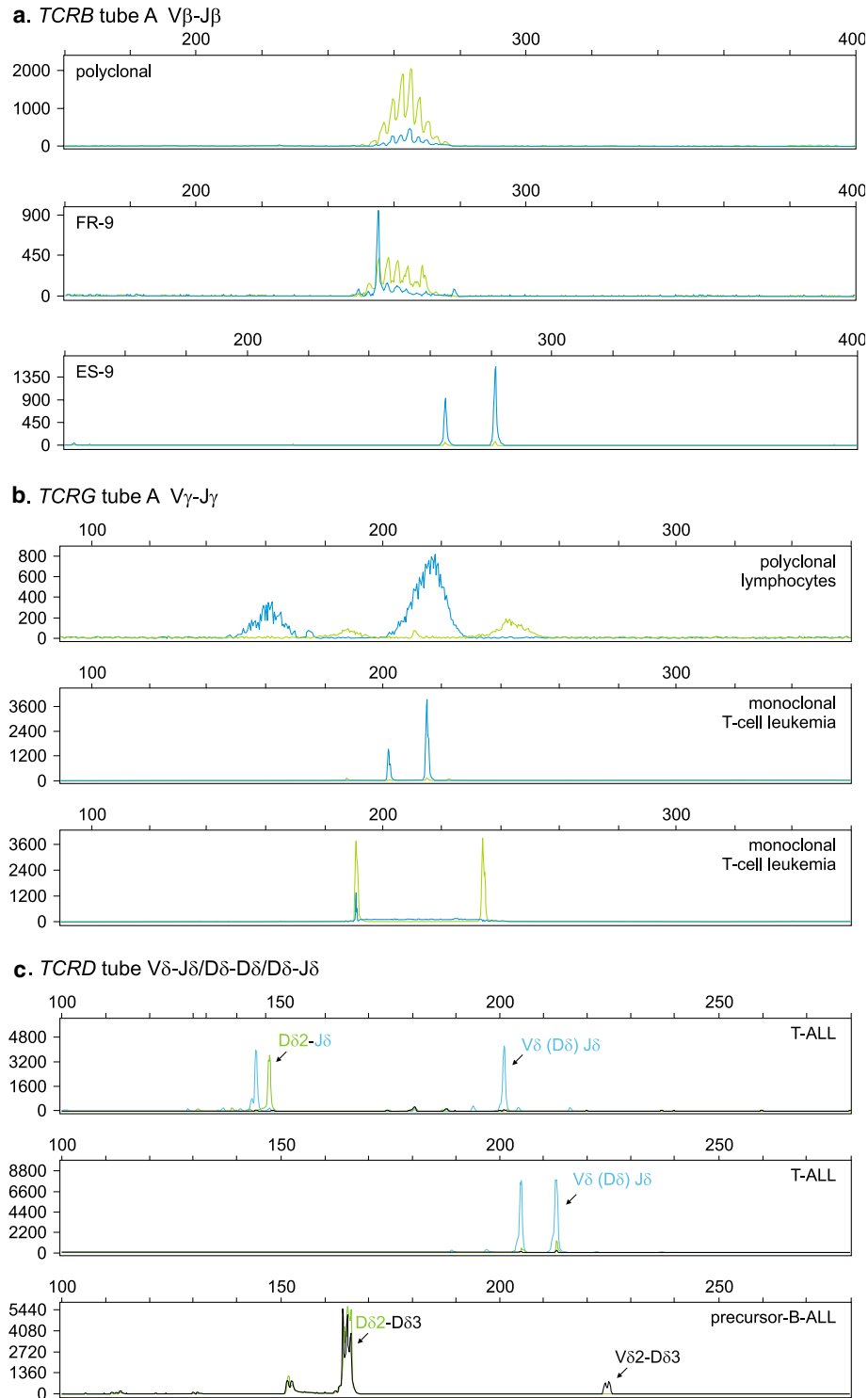


**Figure 14** Multicolor GeneScanning for supporting the rapid and easy identification of TCR gene rearrangements. (a) Two-color analysis of *TCRB* tube A with differential labeling of  $J\beta$ 1 primers (TET labeled; green) and  $J\beta$ 2 primers (FAM labeled; blue), as designed by M Brüggemann and co-workers. The top panel nicely shows the two polyclonal  $J\beta$ 1 and  $J\beta$ 2 rearrangement patterns (cf Figure 8C), whereas the other two panels show clonal  $J\beta$ 2 rearrangements. (b) Two-color analysis of *TCRG* tube A with differential labeling of the  $J\gamma$ 1.3/2.3 primer (FAM-labeled; blue) and the  $J\gamma$ 1.1/2.1 (TET labeled; green), as designed by EA Macintyre and co-workers. The top panel nicely shows the polyclonal rearrangement patterns (cf Figure 9c), whereas the other two panels show clonal  $J\gamma$ 1.3/2.3 and clonal  $J\gamma$ 1.1/2.1 rearrangements, respectively. (c) Three-color analysis of *TCRD* gene rearrangements with differential labeling of  $J\delta$  primers (FAM labeled; blue),  $D\delta$ 2 primer (HEX labeled; green) and  $D\delta$ 3 primer (NED labeled; black), as designed by FL Lavender and co-workers. Within the complex rearrangement patterns of the *TCRD* tube (Figure 10), the three-color analysis allows direct detection of  $V\delta$ - $J\delta$  rearrangements (blue peaks),  $D\delta$ 2- $J\delta$  rearrangements (blue and green peaks, not fully comigrating because of differences in migration speed of the two fluochromosomes),  $V\delta$ 2- $D\delta$ 3 rearrangement (black peaks), and  $D\delta$ 2- $D\delta$ 3 rearrangement (comigrating green and black peaks).

## Detection of MRD

Current cytotoxic treatment protocols induce complete remission in most ALL patient, in some patients with CLL, in most NHL patients, and in a part of the patients with MM. Nevertheless, many of these patients ultimately relapse, implying that not all clonogenic malignant cells had been killed, even though these patients reached complete remission according to cytomorphological criteria. The detection limit of cytomorphological techniques is not lower than 1–5% of malignant cells, implying that these techniques can provide only superficial information about the effectiveness of the treatment.

Detailed insight in treatment effectiveness needs highly sensitive techniques for the detection of low frequencies of malignant cells, that is, MRD. MRD techniques should preferably reach at least sensitivities of  $10^{-4}$  (one malignant cell in  $10^4$  normal cells). Such MRD information appears to have high prognostic value, particularly in ALL, for example, during and after induction therapy<sup>196–200</sup> and before stem cell transplantation.<sup>201–203</sup> In lymphoid malignancies, sensitive and quantitative detection of MRD can be achieved by real-time quantitative PCR analysis of patient-specific junctional regions of rearranged Ig/TCR genes.<sup>68,113,195,204</sup> This requires rapid and easy detection and identification of one (or two) Ig/TCR gene rearrangements in each patient with a lymphoid malignancy. It will be clear from the preceding sections that the BIOMED-2 multiplex PCR tubes are perfectly suited for this purpose.

## Conclusion and future perspectives

The 14 Ig/TCR and 4 *BCL1/BCL2* multiplex tubes have proven to be perfectly suited for PCR-based clonality studies in lymphoproliferative disorders. They have a relatively good sensitivity of 1–10% when heteroduplex analysis is used and 0.5–5% when GeneScanning is used. In particular, the combined use of the *IGH* and *IGK* tubes in suspect B-cell proliferations and the use of *TCRB* and *TCRG* tubes in suspect T-cell proliferations appears to result in unprecedentedly high clonality detection rates.

Currently, the BIOMED-2 laboratories ( $n = 47$ ) are studying a large series of approximately 600 WHO-classified lymphoid malignancies for their Ig/TCR gene rearrangement patterns and the occurrence of *BCL1* and *BCL2* translocations. The first results fully confirm the high clonality detection rates as observed in the General Testing (see Tables 27 and 28).

Whereas the diagnostic power of the BIOMED-2 multiplex tubes is clear, the ongoing studies show that some further improvements might be possible, such as clustering of the DH and V $\kappa$  primers, comparable to the V $\beta$  primers, so that the polyclonal rearrangements are clustered in a single Gaussian curve. Also the design of an additional JH consensus primer (partly overlapping with the existing JH consensus primer) might be useful in case of potential false-negative results due to somatic mutations. Finally, a few extra V $\beta$  primers might be designed for recognition of V $\beta$  gene segments that have not yet been covered by the current primer set. Such further improvements are included in the aims of the EuroClonality group, the continuation of the BIOMED-2 Concerted Action BMH4-CT98-3936 described here.

It should be emphasized that reliable molecular clonality diagnostics is not only determined by the quality and reproducibility of the PCR primers and protocols. Experience in the interpretation of GeneScanning and heteroduplex results is equally important. Finally, the obtained clonality results need to be integrated with the clinical, morphological, and immuno-

phenotypic data to make the final diagnosis and classification, a process that requires multidisciplinary case reviews with hematologists, cytomorphologists, pathologists, and immunologists.

## Acknowledgements

We are grateful to the teams of the National Network Leaders and the technicians of the participating laboratories for their continuous support to make this European collaboration successful. We gratefully acknowledge Professor Martin Dyer, University of Leicester, for the kind gift of cell lines K231, Oz, and SC1. We thank Marieke Comans-Bitter for the design of the high-quality figures, which turned out to be essential for summarizing the Concerted Action results. We are grateful to Gellof van Steenis and Winnie Monster-Hoogendoorn for their support in the completion of the financial administration of the EU project. Finally, we thank the secretaries of the coordinating center in Rotterdam for their continuous support, particularly Danielle Korpershoek, Annella Boon and Bibi van Bodegom.

## Financial support

This Concerted Action was supported financially by the EU BIOMED-2 Grant BMH4-CT98-3936 as well as by national funding, including Revolving Fund 1995 project (JJMvD and AWL), Leukaemia Research Fund Grants 9784, 9917 and 0141 (FLL and HEW), Fondo de Investigaciones Sanitarias Grant PI/20905 (RGS and MG), Fondation Contre la Leucémie of the Fondation de France (ED and EAM), Liga Portuguesa Contra o Cancro Grant 2/1998-2001/LPCC (AP) and Deutsche Krebshilfe Grant Kn-70354-2 (MK).

## References

- van Dongen JJM, Wolvers-Tettero ILM. Analysis of immunoglobulin and T cell receptor genes. Part II: possibilities and limitations in the diagnosis and management of lymphoproliferative diseases and related disorders. *Clin Chim Acta* 1991; **198**: 93–174.
- Jaffe ES, Harris NL, Stein H, Vardiman JW (eds) *World Health Organization Classification of Tumours. Pathology and Genetics of Tumours of Haematopoietic and Lymphoid Tissues*. Lyon: IARC Press, 2001.
- Tonegawa S. Somatic generation of antibody diversity. *Nature* 1983; **302**: 575–581.
- Davis MM, Björkman PJ. T-cell antigen receptor genes and T-cell recognition. *Nature* 1988; **334**: 395–402.
- van Dongen JJM, Szczepanski T, Adriaansen HJ. Immunobiology of leukemia. In: Henderson ES, Lister TA, Greaves MF (eds) *Leukemia*. Philadelphia: WB Saunders Company, 2002, pp 85–129.
- Szczepanski T, Pongers-Willems MJ, Langerak AW, van Dongen JJM. Unusual immunoglobulin and T-cell receptor gene rearrangement patterns in acute lymphoblastic leukemias. *Curr Top Microbiol Immunol* 1999; **246**: 205–215.
- Küppers R, Klein U, Hansmann ML, Rajewsky K. Cellular origin of human B-cell lymphomas. *N Engl J Med* 1999; **341**: 1520–1529.
- Smith BR, Weinberg DS, Robert NJ, Towle M, Luther E, Pinkus GS et al. Circulating monoclonal B lymphocytes in non-Hodgkin's lymphoma. *N Engl J Med* 1984; **311**: 1476–1481.
- Letwin BW, Wallace PK, Muirhead KA, Hensler GL, Kashatus WH, Horan PK. An improved clonal excess assay using flow cytometry and B-cell gating. *Blood* 1990; **75**: 1178–1185.
- Fukushima PI, Nguyen PK, O'Grady P, Stetler-Stevenson M. Flow cytometric analysis of kappa and lambda light chain expression in evaluation of specimens for B-cell neoplasia. *Cytometry* 1996; **26**: 243–252.

- 11 McCoy Jr JP, Overton WR, Schroeder K, Blumstein L, Donaldson MH. Immunophenotypic analysis of the T cell receptor V beta repertoire in CD4+ and CD8+ lymphocytes from normal peripheral blood. *Cytometry* 1996; **26**: 148–153.
- 12 van Dongen JJM, van den Beemd MWM, Schellekens M, Wolvers-Tettero ILM, Langerak AW, Groeneveld K. Analysis of malignant T cells with the V $\beta$  antibody panel. *Immunologist* 1996; **4**: 37–40.
- 13 Van den Beemd MWM, Boor PPC, Van Lochem EG, Hop WCJ, Langerak AW, Wolvers-Tettero ILM et al. Flow cytometric analysis of the V $\beta$  repertoire in healthy controls. *Cytometry* 2000; **40**: 336–345.
- 14 Lima M, Almeida J, Santos AH, dos Anjos Teixeira M, Alguero MC, Queiros ML et al. Immunophenotypic analysis of the TCR-Vbeta repertoire in 98 persistent expansions of CD3(+)/TCR-alpha-beta(+) large granular lymphocytes: utility in assessing clonality and insights into the pathogenesis of the disease. *Am J Pathol* 2001; **159**: 1861–1868.
- 15 Langerak AW, Wolvers-Tettero ILM, van den Beemd MWM, van Wering ER, Ludwig W-D, Hählen K et al. Immunophenotypic and immunogenotypic characteristics of TCR $\gamma\delta$  T cell acute lymphoblastic leukemia. *Leukemia* 1999; **13**: 206–214.
- 16 Langerak AW, van Den Beemd R, Wolvers-Tettero ILM, Boor PP, van Lochem EG, Hooijkaas H et al. Molecular and flow cytometric analysis of the Vbeta repertoire for clonality assessment in mature TCRalpha-beta T-cell proliferations. *Blood* 2001; **98**: 165–173.
- 17 Semenzato G, Zambello R, Starkebaum G, Oshimi K, Loughran Jr TP. The lymphoproliferative disease of granular lymphocytes: updated criteria for diagnosis. *Blood* 1997; **89**: 256–260.
- 18 Triebel F, Faure F, Graziani M, Jitsukawa S, Lefranc MP, Hercend T. A unique V–J–C-rearranged gene encodes a gamma protein expressed on the majority of CD3+ T cell receptor-alpha/beta-circulating lymphocytes. *J Exp Med* 1988; **167**: 694–699.
- 19 Breit TM, Wolvers-Tettero IL, van Dongen JJ. Unique selection determinant in polyclonal V delta 2–J delta 1 junctional regions of human peripheral gamma delta T lymphocytes. *J Immunol* 1994; **152**: 2860–2864.
- 20 Breit TM, Wolvers-Tettero ILM, Hählen K, Van Wering ER, van Dongen JJM. Limited combinatorial repertoire of  $\gamma\delta$  T-cell receptors expressed by T-cell acute lymphoblastic leukemias. *Leukemia* 1991; **5**: 116–124.
- 21 van Dongen JJM, Wolvers-Tettero ILM. Analysis of immunoglobulin and T cell receptor genes. Part I: basic and technical aspects. *Clin Chim Acta* 1991; **198**: 1–91.
- 22 Beishuizen A, Verhoeven MA, Mol EJ, Breit TM, Wolvers-Tettero ILM, van Dongen JJM. Detection of immunoglobulin heavy-chain gene rearrangements by Southern blot analysis: recommendations for optimal results. *Leukemia* 1993; **7**: 2045–2053.
- 23 Breit TM, Wolvers-Tettero ILM, Beishuizen A, Verhoeven M-AJ, van Wering ER, van Dongen JJM. Southern blot patterns, frequencies and junctional diversity of T-cell receptor  $\delta$  gene rearrangements in acute lymphoblastic leukemia. *Blood* 1993; **82**: 3063–3074.
- 24 Beishuizen A, Verhoeven MA, Mol EJ, van Dongen JJM. Detection of immunoglobulin kappa light-chain gene rearrangement patterns by Southern blot analysis. *Leukemia* 1994; **8**: 2228–2236.
- 25 Tümkaya T, Comans-Bitter WM, Verhoeven MA, van Dongen JJM. Southern blot detection of immunoglobulin lambda light chain gene rearrangements for clonality studies. *Leukemia* 1995; **9**: 2127–2132.
- 26 Tümkaya T, Beishuizen A, Wolvers-Tettero ILM, van Dongen JJM. Identification of immunoglobulin lambda isotype gene rearrangements by Southern blot analysis. *Leukemia* 1996; **10**: 1834–1839.
- 27 Moreau EJ, Langerak AW, van Gastel -Mol EJ, Wolvers-Tettero ILM, Zhan M, Zhou Q et al. Easy detection of all T cell receptor gamma (TCRG) gene rearrangements by Southern blot analysis: recommendations for optimal results. *Leukemia* 1999; **13**: 1620–1626.
- 28 Langerak AW, Wolvers-Tettero ILM, van Dongen JJM. Detection of T cell receptor beta (TCRB) gene rearrangement patterns in T cell malignancies by Southern blot analysis. *Leukemia* 1999; **13**: 965–974.
- 29 Hara J, Benedict SH, Mak TW, Gelfand EW. T cell receptor alpha-chain gene rearrangements in B-precursor leukemia are in contrast to the findings in T cell acute lymphoblastic leukemia. Comparative study of T cell receptor gene rearrangement in childhood leukemia. *J Clin Invest* 1987; **80**: 1770–1777.
- 30 Szczepanski T, Beishuizen A, Pongers-Willemsse MJ, Hählen K, van Wering ER, Wijkhuijs JM et al. Cross-lineage T-cell receptor gene rearrangements occur in more than ninety percent of childhood precursor-B-acute lymphoblastic leukemias: alternative PCR targets for detection of minimal residual disease. *Leukemia* 1999; **13**: 196–205.
- 31 Szczepanski T, Langerak AW, van Dongen JJ, van Krieken JH. Lymphoma with multi-gene rearrangement on the level of immunoglobulin heavy chain, light chain, and T-cell receptor beta chain. *Am J Hematol* 1998; **59**: 99–100.
- 32 Przybylski G, Oettle H, Ludwig WD, Siegert W, Schmidt CA. Molecular characterization of illegitimate TCR delta gene rearrangements in acute myeloid leukaemia. *Br J Haematol* 1994; **87**: 301–307.
- 33 Boeckx N, Willemsse MJ, Szczepanski T, van Der Velden VHJ, Langerak AW, Vandekerckhove P et al. Fusion gene transcripts and Ig/TCR gene rearrangements are complementary but infrequent targets for PCR-based detection of minimal residual disease in acute myeloid leukemia. *Leukemia* 2002; **16**: 368–375.
- 34 Szczepanski T, Pongers-Willemsse MJ, Langerak AW, Harts WA, Wijkhuijs JM, van Wering ER et al. Ig heavy chain gene rearrangements in T-cell acute lymphoblastic leukemia exhibit predominant DH6-19 and DH7-27 gene usage, can result in complete V–D–J rearrangements, and are rare in T-cell receptor  $\alpha\beta$  lineage. *Blood* 1999; **93**: 4079–4085.
- 35 Kluin-Nelemans HC, Kester MG, van deCorput L, Boor PP, Landegent JE, van Dongen JJ et al. Correction of abnormal T-cell receptor repertoire during interferon-alpha therapy in patients with hairy cell leukemia. *Blood* 1998; **91**: 4224–4231.
- 36 Sarzotti M, Patel DD, Li X, Ozaki DA, Cao S, Langdon S et al. T cell repertoire development in humans with SCID after non-ablative allogeneic marrow transplantation. *J Immunol* 2003; **170**: 2711–2718.
- 37 Mariani S, Coscia M, Even J, Peola S, Foglietta M, Boccadoro M et al. Severe and long-lasting disruption of T-cell receptor diversity in human myeloma after high-dose chemotherapy and autologous peripheral blood progenitor cell infusion. *Br J Haematol* 2001; **113**: 1051–1059.
- 38 Davis TH, Yockey CE, Balk SP. Detection of clonal immunoglobulin gene rearrangements by polymerase chain reaction amplification and single-strand conformational polymorphism analysis. *Am J Pathol* 1993; **142**: 1841–1847.
- 39 Bourguin A, Tung R, Galili N, Sklar J. Rapid, nonradioactive detection of clonal T-cell receptor gene rearrangements in lymphoid neoplasms. *Proc Natl Acad Sci USA* 1990; **87**: 8536–8540.
- 40 Bottaro M, Berti E, Biondi A, Migone N, Crosti L. Heteroduplex analysis of T-cell receptor gamma gene rearrangements for diagnosis and monitoring of cutaneous T-cell lymphomas. *Blood* 1994; **83**: 3271–3278.
- 41 Langerak AW, Szczepanski T, van der Burg M, Wolvers-Tettero ILM, van Dongen JJM. Heteroduplex PCR analysis of rearranged T cell receptor genes for clonality assessment in suspect T cell proliferations. *Leukemia* 1997; **11**: 2192–2199.
- 42 Kneba M, Bolz I, Linke B, Hiddemann W. Analysis of rearranged T-cell receptor beta-chain genes by polymerase chain reaction (PCR) DNA sequencing and automated high resolution PCR fragment analysis. *Blood* 1995; **86**: 3930–3937.
- 43 Linke B, Bolz I, Fayyazi A, von Hofen M, Pott C, Bertram J et al. Automated high resolution PCR fragment analysis for identification of clonally rearranged immunoglobulin heavy chain genes. *Leukemia* 1997; **11**: 1055–1062.
- 44 Matsuda F, Ishii K, Bourvagnet P, Kuma K, Hayashida H, Miyata T et al. The complete nucleotide sequence of the human immunoglobulin heavy chain variable region locus. *J Exp Med* 1998; **188**: 2151–2162.
- 45 Camacho FI, Algara P, Rodriguez A, Ruiz-Ballesteros E, Mollejo M, Martinez N et al. Molecular heterogeneity in MCL defined by the use of specific VH genes and the frequency of somatic mutations. *Blood* 2003; **101**: 4042–4046.
- 46 Pritsch O, Troussard X, Magnac C, Mauro FR, Davi F, Payelle-Brogard B et al. VH gene usage by family members affected with



- chronic lymphocytic leukaemia. *Br J Haematol* 1999; **107**: 616–624.
- 47 Rettig MB, Vescio RA, Cao J, Wu CH, Lee JC, Han E et al. VH gene usage is multiple myeloma: complete absence of the VH4.21 (VH4–34) gene. *Blood* 1996; **87**: 2846–2852.
- 48 Mortuza FY, Moreira IM, Papaioannou M, Gameiro P, Coyle LA, Gricks CS et al. Immunoglobulin heavy-chain gene rearrangement in adult acute lymphoblastic leukemia reveals preferential usage of J(H)-proximal variable gene segments. *Blood* 2001; **97**: 2716–2726.
- 49 Ghia P, ten Boekel E, Rolink AG, Melchers F. B-cell development: a comparison between mouse and man. *Immunol Today* 1998; **19**: 480–485.
- 50 Corbett SJ, Tomlinson IM, Sonnhammer ELL, Buck D, Winter G. Sequence of the human immunoglobulin diversity (D) segment locus: a systematic analysis provides no evidence for the use of DIR segments, inverted D segments, 'minor' D segments or D–D recombination. *J Mol Biol* 1997; **270**: 587–597.
- 51 Ichihara Y, Matsuoka H, Kurosawa Y. Organization of human immunoglobulin heavy chain diversity gene loci. *EMBO J* 1988; **7**: 4141–4150.
- 52 Bertrand III FE, Billips LG, Burrows PD, Gartland GL, Kubagawa H, Schroeder Jr HW. Ig D(H) gene segment transcription and rearrangement before surface expression of the pan-B-cell marker CD19 in normal human bone marrow. *Blood* 1997; **90**: 736–744.
- 53 Ghia P, ten Boekel E, Sanz E, de la Hera A, Rolink A, Melchers F. Ordering of human bone marrow B lymphocyte precursors by single-cell polymerase chain reaction analyses of the rearrangement status of the immunoglobulin H and L chain gene loci. *J Exp Med* 1996; **184**: 2217–2229.
- 54 Szczepanski T, Willemse MJ, van Wering ER, Weerden JF, Kamps WA, van Dongen JJM. Precursor-B-ALL with DH–JH gene rearrangements have an immature immunogenotype with a high frequency of oligoclonality and hyperdiploidy of chromosome 14. *Leukemia* 2001; **15**: 1415–1423.
- 55 Davi F, Faili A, Gritti C, Blanc C, Laurent C, Sutton L et al. Early onset of immunoglobulin heavy chain gene rearrangements in normal human bone marrow CD34+ cells. *Blood* 1997; **90**: 4014–4021.
- 56 Szczepanski T, van't Veer MB, Wolvers-Tettero ILM, Langerak AW, van Dongen JJM. Molecular features responsible for the absence of immunoglobulin heavy chain protein synthesis in an IgH(–) subgroup of multiple myeloma. *Blood* 2000; **96**: 1087–1093.
- 57 Schroeder Jr HW, Wang JY. Preferential utilization of conserved immunoglobulin heavy chain variable gene segments during human fetal life. *Proc Natl Acad Sci USA* 1990; **87**: 6146–6150.
- 58 Raaphorst FM, Raman CS, Tami J, Fischbach M, Sanz I. Human Ig heavy chain CDR3 regions in adult bone marrow pre-B cells display an adult phenotype of diversity: evidence for structural selection of DH amino acid sequences. *Int Immunol* 1997; **9**: 1503–1515.
- 59 Lebecque SG, Gearhart PJ. Boundaries of somatic mutation in rearranged immunoglobulin genes: 5' boundary is near the promoter, and 3' boundary is approximately 1 kb from V(D)J gene. *J Exp Med* 1990; **172**: 1717–1727.
- 60 Fukita Y, Jacobs H, Rajewsky K. Somatic hypermutation in the heavy chain locus correlates with transcription. *Immunity* 1998; **9**: 105–114.
- 61 Zachau HG. *Immunologist* 1996; **4**: 49–54.
- 62 Lefranc MP. IMGT, the international ImMunoGeneTics database. *Nucleic Acids Res* 2003; **31**: 307–310.
- 63 Lefranc MP. IMGT databases, web resources and tools for immunoglobulin and T cell receptor sequence analysis, <http://imgt.cines.fr>. *Leukemia* 2003; **17**: 260–266.
- 64 Schable KF, Zachau HG. The variable genes of the human immunoglobulin kappa locus. *Biol Chem Hoppe Seyler* 1993; **374**: 1001–1022.
- 65 Weichhold GM, Ohnheiser R, Zachau HG. The human immunoglobulin kappa locus consists of two copies that are organized in opposite polarity. *Genomics* 1993; **16**: 503–511.
- 66 Siminovitch KA, Bakhshi A, Goldman P, Korsmeyer SJ. A uniform deleting element mediates the loss of kappa genes in human B cells. *Nature* 1985; **316**: 260–262.
- 67 Szczepanski T, Langerak AW, Wolvers-Tettero ILM, Ossenkoppele GJ, Verhoef G, Stul M et al. Immunoglobulin and T cell receptor gene rearrangement patterns in acute lymphoblastic leukemia are less mature in adults than in children: implications for selection of PCR targets for detection of minimal residual disease. *Leukemia* 1998; **12**: 1081–1088.
- 68 Van der Velden VHJ, Willemse MJ, van der Schoot CE, van Wering ER, van Dongen JJM. Immunoglobulin kappa deleting element rearrangements in precursor-B acute lymphoblastic leukemia are stable targets for detection of minimal residual disease by real-time quantitative PCR. *Leukemia* 2002; **16**: 928–936.
- 69 van der Burg M, Tumkaya T, Boerma M, de Bruin-Versteeg S, Langerak AW, van Dongen JJM. Ordered recombination of immunoglobulin light chain genes occurs at the IGK locus but seems less strict at the IGL locus. *Blood* 2001; **97**: 1001–1008.
- 70 Cannell PK, Amlot P, Attard M, Hoffbrand AV, Foroni L. Variable kappa gene rearrangement in lymphoproliferative disorders: an analysis of V kappa gene usage, VJ joining and somatic mutation. *Leukemia* 1994; **8**: 1139–1145.
- 71 Fripiat JP, Williams SC, Tomlinson IM, Cook GP, Cherif D, Le Paslier D et al. Organization of the human immunoglobulin lambda light-chain locus on chromosome 22q11.2. *Hum Mol Genet* 1995; **4**: 983–991.
- 72 Williams SC, Fripiat JP, Tomlinson IM, Ignatovich O, Lefranc MP, Winter G. Sequence and evolution of the human germline V lambda repertoire. *J Mol Biol* 1996; **264**: 220–232.
- 73 Kawasaki K, Minoshima S, Nakato E, Shibuya K, Shintani A, Schmeits JL et al. One-megabase sequence analysis of the human immunoglobulin lambda gene locus. *Genome Res* 1997; **7**: 250–261.
- 74 Hieter PA, Korsmeyer SJ, Waldmann TA, Leder P. Human immunoglobulin kappa light-chain genes are deleted or rearranged in lambda-producing B cells. *Nature* 1981; **290**: 368–372.
- 75 Vasicek TJ, Leder P. Structure and expression of the human immunoglobulin lambda genes. *J Exp Med* 1990; **172**: 609–620.
- 76 Taub RA, Hollis GF, Hieter PA, Korsmeyer S, Waldmann TA, Leder P. Variable amplification of immunoglobulin lambda light-chain genes in human populations. *Nature* 1983; **304**: 172–174.
- 77 van der Burg M, Barendregt BH, van Gastel-Mol EJ, Tumkaya T, Langerak AW, van Dongen JJ. Unraveling of the polymorphic C lambda 2–C lambda 3 amplification and the Ke+Oz-polymorphism in the human Ig lambda locus. *J Immunol* 2002; **169**: 271–276.
- 78 Ignatovich O, Tomlinson IM, Jones PT, Winter G. The creation of diversity in the human immunoglobulin V(lambda) repertoire. *J Mol Biol* 1997; **268**: 69–77.
- 79 Bridges Jr SL. Frequent N addition and clonal relatedness among immunoglobulin lambda light chains expressed in rheumatoid arthritis synovia and PBL, and the influence of V lambda gene segment utilization on CDR3 length. *Mol Med* 1998; **4**: 525–553.
- 80 Kiyoi H, Naito K, Ohno R, Saito H, Naoe T. Characterization of the immunoglobulin light chain variable region gene expressed in multiple myeloma. *Leukemia* 1998; **12**: 601–609.
- 81 Tumkaya T, van der Burg M, Garcia Sanz R, Gonzalez Diaz M, Langerak AW, San Miguel JF et al. Immunoglobulin lambda isotype gene rearrangements in B-cell malignancies. *Leukemia* 2001; **15**: 121–127.
- 82 Farner NL, Dorner T, Lipsky PE. Molecular mechanisms and selection influence the generation of the human V lambda J lambda repertoire. *J Immunol* 1999; **162**: 2137–2145.
- 83 Ignatovich O, Tomlinson IM, Popov AV, Bruggemann M, Winter G. Dominance of intrinsic genetic factors in shaping the human immunoglobulin V lambda repertoire. *J Mol Biol* 1999; **294**: 457–465.
- 84 Arden B, Clark SP, Kabelitz D, Mak TW. Human T-cell receptor variable gene segment families. *Immunogenetics* 1995; **42**: 455–500.
- 85 Wei S, Charnley P, Robinson MA, Concannon P. The extent of the human germline T-cell receptor V beta gene segment repertoire. *Immunogenetics* 1994; **40**: 27–36.
- 86 Rowen L, Koop BF, Hood L. The complete 685-kilobase DNA sequence of the human beta T cell receptor locus. *Science* 1996; **272**: 1755–1762.

- 87 Charnley P, Wei S, Concannon P. Polymorphisms in the TCRB-V2 gene segments localize the Tcrb orthon genes to human chromosome 9p21. *Immunogenetics* 1993; **38**: 283–286.
- 88 Robinson MA, Mitchell MP, Wei S, Day CE, Zhao TM, Concannon P. Organization of human T-cell receptor beta-chain genes: clusters of V beta genes are present on chromosomes 7 and 9. *Proc Natl Acad Sci USA* 1993; **90**: 2433–2437.
- 89 Toyonaga B, Yoshikai Y, Vadasz V, Chin B, Mak TW. Organization and sequences of the diversity, joining, and constant region genes of the human T-cell receptor beta chain. *Proc Natl Acad Sci USA* 1985; **82**: 8624–8628.
- 90 Liu D, Callahan JP, Dau PC. Intrafamily fragment analysis of the T cell receptor beta chain CDR3 region. *J Immunol Methods* 1995; **187**: 139–150.
- 91 Tsuda S, Rieke S, Hashimoto Y, Nakauchi H, Takahama Y. IL-7 supports D-J but not V-DJ rearrangement of TCR-beta gene in fetal liver progenitor cells. *J Immunol* 1996; **156**: 3233–3242.
- 92 Weidmann E, Whiteside TL, Giorda R, Herberman RB, Trucco M. The T-cell receptor V beta gene usage in tumor-infiltrating lymphocytes and blood of patients with hepatocellular carcinoma. *Cancer Res* 1992; **52**: 5913–5920.
- 93 Jores R, Meo T. Few V gene segments dominate the T cell receptor beta-chain repertoire of the human thymus. *J Immunol* 1993; **151**: 6110–6122.
- 94 Rosenberg WM, Moss PA, Bell JL. Variation in human T cell receptor V beta and J beta repertoire: analysis using anchor polymerase chain reaction. *Eur J Immunol* 1992; **22**: 541–549.
- 95 Pongers-Willems MJ, Seriu T, Stolz F, d'Aniello E, Gameiro P, Pisa P et al. Primers and protocols for standardized MRD detection in ALL using immunoglobulin and T cell receptor gene rearrangements and *TAL1* deletions as PCR targets. Report of the BIOMED-1 Concerted Action: investigation of minimal residual disease in acute leukemia. *Leukemia* 1999; **13**: 110–118.
- 96 Hansen-Hagge TE, Yokota S, Bartram CR. Detection of minimal residual disease in acute lymphoblastic leukemia by *in vitro* amplification of rearranged T-cell receptor delta chain sequences. *Blood* 1989; **74**: 1762–1767.
- 97 Cave H, Guidal C, Rohrlach P, Delfau MH, Broyart A, Lescoeur B et al. Prospective monitoring and quantitation of residual blasts in childhood acute lymphoblastic leukemia by polymerase chain reaction study of delta and gamma T-cell receptor genes. *Blood* 1994; **83**: 1892–1902.
- 98 Gorski J, Yassai M, Zhu X, Kissella B, Kissella B, Keever C et al. Circulating T cell repertoire complexity in normal individuals and bone marrow recipients analyzed by CDR3 size spectratyping. Correlation with immune status. *J Immunol* 1994; **152**: 5109–5119.
- 99 McCarthy KP, Sloane JP, Kabarowski JH, Matutes E, Wiedemann LM. The rapid detection of clonal T-cell proliferations in patients with lymphoid disorders. *Am J Pathol* 1991; **138**: 821–828.
- 100 Assaf C, Hummel M, Dippel E, Goerdts S, Muller HH, Anagnostopoulos I et al. High detection rate of T-cell receptor beta chain rearrangements in T-cell lymphoproliferations by family specific polymerase chain reaction in combination with the GeneScan technique and DNA sequencing. *Blood* 2000; **96**: 640–646.
- 101 O'Shea U, Wyatt JL, Howdle PD. Analysis of T cell receptor beta chain CDR3 size using RNA extracted from formalin fixed paraffin wax embedded tissue. *J Clin Pathol* 1997; **50**: 811–814.
- 102 Duby AD, Seidman JG. Abnormal recombination products result from aberrant DNA rearrangement of the human T-cell antigen receptor beta-chain gene. *Proc Natl Acad Sci USA* 1986; **83**: 4890–4894.
- 103 Alatrakchi N, Farace F, Frau E, Carde P, Munck JN, Triebel F. T-cell clonal expansion in patients with B-cell lymphoproliferative disorders. *J Immunother* 1998; **21**: 363–370.
- 104 Blom B, Verschuren MC, Heemsker MH, Bakker AQ, van Gastel-Mol EJ, Wolvers-Tettero IL et al. TCR gene rearrangements and expression of the pre-T cell receptor complex during human T-cell differentiation. *Blood* 1999; **93**: 3033–3043.
- 105 Chen Z, Font MP, Loiseau P, Bories JC, Degos L, Lefranc MP et al. The human T-cell V gamma gene locus: cloning of new segments and study of V gamma rearrangements in neoplastic T and B cells. *Blood* 1988; **72**: 776–783.
- 106 Zhang XM, Tonnel C, Lefranc MP, Huck S. T cell receptor gamma cDNA in human fetal liver and thymus: variable regions of gamma chains are restricted to V gamma I or V9, due to the absence of splicing of the V10 and V11 leader intron. *Eur J Immunol* 1994; **24**: 571–578.
- 107 Huck S, Lefranc MP. Rearrangements to the JP1, JP and JP2 segments in the human T-cell rearranging gamma gene (TRG gamma) locus. *FEBS Lett* 1987; **224**: 291–296.
- 108 Quertermous T, Strauss WM, van Dongen JJ, Seidman JG. Human T cell gamma chain joining regions and T cell development. *J Immunol* 1987; **138**: 2687–2690.
- 109 Delfau MH, Hance AJ, Lecossier D, Vilmer E, Grandchamp B. Restricted diversity of V gamma 9-JP rearrangements in unstimulated human gamma/delta T lymphocytes. *Eur J Immunol* 1992; **22**: 2437–2443.
- 110 Porcelli S, Brenner MB, Band H. Biology of the human gamma delta T-cell receptor. *Immunol Rev* 1991; **120**: 137–183.
- 111 Szczepanski T, Langerak AW, Willems MJ, Wolvers-Tettero ILM, van Wering ER, van Dongen JJM. T cell receptor gamma (TCRG) gene rearrangements in T cell acute lymphoblastic leukemia reflect 'end-stage' recombinations: implications for minimal residual disease monitoring. *Leukemia* 2000; **14**: 1208–1214.
- 112 Delabesse E, Burtin ML, Millien C, Madonik A, Arnulf B, Beldjord K et al. Rapid, multicolor fluorescent TCRG Vgamma and Jgamma typing: application to T cell acute lymphoblastic leukemia and to the detection of minor clonal populations. *Leukemia* 2000; **14**: 1143–1152.
- 113 Van der Velden VHJ, Wijkhuijs JM, Jacobs DCH, van Wering ER, van Dongen JJM. T cell receptor gamma gene rearrangements as targets for detection of minimal residual disease in acute lymphoblastic leukemia by real-time quantitative PCR analysis. *Leukemia* 2002; **16**: 1372–1380.
- 114 Taylor JJ, Rowe D, Reid MM, Middleton PG. An interstitial deletion in the rearranged T-cell receptor gamma chain locus in a case of T-cell acute lymphoblastic leukaemia. *Br J Haematol* 1993; **85**: 193–196.
- 115 Castellanos A, Martin-Seisdedos C, Toribio ML, San Miguel JF, Gonzalez Sarmiento R. TCR-gamma gene rearrangement with interstitial deletion within the TRGV2 gene segment is not detected in normal T-lymphocytes. *Leukemia* 1998; **12**: 251–253.
- 116 Verschuren MC, Wolvers-Tettero IL, Breit TM, van Dongen JJ. T-cell receptor V delta-J alpha rearrangements in human thymocytes: the role of V delta-J alpha rearrangements in T-cell receptor-delta gene deletion. *Immunology* 1998; **93**: 208–212.
- 117 WHO-IUIS Nomenclature Sub-Committee on TCR Designation. Nomenclature for T-cell receptor (TCR) gene segments of the immune system. *Immunogenetics* 1995; **42**: 451–453.
- 118 Kabelitz D, Wesch D, Hinz T. Gamma delta T cells, their T cell receptor usage and role in human diseases. *Springer Semin Immunopathol* 1999; **21**: 55–75.
- 119 Shen J, Andrews DM, Pandolfi F, Boyle LA, Kersten CM, Blatman RN et al. Oligoclonality of Vdelta1 and Vdelta2 cells in human peripheral blood mononuclear cells: TCR selection is not altered by stimulation with Gram-negative bacteria. *J Immunol* 1998; **160**: 3048–3055.
- 120 Alaibac M, Daga A, Harms G, Morris J, Yu RC, Zwingerberger K et al. Molecular analysis of the gamma delta T-cell receptor repertoire in normal human skin and in Oriental cutaneous leishmaniasis. *Exp Dermatol* 1993; **2**: 106–112.
- 121 Nordlind K, Liden S. Gamma/delta T cells and human skin reactivity to heavy metals. *Arch Dermatol Res* 1995; **287**: 137–141.
- 122 Deusch K, Pfeffer K, Reich K, Gstretenbauer M, Daum S, Luling F et al. Phenotypic and functional characterization of human TCR gamma delta+ intestinal intraepithelial lymphocytes. *Curr Top Microbiol Immunol* 1991; **173**: 279–283.
- 123 Trejdosiewicz LK, Calabrese A, Smart CJ, Oakes DJ, Howdle PD, Crabtree JE et al. Gamma delta T cell receptor-positive cells of the human gastrointestinal mucosa: occurrence and V region gene expression in *Helicobacter pylori*-associated gastritis, coeliac disease and inflammatory bowel disease. *Clin Exp Immunol* 1991; **84**: 440–444.
- 124 Breit TM, Wolvers-Tettero ILM, Hählen K, Van Wering ER, van Dongen JJM. Extensive junctional diversity of  $\gamma\delta$  T-cell receptors expressed by T-cell acute lymphoblastic leukemias: implications

- for the detection of minimal residual disease. *Leukemia* 1991; **5**: 1076–1086.
- 125 Langlands K, Eden OB, Micallef-Eynaud P, Parker AC, Anthony RS. Direct sequence analysis of TCR V delta 2–D delta 3 rearrangements in common acute lymphoblastic leukaemia and application to detection of minimal residual disease. *Br J Haematol* 1993; **84**: 648–655.
- 126 Schneider M, Panzer S, Stolz F, Fischer S, Gadner H, Panzer-Grumayer ER. Crosslineage TCR delta rearrangements occur shortly after the DJ joinings of the IgH genes in childhood precursor B ALL and display age-specific characteristics. *Br J Haematol* 1997; **99**: 115–121.
- 127 Hettinger K, Fischer S, Panzer S, Panzer-Grumayer ER. Multiplex PCR for TCR delta rearrangements: a rapid and specific approach for the detection and identification of immature and mature rearrangements in ALL. *Br J Haematol* 1998; **102**: 1050–1054.
- 128 Theodorou I, Raphael M, Bigorgne C, Fourcade C, Lahet C, Cochet G et al. Recombination pattern of the TCR gamma locus in human peripheral T-cell lymphomas. *J Pathol* 1994; **174**: 233–242.
- 129 Kanavaros P, Farcet JP, Gaulard P, Haioun C, Divine M, Le Couedic JP et al. Recombinative events of the T cell antigen receptor delta gene in peripheral T cell lymphomas. *J Clin Invest* 1991; **87**: 666–672.
- 130 Przybylski GK, Wu H, Macon WR, Finan J, Leonard DG, Felgar RE et al. Hepatosplenic and subcutaneous panniculitis-like gamma/delta T cell lymphomas are derived from different Vdelta subsets of gamma/delta T lymphocytes. *J Mol Diagn* 2000; **2**: 11–19.
- 131 Kadin ME. Cutaneous gamma delta T-cell lymphomas – how and why should they be recognized? *Arch Dermatol* 2000; **136**: 1052–1054.
- 132 Hodges E, Quin C, Farrell AM, Christmas S, Sewell HF, Doherty M et al. Arthropathy, leucopenia and recurrent infection associated with a TCR gamma delta population. *Br J Rheumatol* 1995; **34**: 978–983.
- 133 Van Oostveen JW, Breit TM, de Wolf JT, Brandt RM, Smit JW, van Dongen JJM et al. Polyclonal expansion of T-cell receptor- $\gamma\delta$  T lymphocytes associated with neutropenia and thrombocytopenia. *Leukemia* 1992; **6**: 410–418.
- 134 Borst J, Wicherink A, van Dongen JJ, De Vries E, Comans-Bitter WM, Wassenaar F et al. Non-random expression of T cell receptor gamma and delta variable gene segments in functional T lymphocyte clones from human peripheral blood. *Eur J Immunol* 1989; **19**: 1559–1568.
- 135 Krejci O, Prouzova Z, Horvath O, Trka J, Hrusak O. TCR delta gene is frequently rearranged in adult B lymphocytes. *J Immunol* 2003; **171**: 524–527.
- 136 Triebel F, Faure F, Mami-Chouaib F, Jitsukawa S, Griscelli A, Genevee C et al. A novel human V delta gene expressed predominantly in the T<sub>H</sub>1 gamma A fraction of gamma/delta+ peripheral lymphocytes. *Eur J Immunol* 1988; **18**: 2021–2027.
- 137 De Boer CJ, van Krieken JH, Schuurung E, Kluin PM. Bcl-1/cyclin D1 in malignant lymphoma. *Ann Oncol* 1997; **8**: 109–117.
- 138 Tsujimoto Y, Yunis J, Onorato-Showe L, Erikson J, Nowell PC, Croce CM. Molecular cloning of the chromosomal breakpoint of B-cell lymphomas and leukemias with the t(11;14) chromosome translocation. *Science* 1984; **224**: 1403–1406.
- 139 Vaandrager JW, Kleiverda JK, Schuurung E, Kluin-Nelemans JC, Raap AK, Kluin PM. Cytogenetics on released DNA fibers. *Verh Dtsch Ges Pathol* 1997; **81**: 306–311.
- 140 Vaandrager JW, Schuurung E, Zwikstra E, de Boer CJ, Kleiverda KK, van Krieken JH et al. Direct visualization of dispersed 11q13 chromosomal translocations in mantle cell lymphoma by multi-color DNA fiber fluorescence *in situ* hybridization. *Blood* 1996; **88**: 1177–1182.
- 141 Pott C, Tiemann M, Linke B, Ott MM, von Hofen M, Bolz I et al. Structure of Bcl-1 and IgH-CDR3 rearrangements as clonal markers in mantle cell lymphomas. *Leukemia* 1998; **12**: 1630–1637.
- 142 Luthra R, Hai S, Pugh WC. Polymerase chain reaction detection of the t(11;14) translocation involving the bcl-1 major translocation cluster in mantle cell lymphoma. *Diagn Mol Pathol* 1995; **4**: 4–7.
- 143 de Boer CJ, Schuurung E, Dreef E, Peters G, Bartek J, Kluin PM et al. Cyclin D1 protein analysis in the diagnosis of mantle cell lymphoma. *Blood* 1995; **86**: 2715–2723.
- 144 Haralambieva E, Kleiverda K, Mason DY, Schuurung E, Kluin PM. Detection of three common translocation breakpoints in non-Hodgkin's lymphomas by fluorescence *in situ* hybridization on routine paraffin-embedded tissue sections. *J Pathol* 2002; **198**: 163–170.
- 145 Williams ME, Swerdlow SH, Meeker TC. Chromosome t(11;14)(q13;q32) breakpoints in centrocytic lymphoma are highly localized at the bcl-1 major translocation cluster. *Leukemia* 1993; **7**: 1437–1440.
- 146 Segal GH, Masih AS, Fox AC, Jorgensen T, Scott M, Braylan RC. CD5-expressing B-cell non-Hodgkin's lymphomas with bcl-1 gene rearrangement have a relatively homogeneous immunophenotype and are associated with an overall poor prognosis. *Blood* 1995; **85**: 1570–1579.
- 147 Janssen JW, Vaandrager JW, Heuser T, Jauch A, Kluin PM, Geelen E et al. Concurrent activation of a novel putative transforming gene, myeov, and cyclin D1 in a subset of multiple myeloma cell lines with t(11;14)(q13;q32). *Blood* 2000; **95**: 2691–2698.
- 148 Troussard X, Mauvieux L, Radford-Weiss I, Rack K, Valensi F, Garand R et al. Genetic analysis of splenic lymphoma with villous lymphocytes: a Groupe Français d'Hématologie Cellulaire (GFHC) study. *Br J Haematol* 1998; **101**: 712–721.
- 149 Limpens J, Stad R, Vos C, de Vlaam C, de Jong D, van Ommen GJ et al. Lymphoma-associated translocation t(14;18) in blood B cells of normal individuals. *Blood* 1995; **85**: 2528–2536.
- 150 Rabbitts P, Douglas J, Fischer P, Nacheva E, Karpas A, Catovsky D et al. Chromosome abnormalities at 11q13 in B cell tumours. *Oncogene* 1988; **3**: 99–103.
- 151 Fukuhara S, Rowley JD, Variakojis D, Golomb HM. Chromosome abnormalities in poorly differentiated lymphocytic lymphoma. *Cancer Res* 1979; **39**: 3119–3128.
- 152 Weiss LM, Warnke RA, Sklar J, Cleary ML. Molecular analysis of the t(14;18) chromosomal translocation in malignant lymphomas. *N Engl J Med* 1987; **317**: 1185–1189.
- 153 Bakhshi A, Jensen JP, Goldman P, Wright JJ, McBride OW, Epstein AL et al. Cloning the chromosomal breakpoint of t(14;18) human lymphomas: clustering around JH on chromosome 14 and near a transcriptional unit on 18. *Cell* 1985; **41**: 899–906.
- 154 Cleary ML, Sklar J. Nucleotide sequence of a t(14;18) chromosomal breakpoint in follicular lymphoma and demonstration of a breakpoint-cluster region near a transcriptionally active locus on chromosome 18. *Proc Natl Acad Sci USA* 1985; **82**: 7439–7443.
- 155 Korsmeyer SJ. BCL-2 gene family and the regulation of programmed cell death. *Cancer Res* 1999; **59**: 1693s–1700s.
- 156 Lithgow T, van Driel R, Bertram JF, Strasser A. The protein product of the oncogene bcl-2 is a component of the nuclear envelope, the endoplasmic reticulum, and the outer mitochondrial membrane. *Cell Growth Differ* 1994; **5**: 411–417.
- 157 Woodland RT, Schmidt MR, Korsmeyer SJ, Gravel KA. Regulation of B cell survival in xid mice by the proto-oncogene bcl-2. *J Immunol* 1996; **156**: 2143–2154.
- 158 Hsu SY, Lai RJ, Finegold M, Hsueh AJ. Targeted overexpression of Bcl-2 in ovaries of transgenic mice leads to decreased follicle apoptosis, enhanced folliculogenesis, and increased germ cell tumorigenesis. *Endocrinology* 1996; **137**: 4837–4843.
- 159 Lee MS, Chang KS, Cabanillas F, Freireich EJ, Trujillo JM, Stass SA. Detection of minimal residual cells carrying the t(14;18) by DNA sequence amplification. *Science* 1987; **237**: 175–178.
- 160 Crescenzi M, Seto M, Herzog GP, Weiss PD, Griffith RC, Korsmeyer SJ. Thermostable DNA polymerase chain amplification of t(14;18) chromosome breakpoints and detection of minimal residual disease. *Proc Natl Acad Sci USA* 1988; **85**: 4869–4873.
- 161 Lee MS. Molecular aspects of chromosomal translocation t(14;18). *Semin Hematol* 1993; **30**: 297–305.
- 162 Buchonnet G, Lenain P, Ruminy P, Lepretre S, Stamatoullas A, Parmentier F et al. Characterisation of BCL2-JH rearrangements in follicular lymphoma: PCR detection of 3' BCL2 breakpoints and evidence of a new cluster. *Leukemia* 2000; **14**: 1563–1569.
- 163 Cleary ML, Galili N, Sklar J. Detection of a second t(14;18) breakpoint cluster region in human follicular lymphomas. *J Exp Med* 1986; **164**: 315–320.

- 164 Akasaka T, Akasaka H, Yonetani N, Ohno H, Yamabe H, Fukuhara S *et al*. Refinement of the BCL2/immunoglobulin heavy chain fusion gene in t(14;18)(q32;q21) by polymerase chain reaction amplification for long targets. *Genes Chromosomes Cancer* 1998; **21**: 17–29.
- 165 Willis TG, Jadayel DM, Coignet LJ, Abdul-Rauf M, Treleaven JG, Catovsky D *et al*. Rapid molecular cloning of rearrangements of the IGHJ locus using long-distance inverse polymerase chain reaction. *Blood* 1997; **90**: 2456–2464.
- 166 Yabumoto K, Akasaka T, Muramatsu M, Kadowaki N, Hayashi T, Ohno H *et al*. Rearrangement of the 5' cluster region of the BCL2 gene in lymphoid neoplasm: a summary of nine cases. *Leukemia* 1996; **10**: 970–977.
- 167 Pezzella F, Ralfkiaer E, Gatter KC, Mason DY. The 14;18 translocation in European cases of follicular lymphoma: comparison of Southern blotting and the polymerase chain reaction. *Br J Haematol* 1990; **76**: 58–64.
- 168 Turner GE, Ross FM, Krajewski AS. Detection of t(14;18) in British follicular lymphoma using cytogenetics, Southern blotting and the polymerase chain reaction. *Br J Haematol* 1995; **89**: 223–225.
- 169 Vaandrager JW, Schuurin E, Raap T, Philippo K, Kleiverda K, Kluin P. Interphase FISH detection of BCL2 rearrangement in follicular lymphoma using breakpoint-flanking probes. *Genes Chromosomes Cancer* 2000; **27**: 85–94.
- 170 Vaandrager JW, Schuurin E, Kluin-Nelemans HC, Dyer MJ, Raap AK, Kluin PM. DNA fiber fluorescence *in situ* hybridization analysis of immunoglobulin class switching in B-cell neoplasia: aberrant CH gene rearrangements in follicle center-cell lymphoma. *Blood* 1998; **92**: 2871–2878.
- 171 Jacobson JO, Wilkes BM, Kwiatkowski DJ, Medeiros LJ, Aisenberg AC, Harris NL. bcl-2 rearrangements in *de novo* diffuse large cell lymphoma. Association with distinctive clinical features. *Cancer* 1993; **72**: 231–236.
- 172 Hill ME, MacLennan KA, Cunningham DC, Vaughan Hudson B, Burke M, Clarke P *et al*. Prognostic significance of BCL-2 expression and bcl-2 major breakpoint region rearrangement in diffuse large cell non-Hodgkin's lymphoma: a British National Lymphoma Investigation Study. *Blood* 1996; **88**: 1046–1051.
- 173 Vaandrager JW, Schuurin E, Philippo K, Kluin PM. V(D)J recombinase-mediated transposition of the BCL2 gene to the IGH locus in follicular lymphoma. *Blood* 2000; **96**: 1947–1952.
- 174 Fenton JA, Vaandrager JW, Aarts WM, Bende RJ, Heering K, van Dijk M *et al*. Follicular lymphoma with a novel t(14;18) breakpoint involving the immunoglobulin heavy chain switch mu region indicates an origin from germinal center B cells. *Blood* 2002; **99**: 716–718.
- 175 Alaibac M, Filotico R, Giannella C, Paradiso A, Labriola A, Marzullo F. The effect of fixation type on DNA extracted from paraffin-embedded tissue for PCR studies in dermatopathology. *Dermatology* 1997; **195**: 105–107.
- 176 An SF, Fleming KA. Removal of inhibitor(s) of the polymerase chain reaction from formalin fixed, paraffin wax embedded tissues. *J Clin Pathol* 1991; **44**: 924–927.
- 177 Camilleri-Broet S, Deveze F, Tissier F, Ducruit V, Le Tourneau A, Diebold J *et al*. Quality control and sensitivity of polymerase chain reaction techniques for the assessment of immunoglobulin heavy chain gene rearrangements from fixed- and paraffin-embedded samples. *Ann Diagn Pathol* 2000; **4**: 71–76.
- 178 Greer CE, Peterson SL, Kiviat NB, Manos MM. PCR amplification from paraffin-embedded tissues. Effects of fixative and fixation time. *Am J Clin Pathol* 1991; **95**: 117–124.
- 179 Legrand B, Mazancourt P, Durigon M, Khalifat V, Crainic K. DNA genotyping of unbuffered formalin fixed paraffin embedded tissues. *Forensic Sci Int* 2002; **125**: 205–211.
- 180 Lo YM, Mehal WZ, Fleming KA. *In vitro* amplification of hepatitis B virus sequences from liver tumour DNA and from paraffin wax embedded tissues using the polymerase chain reaction. *J Clin Pathol* 1989; **42**: 840–846.
- 181 Longy M, Duboue B, Soubeyran P, Moynet D. Method for the purification of tissue DNA suitable for PCR after fixation with Bouin's fluid. Uses and limitations in microsatellite typing. *Diagn Mol Pathol* 1997; **6**: 167–173.
- 182 Sato Y, Sugie R, Tsuchiya B, Kameya T, Natori M, Mukai K. Comparison of the DNA extraction methods for polymerase chain reaction amplification from formalin-fixed and paraffin-embedded tissues. *Diagn Mol Pathol* 2001; **10**: 265–271.
- 183 Tbakhi A, Totos G, Pettay JD, Myles J, Tubbs RR. The effect of fixation on detection of B-cell clonality by polymerase chain reaction. *Mod Pathol* 1999; **12**: 272–278.
- 184 Goelz SE, Hamilton SR, Vogelstein B. Purification of DNA from formaldehyde fixed and paraffin embedded human tissue. *Biochem Biophys Res Commun* 1985; **130**: 118–126.
- 185 Chan PK, Chan DP, To KF, Yu MY, Cheung JL, Cheng AF. Evaluation of extraction methods from paraffin wax embedded tissues for PCR amplification of human and viral DNA. *J Clin Pathol* 2001; **54**: 401–403.
- 186 Coombs NJ, Gough AC, Primrose JN. Optimisation of DNA and RNA extraction from archival formalin-fixed tissue. *Nucleic Acids Res* 1999; **27**: e12.
- 187 Wickham CL, Boyce M, Joyner MV, Sarsfield P, Wilkins BS, Jones DB *et al*. Amplification of PCR products in excess of 600 base pairs using DNA extracted from decalcified, paraffin wax embedded bone marrow trephine biopsies. *Mol Pathol* 2000; **53**: 19–23.
- 188 Cawkwell L, Quirke P. Direct multiplex amplification of DNA from a formalin fixed, paraffin wax embedded tissue section. *Mol Pathol* 2000; **53**: 51–52.
- 189 Diaz-Cano SJ, Brady SP. DNA extraction from formalin-fixed, paraffin-embedded tissues: protein digestion as a limiting step for retrieval of high-quality DNA. *Diagn Mol Pathol* 1997; **6**: 342–346.
- 190 Hoeve MA, Krol AD, Philippo K, Derksen PW, Veenendaal RA, Schuurin E *et al*. Limitations of clonality analysis of B cell proliferations using CDR3 polymerase chain reaction. *Mol Pathol* 2000; **53**: 194–200.
- 191 Zhou XG, Sandvej K, Gregersen N, Hamilton-Dutoit SJ. Detection of clonal B cells in microdissected reactive lymphoproliferations: possible diagnostic pitfalls in PCR analysis of immunoglobulin heavy chain gene rearrangement. *Mol Pathol* 1999; **52**: 104–110.
- 192 Drexler HG. *The Leukemia-Lymphoma Cell Line Facts Book*, Factsbook Series London: Academic Press, 2001.
- 193 Drexler HG, Dirks WG, Matsuo Y, MacLeod RA. False leukemia-lymphoma cell lines: an update on over 500 cell lines. *Leukemia* 2003; **17**: 416–426.
- 194 Beishuizen A, de Bruijn MA, Pongers-Willemsse MJ, Verhoeven MA, van Wering ER, Hahlen K *et al*. Heterogeneity in junctional regions of immunoglobulin kappa deleting element rearrangements in B cell leukemias: a new molecular target for detection of minimal residual disease. *Leukemia* 1997; **11**: 2200–2207.
- 195 Szczepanski T, Flohr T, van der Velden VH, Bartram CR, van Dongen JJ. Molecular monitoring of residual disease using antigen receptor genes in childhood acute lymphoblastic leukaemia. *Best Pract Res Clin Haematol* 2002; **15**: 37–57.
- 196 Willemsse MJ, Seriu T, Hettinger K, d'Aniello E, Hop WC, Panzer-Grumayer ER *et al*. Detection of minimal residual disease identifies differences in treatment response between T-ALL and precursor B-ALL. *Blood* 2002; **99**: 4386–4393.
- 197 Cave H, van der Werff ten Bosch J, Suciu S, Guidal C, Waterkeyn C, Otten J *et al*. Clinical significance of minimal residual disease in childhood acute lymphoblastic leukemia. European Organization for Research and Treatment of Cancer – Childhood Leukemia Cooperative Group. *N Engl J Med* 1998; **339**: 591–598.
- 198 van Dongen JJ, Seriu T, Panzer-Grumayer ER, Biondi A, Pongers-Willemsse MJ, Corral L *et al*. Prognostic value of minimal residual disease in acute lymphoblastic leukaemia in childhood. *Lancet* 1998; **352**: 1731–1738.
- 199 zur Stadt U, Harms DO, Schluter S, Schrappe M, Goebel U, Spaar H *et al*. MRD at the end of induction therapy in childhood acute lymphoblastic leukemia: outcome prediction strongly depends on the therapeutic regimen. *Leukemia* 2001; **15**: 283–285.
- 200 Schmiegelow K, Nyvold C, Seyfarth J, Pieters R, Rottier MM, Knabe N *et al*. Post-induction residual leukemia in childhood acute lymphoblastic leukemia quantified by PCR correlates with *in vitro* prednisolone resistance. *Leukemia* 2001; **15**: 1066–1071.
- 201 Knechtli CJ, Goulden NJ, Hancock JP, Grandage VL, Harris EL, Garland RJ *et al*. Minimal residual disease status before allogeneic bone marrow transplantation is an important determi-

- nant of successful outcome for children and adolescents with acute lymphoblastic leukemia. *Blood* 1998; **92**: 4072–4079.
- 202 van der Velden VH, Joosten SA, Willemse MJ, van Wering ER, Lankester AW, van Dongen JJ *et al*. Real-time quantitative PCR for detection of minimal residual disease before allogeneic stem cell transplantation predicts outcome in children with acute lymphoblastic leukemia. *Leukemia* 2001; **15**: 1485–1487.
- 203 Bader P, Hancock J, Kreyenberg H, Goulden NJ, Niethammer D, Oakhill A *et al*. Minimal residual disease (MRD) status prior to allogeneic stem cell transplantation is a powerful predictor for post-transplant outcome in children with ALL. *Leukemia* 2002; **16**: 1668–1672.
- 204 Guidal C, Vilmer E, Grandchamp B, Cave H. A competitive PCR-based method using TCRD, TCRG and IGH rearrangements for rapid detection of patients with high levels of minimal residual disease in acute lymphoblastic leukemia. *Leukemia* 2002; **16**: 762–764.
- 205 Wagner SD, Luzzatto L. V kappa gene segments rearranged in chronic lymphocytic leukemia are distributed over a large portion of the V kappa locus and do not show somatic mutation. *Eur J Immunol* 1993; **23**: 391–397.
- 206 Wagner SD, Martinelli V, Luzzatto L. Similar patterns of V kappa gene usage but different degrees of somatic mutation in hairy cell leukemia, prolymphocytic leukemia, Waldenstrom's macroglobulinemia, and myeloma. *Blood* 1994; **83**: 3647–3653.
- 207 Solomon A. Light chains of immunoglobulins: structural–genetic correlates. *Blood* 1986; **68**: 603–610.
- 208 Cuisinier AM, Fumoux F, Moinier D, Boubli L, Guigou V, Milili M *et al*. Rapid expansion of human immunoglobulin repertoire (VH, V kappa, V lambda) expressed in early fetal bone marrow. *New Biol* 1990; **2**: 689–699.